

See discussions, stats, and author profiles for this publication at: <https://www.researchgate.net/publication/236496904>

# Preliminary Hydrogeologic Characterization Results from the Wallula Basalt Pilot Study

ARTICLE · NOVEMBER 2009

CITATIONS

6

READS

49

9 AUTHORS, INCLUDING:



[Gretchen Hund](#)

Pacific Northwest National Laboratory, United States

20 PUBLICATIONS 63 CITATIONS

[SEE PROFILE](#)



[Paul david Thorne](#)

Battelle Memorial Institute

67 PUBLICATIONS 212 CITATIONS

[SEE PROFILE](#)



[Stephen Paul Reidel](#)

Washington State University

154 PUBLICATIONS 1,078 CITATIONS

[SEE PROFILE](#)



[F. S. Colwell](#)

Oregon State University

107 PUBLICATIONS 2,311 CITATIONS

[SEE PROFILE](#)

# **Preliminary Hydrogeologic Characterization Results from the Wallula Basalt Pilot Study**

BP McGrail, Principal Investigator

EC Sullivan	PD Thorne
FA Spane	CJ Thompson
DH Bacon	SP Reidel
G Hund	FS Colwell

Battelle  
Pacific Northwest Division  
Richland, Washington 99352

Prepared for  
National Energy Technology Laboratory  
Morgantown, WV 26507-0880  
under Cooperative Agreement DE-FC26-05NT42587

December 2009



## LEGAL NOTICE

This report was prepared by Battelle Memorial Institute (Battelle) as an account of sponsored research activities. Neither Client nor Battelle nor any person acting on behalf of either:

**MAKES ANY WARRANTY OR REPRESENTATION, EXPRESS OR IMPLIED**, with respect to the accuracy, completeness, or usefulness of the information contained in this report, or that the use of any information, apparatus, process, or composition disclosed in this report may not infringe privately owned rights; or

Assumes any liabilities with respect to the use of, or for damages resulting from the use of, any information, apparatus, process, or composition disclosed in this report.

Reference herein to any specific commercial product, process, or service by trade name, trademark, manufacturer, or otherwise, does not necessarily constitute or imply its endorsement, recommendation, or favoring by Battelle. The views and opinions of authors expressed herein do not necessarily state or reflect those of Battelle.



This document was printed on recycled paper.

(9/2003)

# **Preliminary Hydrogeologic Characterization Results from the Wallula Basalt Pilot Study**

BP McGrail, Principal Investigator

EC Sullivan	PD Thorne
FA Spane	CJ Thompson
DH Bacon	SP Reidel <sup>(a)</sup>
G Hund	FS Colwell <sup>(b)</sup>

Battelle  
Pacific Northwest Division  
Richland, Washington 99352

Prepared for  
National Energy Technology Laboratory  
Morgantown, WV 26507-0880  
under Cooperative Agreement DE-FC26-05NT42587

December 2009

---

(a) Washington State University Tri-Cities, Richland, Washington  
(b) Oregon State University, Corvallis, Oregon



## Abstract

The U.S. Department of Energy's Big Sky Regional Carbon Sequestration Partnership has completed drilling the first continental flood basalt sequestration pilot borehole to a total depth of 4110 ft at the Boise White Paper Mill property at Wallula, Washington. Site suitability was assessed before drilling by the 2007 to 2008 acquisition, processing, and analysis of a 4-mi, five-line three component seismic swath, which was processed as a single data-dense line. Analysis of the seismic survey data indicated a composite basalt formation thickness of ~8000 ft and absence of major geologic structures (i.e., faults) along the line imaged by the seismic swath. Drilling of Wallula pilot borehole was initiated on January 13, 2009, and reached total depth on April 6, 2009. Based on characterization results obtained during drilling, three basalt breccia zones were identified between the depth interval of 2716 and 2,910 ft as being a suitable injection reservoir for a subsequent CO<sub>2</sub> injection pilot study. The targeted injection reservoir lies stratigraphically below the massive Umtanum Member of the Grande Ronde Basalt, whose flow-interior section possesses regionally recognized low-permeability characteristics. The identified composite injection zone reservoir provides a unique and attractive opportunity to scientifically study the reservoir behavior of three interconnected reservoir intervals below primary and secondary caprock confining zones.

Drill cuttings, wireline geophysical logs, and thirty-two 1-in. diameter rotary sidewall cores provided geologic data for characterization of rock properties. X-ray fluorescence analyses of selected rock samples provided geochemical characterizations of the rocks and stratigraphic control for the basalt flows encountered by the Wallula pilot borehole. Based on the geochemical results, the pilot borehole was terminated in the Wapshilla Ridge 1 flow of the Grande Ronde Basalt Formation.

Detailed hydrologic test characterizations of 12 basalt interflow reservoir zones and 3 flow-interior/caprock intervals were performed during drilling, and immediately thereafter reached the final borehole drilling depth (i.e., 4110 ft). In addition, 6 of the 12 basalt interflow zones were selected for detailed hydrochemical characterization. Results from the detailed hydrologic test characterization program provided the primary information on basalt interflow zone transmissivity/injectivity and caprock permeability characteristics.



# Executive Summary

Continental flood basalts represent one of the largest geologic structures on the planet and exist in regions of the United States (and other countries such as India) where sedimentary basin storage capacity is limited. Consequently, demonstration of commercial-scale storage in deep flood basalts is important in meeting global CO<sub>2</sub> emissions targets. Because of extensive prior characterization of the flood basalts in southeastern Washington State, this region has been the focus of these first field studies.

Before commencement of drilling, analysis of a 4-mi, five line three-component seismic swath near the field site location showed no major faults and basalt thickness is about 8000 ft along the line imaged by the seismic swath. Consequently, the U.S. Department of Energy's Big Sky Regional Carbon Sequestration Partnership initiated and completed drilling the first continental flood basalt sequestration pilot borehole to a total depth of 4110 ft on the Boise White Paper mill property at Wallula, Washington. A suite of wireline logs were acquired (some for the first time in basalts) that included the following:

- Platform Express with Array Induction Imager Tool
- Elemental Capture Spectroscopy log
- Reservoir Saturation Tool: Sigma Saturation log
- Fluid temperature log
- Sonic Scan including SonicScanAdvancedAnswer, anisotropy analysis, primary and secondary wave compression and shear with summary interpretation
- Formation Micro Imager with summary fracture interpretation over 1600 ft of interval
- Rotary sidewall cores.

Logging data combined with X-ray fluorescence stratigraphy indicate there are no major faults intersected by the well. Observed dip reversals are stratigraphic rather than due to faults, and regional structural dip is two degrees to the northwest.

Hydrogeologic information was obtained primarily during borehole drilling/advancement using a progressive drill-and-test characterization strategy. A general decreasing transmissivity trend with depth pattern was observed, which is consistent with results exhibited for Columbia River basalt interflow zones at a number of other deep wells in the region. Based on the comparative results from 10 test intervals, a candidate injection test zone was identified between the general depth interval of ~2716 and 2870 ft below ground surface. Over this interval, three brecciated interflow zones were selected for future CO<sub>2</sub> injection: the Ortleigh flow top, the Slack Canyon #1 flow top, and the Slack Canyon #2 flow top. The flow tops have relatively high permeabilities and are bounded by thick-flow interiors that have extremely low permeabilities. The borehole configuration established at the Wallula pilot site provides a unique and very attractive opportunity to scientifically study the reservoir behavior of three connected reservoir intervals below primary and secondary caprock zones. Simulations of a 1000 metric tons (MT) open-borehole injection over a period of 14 days into the three brecciated zones show that most of the injected CO<sub>2</sub> flows into the Slack Canyon #2 flow top because of its higher permeability. The increase in pressure in the well bore is less than 110 psi to achieve this injection rate, and the radius of the injected supercritical CO<sub>2</sub> increases to a maximum of 180 ft at 1 year after the start of injection. No CO<sub>2</sub>

migration into the overlying Slack Canyon #3 flow interior is predicted even after 1 year of simulation time. Based on the cumulative analyses completed to date, the Wallula basalt pilot borehole appears to be well suited to conduct the world's first supercritical CO<sub>2</sub> injection test into a continental flood basalt formation.



# Acronyms

bgs	below ground surface
BSCSP	Big Sky Carbon Sequestration Partnership
CCS	carbon capture and storage
CRB	Columbia River basalts
CRBG	Columbia River Basalt Group
DOECAP	U.S. Department of Energy's Consolidated Audit Program
DST	drill-stem test
ECS	Elemental Capture Spectroscopy
FMI	Formation Micro Imager
FSM	Frenchman Springs Member
GCM	Grouse Creek Member
GEL	General Engineering Laboratories
gpm	gallons per minute.
Gt	billion metric tons
Hz	hertz
ID	inside diameter
IGCC	integrated gasification combined cycle
MCL	maximum concentration limits
msl	mean sea level
MW	megawatt
MT	metric ton
ND	not determined
OD	outside diameter
OFT	Ortley flow top
OM	Ortley Member
PCR	polymerase chain reaction
PNWD	Battelle Pacific Northwest Division
SBM	Sentinel Bluffs Member
SCFT1	Slack Canyon #1 flow top
SCFT2	Slack Canyon #2 flow top
SP	spontaneous potential
SW	slug withdrawal
TD	total depth
VSP	vertical seismic profile
WRM	Wapshilla Ridge Member
XRD	X-ray diffraction
XRF	X-ray fluorescence



# Contents

Abstract.....	iii
Executive Summary .....	v
1.0 Introduction .....	1.1
1.1 Regional Setting .....	1.1
1.2 Site Selection Overview .....	1.2
2.0 Site Characterization.....	2.1
2.1 Soil Gas Monitoring Wells.....	2.1
2.2 Seismic Survey.....	2.2
2.3 Borehole Drilling and Characterization .....	2.5
2.3.1 Drilling Program and Well Construction .....	2.6
2.3.2 Stratigraphy and Geochemical Sampling .....	2.11
2.3.3 Wireline Geophysics .....	2.13
2.3.4 Hydrologic Testing.....	2.21
2.3.5 Hydrochemistry and Isotopic Sampling .....	2.34
2.3.6 Microbiological Studies .....	2.36
3.0 Injection Discussion and Planning .....	3.1
3.1 Target Formation Description .....	3.1
3.2 Injection Simulation Analysis .....	3.1
3.2.1 Hydraulic Properties.....	3.1
3.2.2 Simulation Results.....	3.3
3.3 Injection Procedures.....	3.13
3.4 Monitoring Program.....	3.14
3.4.1 Atmospheric Monitoring .....	3.14
3.4.2 Soil Monitoring .....	3.14
3.4.3 Water Chemistry .....	3.15
3.4.4 Preclosure Characterization.....	3.15
4.0 Public Outreach .....	4.1
4.1 Historical Background.....	4.1
5.0 References .....	5.1
Appendix A – Stratigraphy/XRF .....	A.1
Appendix B – Wireline Geophysics.....	B.1
Appendix C – Hydrologic Test Methods/Analyses .....	C.1
Appendix D – Hydrologic Test Equipment .....	D.1
Appendix E – Hydrochemical Data for Wallula Pilot Groundwater Samples.....	E.1

# Figures

1.1	Surface Areal Extent of Basalt Formations of the Columbia River Basalt Group.....	1.1
1.2	Aerial Photograph of Boise Mill Site, Borehole Location, and Seismic Survey .....	1.2
2.1	Location of Three-Component Seismic Swath Near Boise Plant at Attalia Station .....	2.2
2.2	Two Vibroseis Trucks on Location at the Wallula Site .....	2.2
2.3	Novel Four Mile, Five Line Three-Component Seismic Swath Designed by CCGVeritas.....	2.3
2.4	P-P Image Produced in an Intermediate-Stage Processing of the Wallula Data .....	2.4
2.5	Final P-P Image as Processed by CCGVeritas .....	2.4
2.6	Rotary Sidewall Core Samples Shown as They were Examined at the Wellsite .....	2.12
2.7	Structures of a Single Idealized Flood Basalt Flow .....	2.13
2.8	Schlumberger Platform Express Logs Through the Proposed Injection Zone .....	2.14
2.9	Sonic Porosity Log over the Seals and Injection Zones.....	2.16
2.10	Drilling Induced Fractures Above 2900 ft in the Wallula Pilot Borehole, as Imaged by the FMI Log .....	2.17
2.11	Northwest-Southeast Oriented Stress-Induced Fractures in the Wallula Pilot Borehole, as Tabulated from the FMI Log.....	2.18
2.12	Natural Fractures in a Highly Vesicular Zone in the Wallula Pilot Borehole.....	2.19
2.13	Rose Plot of Azimuth of Natural Fractures as Determined from the FMI Log.....	2.19
2.14	Rose Plot of Fast Shear Azimuth from the Full Waveform Sonic .....	2.19
2.15	Computer Generated Facies Model Based on Bedding Dips Interpreted from the FMI.....	2.20
2.16	Location of the Shell 1-10 Darcell Gas Exploration Well and Other Deep Wells in the Region .....	2.22
2.17	As-Built Completion for the Wallula Pilot Borehole.....	2.23
2.18	General Deployment of the Downhole Packer Test System during Borehole Advancement .....	2.24
2.19	Downhole Test System Configuration with Installed Submersible Pump within Cross-Over Test Tubing-String Section.....	2.25
2.20	Depth Location of Wallula Pilot Basalt Interflow Test Zones .....	2.25
2.21	Wallula Pilot Basalt Interflow Transmissivity versus Borehole Depth .....	2.27
2.22	Borehole Hydrologic Test Zones within the Completed Well Injection Zone Horizon .....	2.30
2.23	Slug Test Zone Response Comparison .....	2.30
2.24	Hydrologic Test Characterization Sequence: Zone 8B .....	2.31
2.25	Preliminary Zone 8B Slug Test Analysis.....	2.32
2.26	Caprock Hydrologic Test Zones above the Completed Well Injection Zone Horizon .....	2.33
2.27	Five Intervals were Packed Off in the Wallula Pilot Well and Sampled for Free- Living Microbial Cells in Groundwater and Terminal Restriction Fragment Length Polymorphism Profiles from the Five Respective Intervals .....	2.37

3.1	Lithologic Units for Simulation of Pilot-Scale CO <sub>2</sub> Injection at Wallula .....	3.3
3.2	CO <sub>2</sub> Saturation in the Ortley, Slack Canyon #1 and Slack Canyon #2 Flow Tops Immediately after 1000 MT Supercritical CO <sub>2</sub> Injection .....	3.4
3.3	Fluid Density in the Ortley, Slack Canyon #1, and Slack Canyon #2 Flow Tops Immediately after 1000 MT Supercritical CO <sub>2</sub> Injection .....	3.4
3.4	CO <sub>2</sub> Saturation in the Ortley, Slack Canyon #1 and Slack Canyon #2 Flow Tops 1 Year after Start of 1000 MT Supercritical CO <sub>2</sub> Injection .....	3.5
3.5	Radii Containing 50%, 90%, and 100% of 1000 MT of Supercritical CO <sub>2</sub> Injected into the Ortley, Slack Canyon #1 and Slack Canyon #2 Flow Tops .....	3.5
3.6	Increase in Well Pressure during Injection of Supercritical CO <sub>2</sub> into the Ortley, Slack Canyon #1, and Slack Canyon #2 Flow Tops .....	3.6
3.7	Phase Distribution of 1000 MT of Supercritical CO <sub>2</sub> Injected into the Ortley, Slack Canyon #1 and Slack Canyon #2 Flow Tops .....	3.6
3.8	CO <sub>2</sub> Saturation in the Slack Canyon #2 Flow Top, Immediately after 1000 MT Supercritical CO <sub>2</sub> Injection .....	3.7
3.9	Fluid Density in the Slack Canyon #2 Flow Top, Immediately after 1000 MT Supercritical CO <sub>2</sub> Injection .....	3.7
3.10	CO <sub>2</sub> Saturation in the Slack Canyon #2 Flow Top, 1 Year after Start of 1000 MT Supercritical CO <sub>2</sub> Injection .....	3.8
3.11	Radii Containing 50%, 90%, and 100% of 1000 MT of Supercritical CO <sub>2</sub> Injected into the Slack Canyon #2 Flow Top .....	3.8
3.12	Increase in Well Pressure During Injection of Supercritical CO <sub>2</sub> into the Slack Canyon #2 Flow Top .....	3.9
3.13	Phase Distribution of 1000 MT of Supercritical CO <sub>2</sub> Injected into the Slack Canyon #2 Flow Top .....	3.9
3.14	CO <sub>2</sub> Saturation in the Ortley Flow Top Immediately after 1000 MT Supercritical CO <sub>2</sub> Injection .....	3.10
3.15	Fluid Density in the Ortley Flow Top, Immediately after 1000 MT Supercritical CO <sub>2</sub> Injection .....	3.11
3.16	CO <sub>2</sub> Saturation in the Ortley Flow Top, 1 Year after Start of 1000 MT Supercritical CO <sub>2</sub> Injection .....	3.11
3.17	Radii Containing 50%, 90%, and 100% of 1000 MT of Supercritical CO <sub>2</sub> Injected into the Ortley Flow Top .....	3.12
3.18	Increase in Well Pressure during Injection of Supercritical CO <sub>2</sub> into the Ortley Flow Top .....	3.12
3.19	Phase Distribution of 1000 MT of Supercritical CO <sub>2</sub> Injected into the Ortley Flow Top .....	3.13

## Tables

2.1	Gas Chromatography Results on Gas Samples Collected from Soil Gas Probes BAM 126 and BAM 127 and Background .....	2.1
2.2	Borehole Stratigraphy of the Wallula Pilot Borehole Well Based on X-Ray Fluorescence Data, Lithology, and Stratigraphic Position.....	2.7
2.3	Borehole Drilling/Test Activity Log.....	2.8
2.4	Test Zone Characterization Activity Log .....	2.10
2.5	Summary of Hydrologic Test Methods Used for Wallula Pilot Test Site Characterization Investigation .....	2.26
2.6	Preliminary Observed Hydraulic Head Measurements.....	2.28
2.7	Pertinent Information Pertaining to Hydrochemical/Microbiological Sampling.....	2.34
3.1	Hydraulic Properties and Depth of Basalt Flows at Wallula .....	3.2
3.2	Brooks-Corey Function Parameters .....	3.2

# 1.0 Introduction

Continental flood basalts represent one of the largest geologic structures on the planet but have received comparatively little attention for geologic storage of CO<sub>2</sub>. Because flood basalt formations exist in regions of the United States (and other countries such as India) where sedimentary basin storage capacity is limited, demonstration of commercial-scale storage in deep flood basalts is important in meeting global CO<sub>2</sub> emissions targets. That fact is now being increasingly realized. Since the original concepts for sequestration in basalts were proposed (McGrail et al. 2003; McGrail et al. 2006), interest has grown rapidly with laboratory (White et al. 2006; Matter et al. 2007; Flaathen et al. 2008; Goldberg et al. 2008; Gysi and Stefansson 2008; Prasad et al. 2009; Schaef and McGrail 2009) and other field trials (Alfredsson et al. 2008; Khalilabad et al. 2008) now underway around the world. Nevertheless, the field pilot study undertaken by the Big Sky Carbon Sequestration Partnership (BSCSP) described in this report remains unique in the world for confirming the feasibility of permanently and safely sequestering large quantities of supercritical CO<sub>2</sub> within deep flood basalt formations.

## 1.1 Regional Setting

Southeastern Washington State, and indeed a large portion of the entire Pacific Northwest east of the Cascade Mountain Range, belongs to the Columbia Plateau Province that hosts a world-class set of continental flood basalt deposits. The Miocene Columbia River Basalt Group (CRBG) covers over 77,200 mi<sup>2</sup> of portions of eastern Washington State, northeastern Oregon, and western Idaho (Figure 1.1), with a total estimated volume of more than 53,700 mi<sup>3</sup> (Reidel et al. 2002). Collectively, over 300 individual CRBG flows have been identified within the region, which attain a maximum composite thickness of greater than 16,000 ft within the central portion of the Columbia Basin. Conservative estimates of CO<sub>2</sub> storage capacity in the CRBG are approximately 10 to 50 billion metric tons (Gt) of CO<sub>2</sub> (McGrail et al. 2006). Groundwater within and below the Grande Ronde Basalt in this region of the Columbia Basin is brackish and sulfide-rich, with high concentrations of fluoride that exceed maximum concentration limits (MCLs) as specified in National Primary Drinking Water Regulations (40 CFR 141.62). Exceedance of MCLs listed in 40 CFR 141.62 is the standard adopted in Washington State for permitting geologic sequestration projects under WAC 173-218-115.

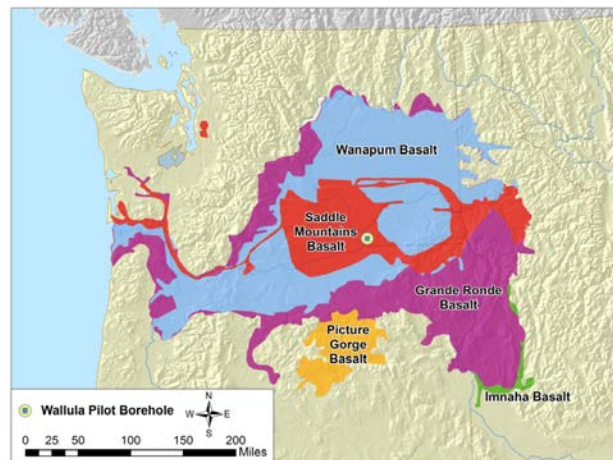


**Figure 1.1.** Surface Areal Extent of Basalt Formations of the Columbia River Basalt Group (modified from Reidel et al. 2002)

## 1.2 Site Selection Overview

In April 2007, Battelle Pacific Northwest Division (PNWD) and the BSCSP were invited by the Port of Walla Walla to conduct a field pilot study on Port-owned land in Walla Walla County. The demonstration site was at that time under consideration by industry for construction of a 750-megawatt (MW) integrated gasification combined cycle (IGCC) power plant that would require carbon capture and storage (CCS). The site is located in a rural area and is zoned heavy industrial; agriculture and livestock management are the principal businesses in the surrounding region. As a result of this invitation from the Port, PNWD began planning field work on the Port site, which included conducting a seismic survey prior to drilling a pilot test well.

In November 2007, the Port of Walla Walla signed a land use agreement giving Battelle permission to conduct a seismic survey on its property. After obtaining the necessary surrounding land owner permits, Battelle completed a seismic survey at the Port site in December 2007. Following completion of the seismic survey, the pilot borehole was delayed by public opposition to the proposed IGCC plant (see Section 4.0, “Public Outreach”). In April 2008, a decision was made at the request of the Port and Walla Walla County Commissioners to find an alternative site location. In May 2008, Battelle staff contacted management at the Boise Whitepaper mill located approximately one-half mile from the Port property site regarding interest in conducting the pilot study on its property. This location ensured the pilot study could be conducted on private property, but was still near enough to the seismic survey line to preserve relevance of the \$750,000 investment in the seismic survey. Negotiations for a land use agreement were successfully concluded in August 2008. PNWD staff surveyed the Boise mill site to identify a suitable location for the borehole. Site constraints, such as size of unobstructed areas, proximity to structures, and access to electrical power and water dictated the final selected site location illustrated in Figure 1.2.

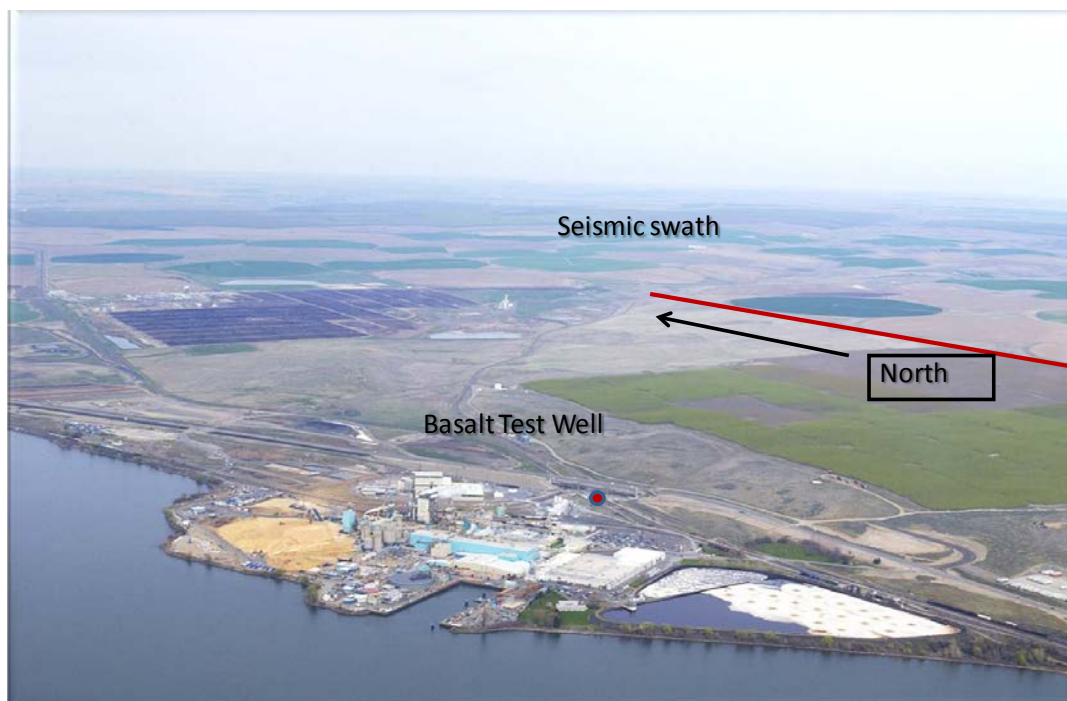


**Figure 1.2.** Aerial Photograph of Boise Mill Site, Borehole Location, and Seismic Survey



## 2.0 Site Characterization

Site characterization activities conducted at the Wallula pilot site included the following:

- installation of two shallow soil gas monitoring wells
- surface seismic survey
- borehole characterization activities conducted in association with drilling the pilot borehole.

Details and results and conclusions from each of these activities are provided in the following sections.

### 2.1 Soil Gas Monitoring Wells

On July 7, 2007, two soil gas probes (BAM 126 and BAM 127) were installed approximately 0.5 mi from the Wallula site by Boart Longyear Company (Milton, Washington). The 1.9-cm diameter probes were spaced approximately 275 m apart and installed ~7.6 m deep and included a bottom screened interval of 2.54 m. Sand was used for packing around the probes and commercial dry granular bentonite was used for sealing. Above ground risers with padlocks were installed in concrete to protect the soil gas probes from adverse weather conditions.

Gas samples were collected using a Pulse Pump III (MiDan) and 1-L Tedlar® bags.<sup>1</sup> Initially, each gas probe was purged approximately six well volumes before collecting samples into Tedlar sample bags. A single air sample was collected near one of the wells and used as a background sample. Gas chromatography was used to measure concentrations of H<sub>2</sub>, CO<sub>2</sub>, C<sub>2</sub>H<sub>4</sub>, C<sub>2</sub>H<sub>6</sub>, O<sub>2</sub>, N<sub>2</sub>, CH<sub>4</sub>, and CO in these gas samples. Results from the gas chromatography analysis (July 25, 2007) showed slightly elevated readings (above background) for N<sub>2</sub> and O<sub>2</sub> (Table 2.1). Concentrations of CO<sub>2</sub> in the wells were identical or lower than background levels. Remaining gas compounds of interest (especially methane) were below detectable limits in both wells and the air sample (Table 2.1). Gas chromatography results from the second sampling, collected on August 21, 2007, are also presented in Table 2.1. Concentrations for CO<sub>2</sub>, N<sub>2</sub>, and O<sub>2</sub> from both wells are similar to the first sampling. The background sample, collected near well 126 compares well to the first background sample collected near well 127. No significant differences were noted between the two gas samplings.

**Table 2.1.** Gas Chromatography Results on Gas Samples Collected from Soil Gas Probes BAM 126 and BAM 127 and Background (air)

Component	07/25/07			08/21/07		
	Air	126	127	Air	126	127
CO <sub>2</sub>	0.03	0.02	0.03	0.02	0.03	0.03
N <sub>2</sub>	51.36	52.43	54.33	48.98	52.63	50.71
O <sub>2</sub>	2.09	4.39	2.62	0.41	0.74	0.76
C <sub>2</sub> H <sub>4</sub> , CH <sub>4</sub>	DL	DL	DL	DL	DL	DL
H <sub>2</sub> , CO, C <sub>2</sub> H <sub>6</sub>	DL	DL	DL	DL	DL	DL

Concentration in percent.  
DL = detection limit.

<sup>1</sup>Tedlar is a registered trademark of E. I. du Pont de Nemours & Co., Inc.

## 2.2 Seismic Survey

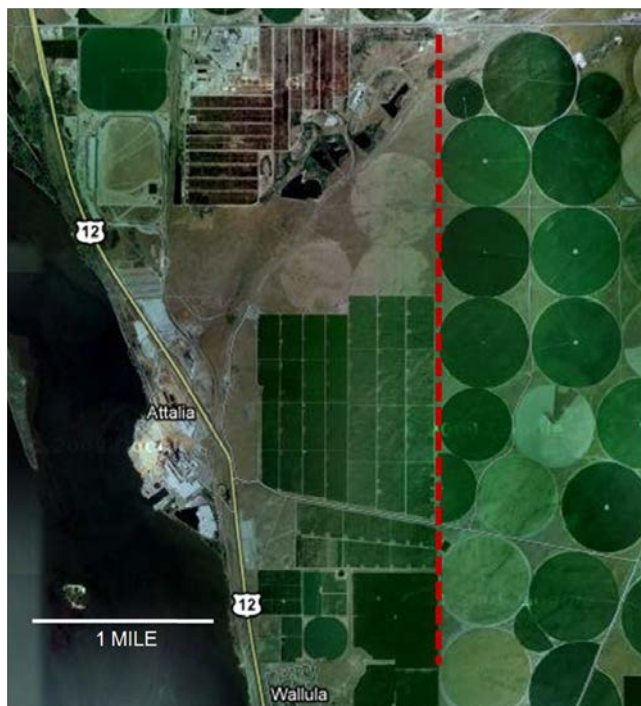


**Figure 2.1.** Location of Three-Component Seismic Swath Near Boise Plant at Attalia Station. Satellite view from Google Maps™ mapping service.<sup>1</sup>



**Figure 2.2.** Two Vibroseis Trucks on Location at the Wallula Site

An innovative three-component, two-dimensional surface seismic swath profile acquired near Wallula, Washington State, in December 2007 (Figure 2.1) provided the framework for fault detection and first order characterization of subsurface stratigraphy and structure at the site of the proposed Big Sky CO<sub>2</sub> sequestration test. The results from this seismic acquisition and processing experiment greatly reduced uncertainty associated with site selection by showing there are no deep-seated surface or subsurface faults along the seismic line. Experiment results also showed that a thick succession of basalt layers are present and undisturbed by large scale faulting. The seismic survey represents the first known success of surface-based seismic imaging of basalt that has a thin sediment cover. The results provide a critical key for subsurface characterization and monitoring of CO<sub>2</sub> sequestration in basalts. This experiment has important implications for sequestration not only in the Pacific Northwest but also in other worldwide basalt terrains.

The 2007 4-mi reflection survey used a seismic signal produced by vibrator trucks (Figure 2.2). Approximately 3000 receivers recorded various modes of compression (P) and shear (S) waves, including waves that are converted from one mode to the other as they encounter sharp boundaries of subsurface rock layers. The three-component receivers, consisting of vertical compression wave and two orientations of shear wave sensors, were arranged in a five-line (440-ft) swath that extended north-south for 4 mi, near the proposed CO<sub>2</sub> injection test site. Two vibrator trucks generated a synchronized seismic signal at closely spaced stations along each of the long (4 mi) sides of the rectangular swath.

Prior to acquiring the survey data, the vibrators were tested to ensure their electronics

<sup>1</sup> Google Maps is a trademark of Google, Inc.

and control systems preformed within specifications. Finally, acquisition tests were conducted to determine the optimal combination of vibration frequency, length of vibration time (“sweep”) and number of sweeps that created the strongest signal-like reflections of the basalt layers below about 3000 ft that are targeted for detailed sequestration characterization. The seismic design (Figure 2.3) and processing was performed by CCGVeritas, and the swath acquisition was conducted by Paragon Geophysical Services, Inc.

Field data are not suitable for immediate interpretation of the subsurface geology. To create an accurate depiction of the subsurface, a number of types of data artifacts must be removed or at least minimized. These artifacts are related to the instrumentation and method of acquisition, missing data due to the presence of agricultural or other surface obstacles, the topography of the ground surface, and a number of types of noise in the data that obscure or misplace the subsurface image. Because the Wallula data set involved five lines of receiver data, each 4 mi long, and because three modes of seismic waves (P wave, converted P-SV wave, and shear wave SV-SV) exist for each line, processing the Wallula data set was particularly labor and computer intensive.

Processing of the Wallula data set included more than 30 individual processing steps, many of them iterative. Processing addresses six main functions: database building, editing and basic corrections, signal-to-noise enhancement, enhancement of resolution in time (the vertical part of data display), and enhancement of resolution in space (the lateral location of geologic features). Finally, processing involves producing images that make different types of geologic features easier to detect and recognize. Because the survey was designed to allow for identification of converted waves that can behave as noise and can obscure the seismic image, full elastic numerical modeling of seismic wave behavior was required. This work was conducted by CCGVeritas, using known local geology and rock properties gained during years of basalt research at the Hanford Site.

Results of the numerical modeling allowed the identification and removal of converted wave noise, and identified causes of loss of P wave signal at shallow depths and at basalt flow interfaces. An intermediate processing image (Figure 2.4) shows that in the subsurface geology intersected by the seismic swath, a thick succession of basalts (about 8000 ft) is present, with no indications of major faulting. At this stage, the data in the zone of interest (about 0.5 sec two-way time) are relatively low frequency (about 15 hertz [Hz]). Figure 2.5 shows the final P-P image with higher dominant frequency data (about 30 Hz). Additional processing, particularly if a vertical seismic profile (VSP) is acquired for calibration, is expected to further enhance imaging.

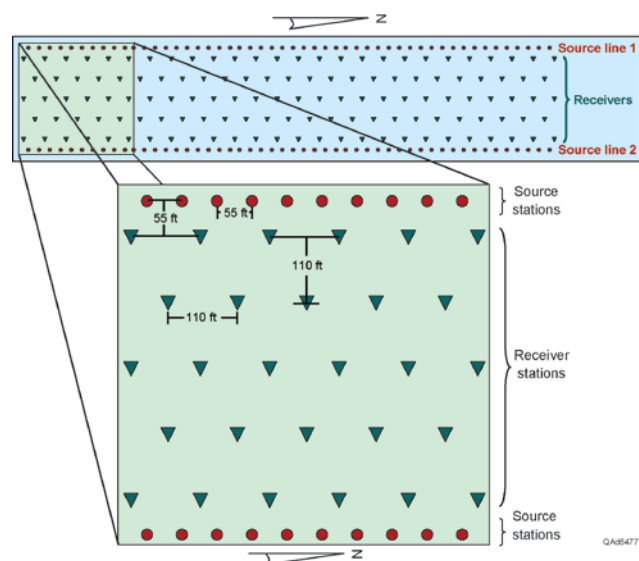


**Figure 2.3.** Novel Four Mile, Five Line Three-Component Seismic Swath Designed by CCGVeritas



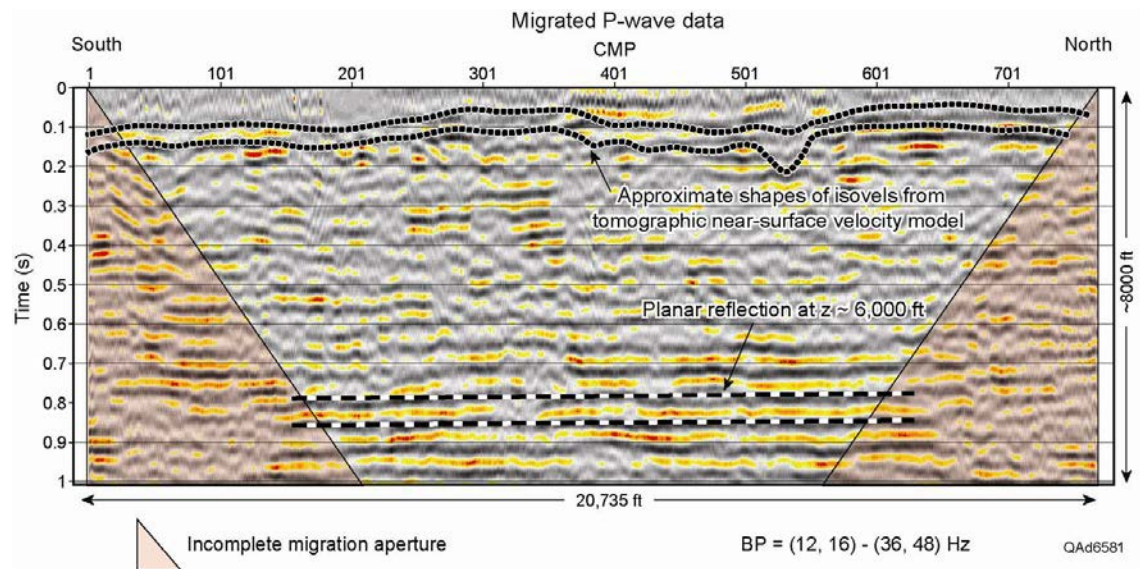


**Figure 2.4.** P-P Image Produced in an Intermediate-Stage Processing of the Wallula Data. The shaded triangular areas at the ends of the profile show end of line affects on the data redundancy. The flat lying reflectors at about 0.8 seconds (two-way time) are evidence for lack of deep-seated faulting. B.P is bandwidth; Hz is frequency. Dominant frequency is only about 15 Hz at this processing stage.

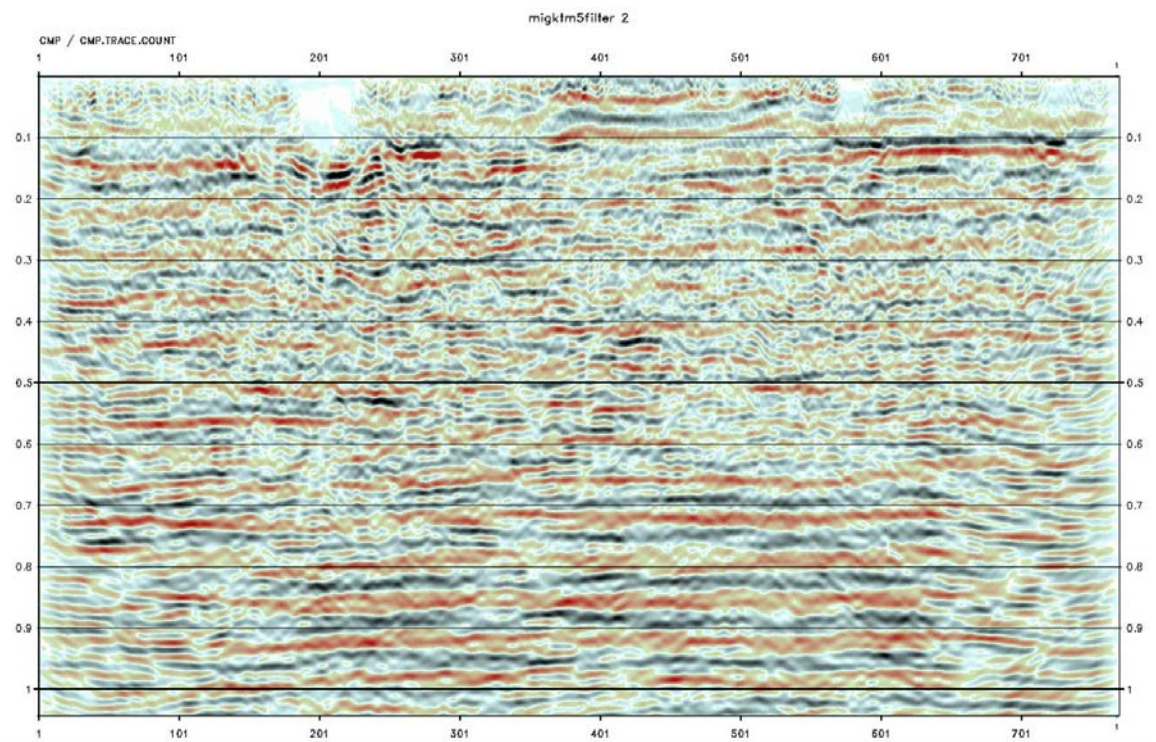


**Figure 2.5.** Final P-P Image as Processed by CGGVeritas. The frequency bandwidth is doubled (approximately) compared to the image shown as Figure 2.4. The dominant frequency is about 30 Hz. Again, there is no evidence of vertical faulting within the deeper basalt units (0.8 seconds to 1.0 seconds).

As with images generated during the intermediate processing stages, the final migrated P-wave images indicate that no east-west striking faults disrupt the deep basalt interval along the seismic swath, and thus no major deep-seated breaks are likely to penetrate the shallower basalt section. Because the dominant wavelength of the data is approximately 600 ft, there could be small-throw faults with vertical displacements of 50 or 60 ft (0.1 »dom) that cannot be recognized on the currently processed two-dimensional images. In addition, faults parallel to the seismic swath would not be imaged by this transect. Data gaps near the surface and underlying disruption of the seismic image were caused by avoidance of irrigation waterlines and surface infrastructure. Data interpreted from this seismic line do not eliminate risk of a fault being present at the well site, but do reduce uncertainty associated with existence of hidden east-west striking faults that are associated with major structures in the Pasco Basin.

Researchers' most important findings for understanding the problems with acquiring seismic reflection data in basalts are as follows:

- A wide variety of shear wave energy modes swamp the P-wave seismic records.
- Except at very short geophone offsets, ground roll overprints P-wave signal.
- Because of extreme velocity contrasts, primary wave events are refracted at incidence angles greater than about 7–15 degrees.
- P-wave energy is converted to down-going shear wave energy at the top of the uppermost basalt layer. This creates a shear wave-shear wave volume that may lead to new techniques for evaluating azimuthal seismic anisotropy, fractures, and stratigraphic heterogeneity.

These scientific insights gained during acquisition and processing of the three-component two-dimensional swath have already resulted in a breakthrough in application of seismic imaging to basalt geology. Identification of the specific causes of poor data quality allow the development of processing steps to remove unwanted energy modes, improve the signal-to-noise ratio, and increase resolution. Borehole geophysical data from the pilot borehole will facilitate additional customized processing steps that could further enhance accuracy of the seismic imaging.

## **2.3 Borehole Drilling and Characterization**

The Wallula pilot borehole used the progressive “drill-and-test” characterization strategy that emphasizes the acquisition of detailed hydrogeologic characterization information concurrent with drilling and borehole advancement. This is in contrast to characterization strategies that are initiated after a borehole has reached the final well completion depth. As discussed in Reidel et al. (2002), information acquired using a progressive drill-and-test strategy provides characterization information of higher quality, particularly for those hydrologic parameters that are sensitive or more significantly impacted by the borehole drilling process (e.g., hydrochemistry, microbiology). This is also the preferred characterization strategy for boreholes—such as the Wallula pilot borehole—that are drilled in areas not having significant subsurface information available from surrounding wells drilled to comparable depths. In the case of the Wallula pilot project, the deepest well drilled within a 6-mi radius of the pilot borehole location is only 915 ft. Because of this lack of subsurface hydrogeologic information, characterization activities at the Wallula pilot borehole were more extensive than normally used at deep boreholes that are situated in more characterized areas. The Wallula pilot borehole represents the first detailed-characterization, reconnaissance-level borehole for deep Columbia River basalt formations within this

region of the State. A discussion of the Wallula pilot borehole drilling, characterization activities, and well completion details is provided in the following sections of the topical report.

Table 2.2 presents a summary and sequence of associated borehole drilling and characterization activities occurring at the Wallula pilot project between January 10 and May 19, 2009.

### **2.3.1 Drilling Program and Well Construction**

Drilling services for the Wallula pilot borehole were provided by Boart Longyear drilling services, based in Salt Lake City, Utah, using a LM-140 rotary drilling rig originally constructed by Lang Drilling Company. Particular attributes of the LM-140 include a top-head drive, with pull-back load-lifting capacity of 140,000 lbs, and drilling rotating torque of 14,000 foot-lbs. It can employ standard or reverse-flood circulation methods and can use a variety of drilling fluids (polymer/bentonite, water, air, foam), all of which meet general standards listed in WAC-173-160-442 and WAC-173-160-444. Drilling was initiated on January 14, 2009, and continued to a depth of 56 ft below ground surface (bgs) using a 24.0-in. diameter drill-bit. A 20-in. diameter surface conductor casing was set to this depth and an annular cement seal emplaced from depth to land surface using a tremie-pipe delivery system. Cementing protocols followed recommended Washington State regulations specified for resource protection well construction/completions (WAC-173-160-420, WAC-173-160-430, and WAC-173-160-450). The borehole was drilled below 56 ft using a 19-in. bit, and continued to a depth of 1108 ft bgs. Conventional circulation using primarily a bentonite-based drilling fluid was used to a depth of 190 ft. Below 190 ft, the reverse-flood drilling method using primarily bentonite-based drilling fluid was employed. A 14-in. diameter casing was welded and installed from land surface to 1108 ft. The casing annulus was sealed with neat cement and State-approved additive accelerants (calcium chloride) using a tremie-pipe delivery system. The borehole was drilled below 1108 ft using a 12.25-in. drill bit, and advanced to a final depth of 4110 ft.

As noted in Tables 2.3 and 2.4, numerous characterization activities were conducted during the process of drilling the borehole section from 1108 to 4110 ft. Preliminary results obtained from these characterization activities are discussed in subsequent report sections. These characterization results were used in selecting the pilot study injection zone, and for the final well-completion design.

As part of the well-completion design, the lower borehole section of the pilot borehole was cemented back to a targeted depth of 2910 ft, using a tremie-pipe delivery system. Near the targeted top of the borehole cement plug, the tremie-pipe system became stuck within the borehole at a depth of 2835 ft. Approximately 1 week of drilling-rig remedial activities (May 1–8, 2009) were required to free the tremie-pipe system from the borehole. Following successful removal of the tremie pipe, spot cement, and drilling slough debris from the borehole, the top of the cement plug was tagged at a depth of 2985 ft. The borehole was circulated clean and the lower borehole cement plug completed to a depth of 2910 ft.

**Table 2.2.** Borehole Stratigraphy of the Wallula Pilot Borehole Well Based on X-Ray Fluorescence Data, Lithology, and Stratigraphic Position. Depths are in feet. The target zone is 2720 to 2875 ft.

Geologic Unit	Depth to Top of Unit, (ft below ground surface)
Surficial Sediment	0
<b>Saddle Mountain Basalt Formation</b>	<b>44</b>
Ice Harbor Member	44
Levy Sedimentary Interbed	140
Elephant Mountain Member	206
Rattlesnake Ridge Interbed	307
Pomona Member	365
Selah Interbed	515
Umatilla Member	527
<b>Wanapum Basalt Formation</b>	<b>1058</b>
Priest Rapids Member	1058
Frenchman Springs Member (FSM)	1135
FSM Flow 1	1135
FSM Flow 2	1256
FSM Flow 3	1328
FSM Flow 4	1449
Vantage Interbed	1588
<b>Grande Ronde Basalt Formation</b>	<b>1594</b>
Sentinel Bluffs Member (SBM)	1594
SBM Flow 1	1594
SBM Flow 2	1755
SBM Flow 3	1838
SBM Flow 4	1932
SBM Flow 5	2010
SBM Flow 6	2085
SBM Flow 7	2139
SBM Flow 8	2250
Winterwater Member	2320
Umtanum Member	2418
Slack Canyon Member (SC)	2590
SC Flow 1	2590
SC Flow 2	2730
SC Flow 3	2808
Ortley Member (OM)	2850
OM Flow 1	2850
OM Flow 2	2940
OM Flow 3	3219
OM Flow 4	3385
Grouse Creek Member (GCM) (tentative ID)	3463
GCM Flow 1	3463
GCM Flow 2	3607
Wapshilla Ridge Member (WRM) (tentative ID)	3810
WRM Flow 1	3810
WRM Flow 2	4068
<b>Borehole – Total Depth</b>	<b>4110.5</b>

**Table 2.3.** Borehole Drilling/Test Activity Log

Test Date	Borehole Activity	Borehole Depth, ft bgs <sup>(a)</sup>	Comments
1/10–14/09	Drilling rig mobilization and site development	--	Arrival of Boart Longyear drilling rig; site preparation provided by Boart Longyear and Boise White Paper
1/14–15/09	Drilling and surface conductor casing installation	56	Borehole drilling initiated 1/14/09 using 24-in. diameter bit; basalt encountered at a depth of 44 ft; 20-in. surface conductor casing set 0–56 ft and casing annulus cemented to land surface
1/15–29/09	Drilling of 19-in. diameter borehole	56–1108	Drilling of 19-in. diameter borehole using primarily conventional circulation and bentonite-based drilling fluid; reverse-flood circulation used below a depth of 190 ft
1/29–2/5/09	Installation/cementing of 14-in. diameter casing	0–1108	14-in. diameter welded casing set 0–1108 ft, and casing annulus cemented to land surface using tremie-pipe delivery system
2/5–2/7/09	Drilling of 12.25-in. diameter borehole	1108–1474	Drilling of 12.25-in. diameter borehole using the reverse-flood circulation method and using primarily water as drilling circulation fluid
2/7–14/09	Zone 1 characterization	1108–1474	High capacity hydrologic tests conducted for Boise White Paper aquifer storage project; hydrochemical and microbiological sampling
2/14–17/09	Drilling of 12.25-in. diameter borehole	1474–1814	Drilling of 12.25-in. diameter borehole using the reverse-flood circulation method and using primarily water as drilling circulation fluid
2/17–21/09	Zone 2 characterization	1700–1814	Baski borehole packer/pressure probe test system used to isolate test zone; see Table 2.2 for characterization summary
2/21–27/09	Drilling of 12.25-in. diameter borehole	1814–2345	Drilling of 12.25-in. diameter borehole using the reverse-flood circulation method and using primarily water as drilling circulation fluid
2/27–3/2/09	Zone 3 characterization	1895–2345	Baski borehole packer/pressure probe test system used to isolate test zone; see Table 2.2 for characterization summary
3/2–7/09	Drilling of 12.25-in. diameter borehole	2345–2798	Drilling of 12.25-in. diameter borehole using the reverse-flood circulation method and using primarily water as drilling circulation fluid
3/7–3/10/09	Zone 4 characterization	2516–2798	Baski borehole packer/pressure probe test system used to isolate test zone; see Table 2.2 for characterization summary
3/10–18/09	Drilling of 12.25-in. diameter borehole	2798–3279	Drilling of 12.25-in. diameter borehole using the reverse-flood circulation method and using primarily water as drilling circulation fluid
3/18–20/09	Zone 5A characterization Zone 5B characterization	3159–3279 2910–3279	Baski borehole packer/pressure probe test system used to isolate test zones; see Table 2.2 for characterization summary
3/20–4/7/09	Drilling of 12.25-in. diameter borehole	3279–4110	Drilling of 12.25-in. diameter borehole using the reverse-flood circulation method and using primarily water as drilling circulation fluid



**Table 2.3.** (contd)

Test Date	Borehole Activity	Borehole Depth, ft bgs <sup>(a)</sup>	Comments
4/7–16/09	Zone 6A characterization Zone 6B characterization Zone 6C characterization	3340–4110 3700–4110 3510–4110	Baski borehole packer/pressure probe test system used to isolate test zones; see Table 2.2 for characterization summary
4/16–18/09	Zone 7 characterization	2698–4110	Baski borehole packer/pressure probe test system used to isolate test zone; see Table 2.2 for characterization summary
4/18–4/19	Detailed wireline geophysical survey	1108–4110	Detailed wireline geophysical survey suite of open borehole section conducted by Schlumberger, Inc.
4/20–24/09	Zone 8A characterization Zone 8B characterization	2790–2913 2688–2913	Baski borehole packer/pressure probe test system and underlying Weatherford bridge plug packer used to isolate test zone; see Table 2.2 for characterization summary
4/25/09	Caprock characterization Zone 9	2668–2708	Baski borehole packer/pressure probe test system and underlying Weatherford bridge plug packer used to isolate test zone; see Table 2.2 for characterization summary
4/26–27/09	Caprock characterization Zone 10A Zone 10B	2460–2563 2510–2563	Baski borehole packer/pressure probe test system and underlying Weatherford bridge plug packer used to isolate test zone; see Table 2.2 for characterization summary
4/28–29/09	Wireline geophysical survey	1108–4110	Televiewer survey conducted by Stoller Corporation
4/29–5/1/09	Borehole plug-back cementing	2985–4110	Lower borehole section cemented back to a depth of 2998 ft using tremie-pipe delivery system; tremie-pipe inadvertently stuck within borehole at a depth of ~2835 ft
5/1–8/09	Remedial well completion activities	2910–2985	Remedial activities were successful in removing the stuck tremie-pipe from the borehole at a depth of 2835 ft; borehole cleaned and cement seal tagged at a depth of 2985; plug-back cementing continued to a depth of 2910
5/8–11/09	Well completion activities	0–2910	Well completion activities included: installation of a protective sand/gravel layer between 2716 and 2910 ft; and installation of 7-in. diameter casing between 0 and 2716 ft
5/11–15/09	Well casing cementing	0–2716	7-in. diameter casing annulus cemented to land surface using tremie-pipe delivery system
5/15–18/09	Test zone development	2716–2910	Protective sand and gravel layer between 2716 and 2910 ft removed by air-lifting; test zone developed using the air-lift pumping method
5/18–19/09	Site demobilization	--	Boart/Longyear removed drilling rig and support equipment from the site
(a) ft bgs = feet below ground surface; ground-surface elevation = 363.99 ft above mean sea level; NAVD 88 (Note: final vertical well survey conducted following well completion).			

**Table 2.4.** Test Zone Characterization Activity Log

Test Date	Characterization Activity	Test Interval Depth, ft bgs <sup>(a)(b)</sup>	Formation	Comments
2/7–14/09	<b>Zone 1</b> hydrologic testing hydrochemical and microbiological sampling	1108–1474	Wanapum Basalt	High capacity hydrologic tests conducted for Boise White Paper aquifer storage project; tests included a 3-stage, step-drawdown test and a ~24-hr constant-rate pumping test and recovery
2/17–21/09	<b>Zone 2</b> wireline geophysics hydrologic testing hydrochemical and microbiological sampling	1700–1814	Grande Ronde Basalt	Wireline geophysics conducted by Stoller Corporation; hydrologic tests included slug tests, and ~21-hr constant-rate pumping test and recovery
2/27–3/2/09	<b>Zone 3</b> wireline geophysics hydrologic testing hydrochemical and microbiological sampling	1895–2345	Grande Ronde Basalt	Wireline geophysics conducted by Stoller Corporation; hydrologic tests included slug tests, and ~19-hr constant-rate pumping test and recovery
3/7–3/10/09	<b>Zone 4</b> wireline geophysics hydrologic testing hydrochemical and microbiological sampling	2516–2798	Grande Ronde Basalt	Wireline geophysics conducted by Stoller Corporation; hydrologic tests included slug, DST, and ~27-hr constant-rate pumping test and recovery
3/18–19/09	<b>Zone 5A</b> wireline geophysics hydrologic testing	3159–3279	Grande Ronde Basalt	Wireline geophysics conducted by Stoller Corporation; due to extremely low groundwater production conditions, testing was suspended
3/19–20/09	<b>Zone 5B</b> hydrologic testing	2910–3279	Grande Ronde Basalt	Hydrologic tests included slug and pulse tests
4/7–14/09	<b>Zone 6A</b> wireline geophysics hydrologic testing hydrochemical and microbiological sampling	3340–4110	Grande Ronde Basalt	Wireline geophysics conducted by Stoller Corporation; hydrologic tests included slug, DST, and ~94-hr cyclical pumping test and recovery
4/14–15/09	<b>Zone 6B</b> hydrologic testing	3700–4110	Grande Ronde Basalt	Hydrologic tests included slug and pulse tests
4/15–16/09	<b>Zone 6C</b> hydrologic testing	3510–4110	Grande Ronde Basalt	Hydrologic tests included slug and DST tests
4/16–18/09	<b>Zone 7</b> hydrologic testing	2698–4110	Grande Ronde Basalt	Hydrologic tests included slug and DST tests and ~6 hr cyclical pumping test
4/20–22/09	<b>Zone 8A</b> hydrologic testing	2790–2913	Grande Ronde Basalt	Hydrologic tests included a slug and DST test

**Table 2.4. (contd)**

Test Date	Characterization Activity	Test Interval Depth, ft bgs <sup>(a)(b)</sup>	Formation	Comments
4/22–24/09	<b>Zone 8B</b> hydrologic testing hydrochemical sampling	2688–2913	Grande Ronde Basalt	Hydrologic tests included slug, DST and ~15-hr cyclical pumping test and recovery
4/25/09	<b>Zone 9</b> caprock hydrologic testing	2668–2708	Grande Ronde Basalt	Low-permeability, multistep constant-pressure injection test
4/26/09	<b>Zone 10A</b> caprock hydrologic testing	2460–2563	Grande Ronde Basalt	Low-permeability, multistep constant-pressure injection test
4/27/09	<b>Zone 10B</b> caprock hydrologic testing	2510–2563	Grande Ronde Basalt	Low-permeability, multistep constant-pressure injection test

(a) ft bgs = feet below ground surface; ground-surface elevation = 363.99 ft above mean sea level; NAVD 88 (Note: final vertical well survey conducted following well completion).

(b) Upper test interval depth indicative of top of packer depth setting or well casing depth; lower test interval depth indicates either bottom of borehole at the time of testing (for Zones 1 through 7) or top of lower bridge plug packer (for Zones 8 through 10). Note: top packer = 4.5 ft in length.

DST = drill-stem test.

Following completion of the plug-back cementing from 4110 to 2910 ft, a protective sand/gravel layer was installed over the targeted open-well completion depth interval 2716 to 2910 ft. Following installation of the protective sand/gravel layer, 7-in. diameter casing was installed from land surface to 2716 ft. The 7-in. casing annulus was sealed with neat cement and State-approved additive accelerants (calcium chloride) using a tremie-pipe delivery system. Following successful sealing of the 7-in. casing, the protective sand and gravel layer was removed using the air-lift method, and the 194-ft open-well/test zone interval between 2716 and 2910 ft was developed using the air-lift pumping technique. This final test zone development marked the end of well completion activities and Boart Longyear demobilized from the Wallula pilot location on May 19, 2009.

### 2.3.2 Stratigraphy and Geochemical Sampling

This section provides a discussion and summary characterization of the rock data collected from the basalt pilot well, including rock cuttings, geologist descriptions, and rotary sidewall cores. The reverse circulation drilling method produced optimal cuttings sizes for observation of important textural rock characteristics. Onsite geologists collected rock cuttings every 10 ft (more frequently in zones of interest), and following written, standardized procedures (Bjornstad 2009), recorded macroscopic and microscopic lithology descriptions, as well as degree of fracture surfaces observed. The geologist's log is in Appendix A.1.

Basalt cutting samples taken at key points in drilling and sent to Eastern Washington University in Washington State for X-ray fluorescence (XRF) analyses provided whole rock geochemistry and stratigraphic control for the well. Interpretation of the wellbore data indicates that no faults were cut within the well, and that the stratigraphic level at total depth (4110 ft) is within the Wapshilla Ridge 1 basalt flow (Table 2.2).

Deviation surveys taken when total depth was at 1800 ft and again from 4110 ft to the surface show that the wellbore remained vertical with a deviation of 0.52 degrees with an azimuth of 118.4 degrees (east-southeast) at 1800 ft; at a total depth of 4110 ft, the bottom hole location was at a lateral distance of 50 ft from the top, with an azimuth of N50° east.

Thirty-two rotary sidewall cores (Figure 2.6) were cut between 4110–1542 ft and are listed in table format in Appendix A.2. The field print of the Formation Micro Imager (FMI) log (resolution about 1/8 in.) was used to determine precise intervals to be cored. This resulted in an increased success rate on retrieving cores, as researchers were able to avoid vugs, cavities, and severe washouts. This technique also allowed researchers to more precisely sample a wide variety of basalt lithofacies (Figure 2.7). Depths of the cores in and proximal to the injection zone are shown in Figure 2.8; 3 out of 35 selected coring targets were abandoned because of borehole rugosity, or continued breakage of core during drilling. The sidewall core samples are awaiting analysis that will include thin section petrography. Preliminary petrographic analysis of thin sections from well cuttings indicates the basalt lithologies are dominated by plagioclase, augite, and glassy mesostasis. Hematite is one of the few accessory minerals. Vein, fracture, and vesicle filling materials include calcite and quartz (several crypto-, micro-, and mega crystalline forms). The most common alteration products, as determined from X-ray diffraction (XRD) and megascopic identification are illite, zeolites, clinoptilolite, and celadonite. Pyrite is also locally present.



**Figure 2.6.** Rotary Sidewall Core Samples Shown as They were Examined at the Wellsite. Field print of the FMI allowed precise targetting of core samples.

Previous detailed study and mapping of the Columbia River flood-basalts has resulted in the establishment of stratigraphic units that can be reliably identified and correlated on a regional basis (see Reidel et al. [2002] for a discussion and important references). The CRBG has been divided into six formal formations in ascending stratigraphic order: the Imnaha, Grande Ronde, Prineville, Picture Gorge, Wanapum, and Saddle Mountains Basalts.

CRBG units are identified and mapped in outcrop using a combination of lithology, paleomagnetic properties, and geochemical composition in regards to superposition, but borehole samples are not easily identified using only these techniques. Additional major and minor oxides, and trace and rare earth elements provide the key data, with  $\text{TiO}_2$ ,  $\text{P}_2\text{O}_5$ , Cr, MgO, Zr, and Ba being the most diagnostic elements to consider. The most definitive identification technology of discrete basalt sub-groups, formations, members and individual flows is the high-precision, rapid analysis of major and trace elements by XRF analysis. The GeoAnalytical Laboratory at Washington State University provided the high-quality analyses that are the standard for identification of CRBG flows. The analytical and sample preparation techniques are described in Johnson et al. (1999).

A major reason that CRBG geochemical stratigraphy is possible on a regional scale is due to the remarkable “bulk” geochemical homogeneity of individual CRBG eruptions despite their huge volumes and great distances traveled. Typically, a single sample will identify a flow, but when a known compositional variation exists in a flow (Reidel 2005), several samples may be required.

Major distinctions occur between the three basalt formations. The Saddle Mountains Basalt Formation is the youngest set of flows and typically has a much wider and diverse range of geochemical composition than the two older CRBG formations. Flows of the Wanapum Basalt typically will have higher  $\text{TiO}_2$  than the Grande Ronde Basalt. Grande Ronde Basalt members, which are our sequestration target, display a relatively narrow range of geochemical compositions that typically exhibit small, but significant, variations in  $\text{TiO}_2$ ,  $\text{P}_2\text{O}_5$ , Cr, and MgO. The XRF geochemistry data used to establish the wellbore stratigraphy are in Appendix A.3.

### 2.3.3 Wireline Geophysics

Two companies performed wireline logging activities at the pilot borehole. Stoller Corp., a local logging company that accommodated the logging schedule driven by drilling and geologic conditions, conducted a sonic-based cement bond log across the shallow 14-in. casing from 1108 ft to surface, as well as a cement bond log across the 7-in. casing from 2720 ft to surface. Stoller Corp. also collected data in five logging runs in the deeper, 12-1/4-in. open borehole over separate logging intervals. Gamma,

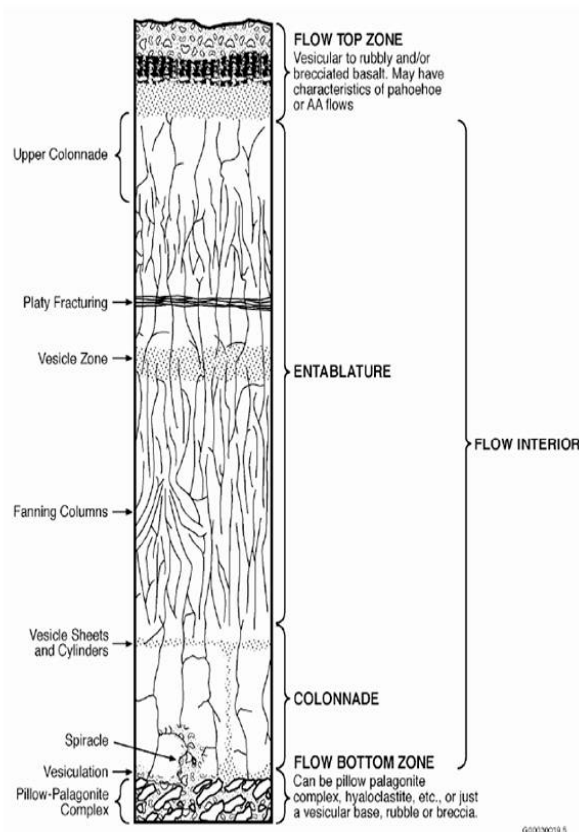


**Figure 2.7.** Structures of a Single Idealized Flood Basalt Flow

spontaneous potential (SP), four-arm caliper, dipole sonic, and resistivity data were acquired as needed to determine rock quality and select competent rock intervals for seating the down-hole packer tool for hydrologic tests. These logs were run from 1108 ft to borehole total depth (TD) of 4110 ft. An acoustic borehole imager was run from TD to 1108 ft to allow evaluation of data gathered through acoustic-based imaging and resistivity-based imaging. All tools performed well; caliper, resistivity and sonic instruments were especially helpful in picking unfractured intervals for seating the packer. To protect against aquifer cross-flow, and to prevent drilling complications from possible borehole instability, no open-hole wireline logs were acquired above 1100 ft.

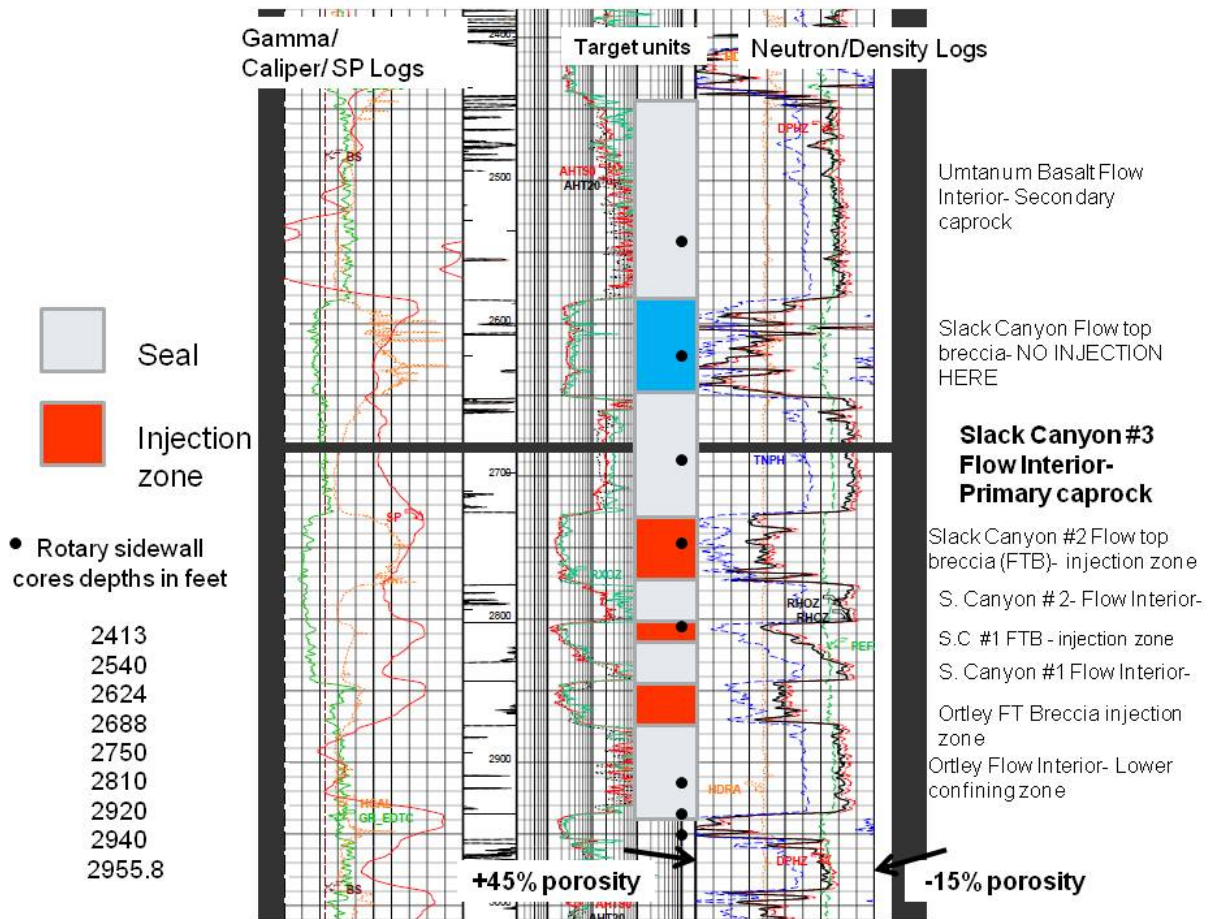


**Figure 2.8.** Schlumberger Platform Express Logs Through the Proposed Injection Zone. Note on this display, porosity increases to the left. The thermal neutron curve is thermal neutron porosity and the density porosity is on channel DPHZ. Other acronyms are in Schlumberger logs in Appendix B.

The most important element of the Stoller Corp. log data for progressing with permitting activities are the cement bond logs. Acoustic cement bond logs can be interpreted as percent of cement behind casing. Acoustic signals propagated in steel casing have large amplitude in free casing because much of the energy is retained in the casing. The opposite effect is found in casing that is in contact with a solid such as cement. The signal from the casing is much smaller because the acoustic energy is coupled into the surrounding cement and formation.

Cement bond logs generated by Stoller Corp. (Appendix B.1) indicate that in the shallow 14-in. casing, there is less than 50% cement bond over several of the sedimentary interbeds of the Ellensburg Formation. This is consistent with washout and some loss of circulation experienced while drilling these beds. The cement bond log indicates these intervals are separated by intervals that have 95% to 100% bond. The bond is consistently higher below a depth of about 950 ft. The bond for the 7-in. casing is consistently high, at or near 100% bond except in rare, isolated 4- to 6-ft intervals that have 95% bond. Only in one short, isolated interval from 2392 to 2398 ft does the bond go below 90%. Thus, the sedimentary beds of the Ellensburg Formation appear to be isolated from each other and from the deeper basalts flow tops.

Schlumberger Wireline Services acquired the open-hole logs that required sealed source neutron logging and heavier tool strings of combined tools. The complete list of Schlumberger Wireline Services is as follows:

- Platform Express with Array Induction Imager Tool
- Elemental Capture Spectroscopy (ECS) log
- Reservoir Saturation Tool: Sigma Saturation Mode
- Fluid temperature log
- Sonic scan including SonicScanAdvancedAnswer, anisotropy analysis, P/S compression and shear with summary interpretation
- FMI with summary fracture interpretation over 1600 ft of interval
- Rotary sidewall cores.

Schlumberger Wireline Services' open-hole caliper, gamma, SP, photoelectric cross-section, array induction, neutron, density, pulsed neutron sigma, and full waveform sonic logs were run from total depth of 4110 ft up into the shallow casing to a depth of 950 ft. The gamma, thermal neutron, and full waveform sonic logs continued inside the 14-in. casing to the surface. The FMI resistivity-based image log was run from 4110 ft to the base of the shallow casing; however, for budgetary reasons, the log was processed only up to 2000 ft. The remaining data can be processed at any time as needed.

The borehole was drilled with water rather than drilling mud to protect fracture porosity and prevent borehole damage due to invasion of fines. This resulted in washout zones when brecciated flow tops occurred above dense basalt flow interiors. Although neutron and density logs do not give reliable measurements in these zones, sonic logs—when calibrated with core-based acoustic measurements—may ultimately provide more reliable measures of porosity. Hydrologic testing data provide additional constraints on the borehole data in these zones.

Porosity was measured with the thermal neutron, density and sonic tools, and tied to basalt lithofacies and structure through image logs. All porosity and permeability displays on these preliminary logs are uncalibrated, and were not used in calculating injectivity, transmissivity, or storage capacity within the targeted composite injection zone. The matrix values for density, neutron, and sonic porosity will be calibrated with laboratory data from the rotary sidewall cores or from core material from equivalent formations at the Hanford Site. However, even in this early stage of evaluation, the log signatures provide important clues for identification of basalt lithofacies. Both uncalibrated cross-plot



density/neutron porosity and sonic porosity are essentially zero in the massive basalt flow interiors, and range from 0% to 3% in the entablature zones (Figure 2.7). In zones of washout in the brecciated flow tops, the neutron-density porosity will be less reliable, even when calibrated to core (see Figure 2.8, where the thermal neutron curve is labeled TNPHI and the density porosity is labeled DPHZ). Uncalibrated sonic porosities are from 15% to 30% in the brecciated flow tops; and from 15% to 25% in the proposed injection zones (Figure 2.9). The Platform Express log is attached as Appendix B.2; the Sonic Scanner log is Appendix B.3. A preliminary montage of Schlumberger logs is included in Appendix B.4.

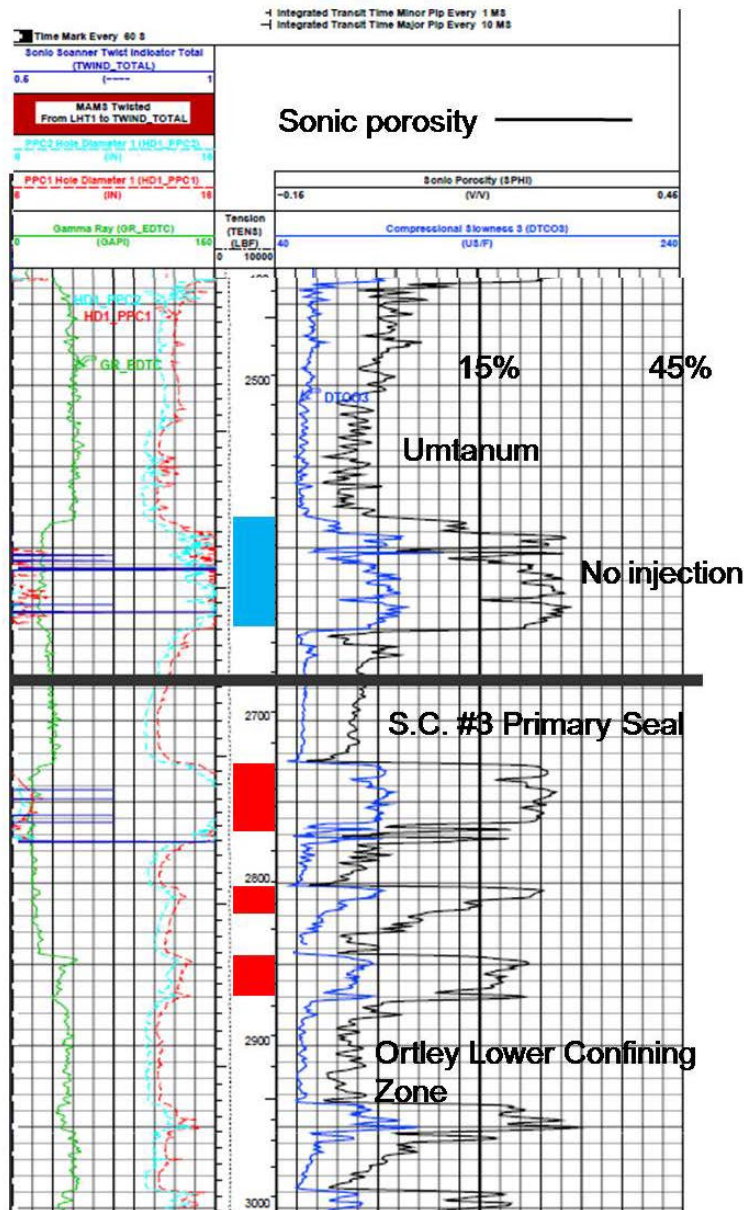


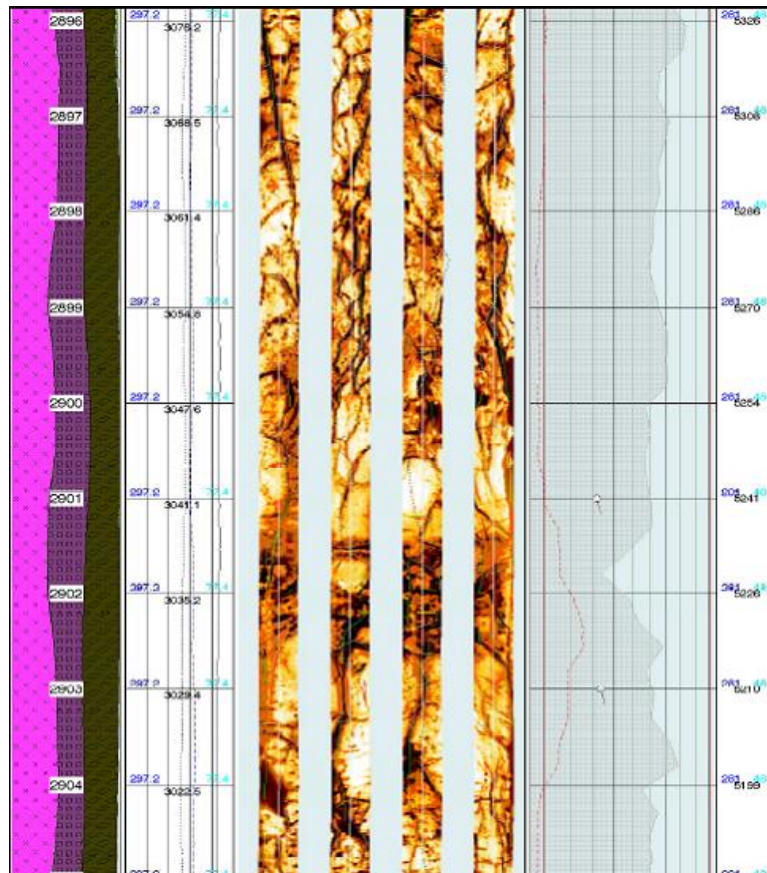
**Figure 2.9.** Sonic Porosity Log over the Seals and Injection Zones. Note on this display, uncalibrated porosity (black curve) increases to the right. Red indicates proposed injection zones. Blue is the Slack Canyon #3 flow top, below the base of the Umtanum Basalt Flow.



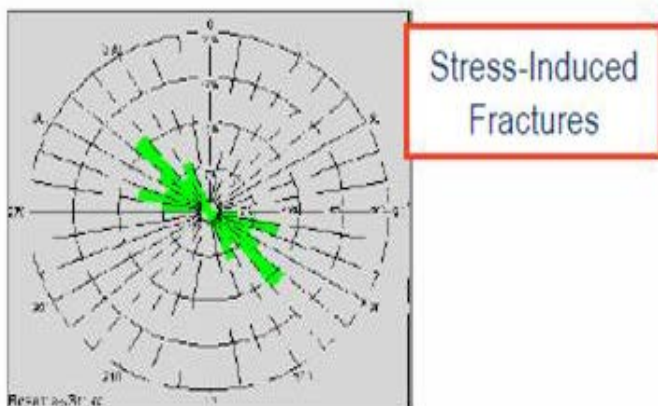
Resistivity-based image logs provide both structural and stratigraphic data, as well as input for seating packers for hydrologic testing, and selecting precise intervals for cutting rotary sidewall cores. Additional remarks on acoustic and resistivity-based image logs are included in Appendix B. The following section provides structural information.

Image logs provide important data on the horizontal components of stress tensors near the borehole through analysis of borehole breakout and drilling induced fractures (Tingay et al. 2008). Borehole breakout refers to the compressive-stress induced spalling and enlargement of the borehole cross-section; spalling is greatest in the direction of the horizontal component of minimum compressive stress ( $S_h$ ). Thus, the long axis of borehole breakout is roughly perpendicular to the horizontal component of maximum compressive stress ( $S_H$ ).

Image logs can aid in the identification of drilling induced fractures. Drilling induced fractures, in contrast to borehole breakout features, are caused by tensile failure of the borehole wall and typically develop as short, narrow fractures that are sub-parallel or slightly inclined to vertical (Figure 2.10), as “centerline” fractures. Drilling induced fractures may cause minor spalling, but do not usually result in borehole enlargement. The stress concentration around a vertical borehole is at a minimum in the  $S_H$  direction. Thus, drilling induced fractures are parallel to the horizontal component of maximum stress or approximately parallel to the  $S_H$  orientation.



**Figure 2.10.** Drilling Induced Fractures Above 2900 ft in the Wallula Pilot Borehole, as Imaged by the FMI Log. Natural, short platy cooling fractures are also present.



**Figure 2.11.** Northwest-Southeast Oriented Stress-Induced Fractures in the Wallula Pilot Borehole, as Tabulated from the FMI Log. North (zero degrees) is at the top of the circle. These data approximate the azimuth of the horizontal component of maximum compressive stress ( $S_H$ ).

Evidence of borehole breakout is observed in image logs by two opposite quadrants of the image log having a darker image. No borehole breakout was observed in the image logs from the Wallula Pilot borehole. In contrast to the lack of breakout, drilling induced fractures are common, and are strongly oriented northwest-southeast (Figure 2.11). The induced fractures are parallel to the horizontal component of maximum stress or approximately parallel to the  $S_H$  orientation, indicated by the FMI data to be northwest-southeast. Further analysis of these data will be conducted to determine formation-specific differences in maximum horizontal stress tensor. A copy of the FMI is attached as Appendix B.5.

Natural tectonic fractures are generally easy to identify in the image logs from the Wallula pilot borehole (Figure 2.12) by their distinct, high dip, sinusoidal low resistive curves that cross the entire borehole. Note the high density of vesicles in this example. Green sinusoid lines are interpreted as basalt flow features; these flows dip to the west at about 20 to 30 degrees. Flow stress features are seen in the elongation of some of the larger vesicles. The natural fractures are dipping to the northeast and striking northwest-southeast.

Natural fractures are common in the Wallula pilot borehole. The majority are cooling joints and short irregular fractures that do not appear to be permeable. Tectonic natural fractures in the Wallula borehole strike dominantly parallel to the horizontal azimuth of maximum stress (Figure 2.13). The tectonic fractures that are parallel to  $S_H$  are more likely to be open and transmissive than fractures not parallel to  $S_H$  (Zoback 1999).

Analysis of the P and S modes of the full waveform sonic log data is in progress and will be calibrated and integrated with the FMI data to yield more detail on Young's modulus, Poisson's ratio, and other geomechanical properties of the basalts. Of particular interest is the azimuth of the fast shear mode, which is parallel to maximum stress, and does not depend on calibration with matrix velocities to yield azimuthal data on stress tensors. Preliminary analysis by Schlumberger indicates two directions of the fast shear mode. One direction is approximately N45°W, in agreement with the drilling induced and tectonic fracture orientation. The other major orientation of the fast shear is east-west, and is in agreement with the azimuth of the short fracture segments that appear to be cooling and basalt flow features. These data may reflect stresses related to basalt emplacement and cooling (Figure 2.14).

Structural dip is about two degrees to the northwest, but is prominently overprinted by a stratigraphic dip of the basalt flow structures. Dips shown in the Schlumberger computer-generated facies model (Figure 2.15) integrate several wireline logs with the image log to discriminate facies and structure. Dip reversals are shown in the right-hand track for the interval from 2500 to 3400 ft.

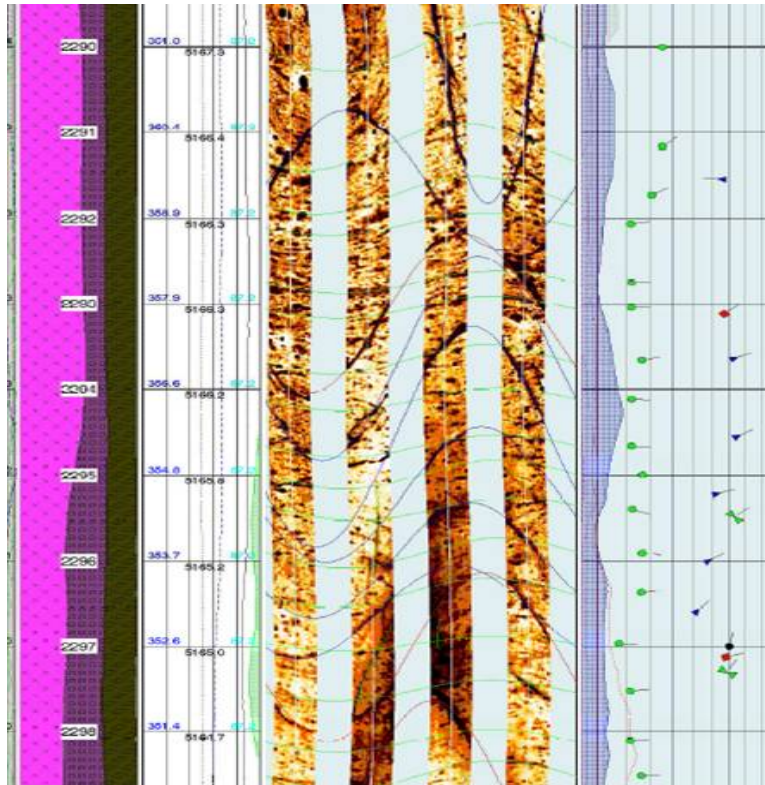


**Figure 2.12.** Natural Fractures in a Highly Vesicular Zone in the Wallula Pilot Borehole

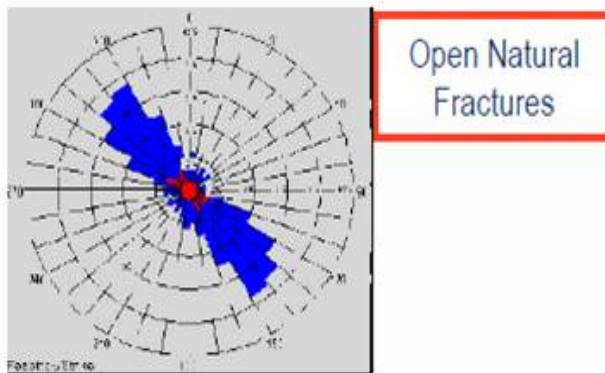


**Figure 2.13.** Rose Plot of Azimuth of Natural Fractures as Determined from the FMI Log. North (zero degrees) is at the top of the circle.

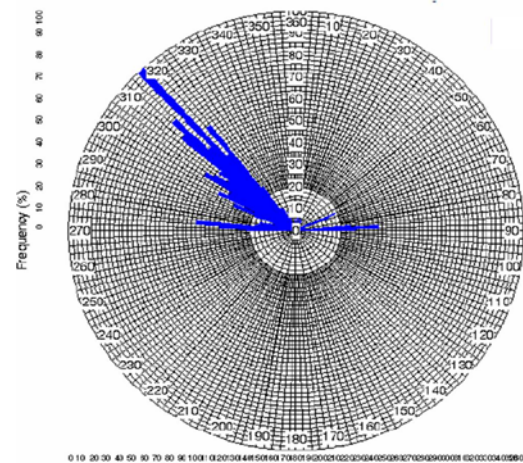


**Figure 2.14.** Rose Plot of Fast Shear Azimuth from the Full Waveform Sonic. North (zero degrees) is at the top of the circle. East-west azimuth may be related to flow emplacement.



Facies and dips are plotted against borehole depth in the left track. The center image is the resulting model with the borehole intersected by a line representing the point of maximum dip reversal. Examination of the image log indicates this dip reversal is stratigraphic rather than fault related. If any faults exist in the well, they would have to have extremely low throw or be parallel to bedding planes.

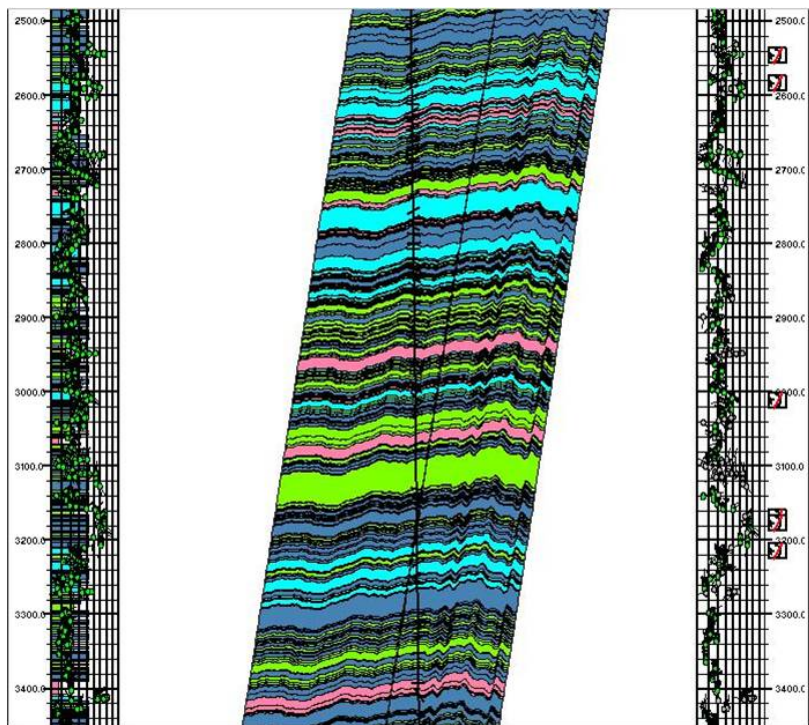


**Figure 2.15.** Computer Generated Facies Model Based on Bedding Dips Interpreted from the FMI. These data were combined with other log data to determine basalt “facies.”

Logging data combined with XRF stratigraphy indicate there are no major faults in the well. In particular, image log analysis indicates that dip reversals are stratigraphic rather than caused by faults (Figure 2.15). Regional structural dip, as interpreted by Schlumberger, is two degrees to the northwest; stratigraphic dips are commonly 10 to 30 degrees, vary considerably in azimuth and magnitude, and appear to be related to basalt emplacement.

An analysis of drilling induced fractures yields the horizontal azimuth of maximum earth stress. Borehole breakout was insufficient to yield a borehole signature. Tectonic fractures (natural fractures) dip northeast and strike northwest-southeast. Fractures with this northwest-southeast azimuth may be transmissive but do not represent large storage volumes.

Shallow sedimentary interbeds of the Ellensburg Formation correlated well with regional data; the 6-ft thick Vantage clay interbed between the Wanapum and the Grande Ronde Formation was the lowest recognized regional sedimentary marker. Although several of the sedimentary interbeds behind the 14-in. casing are marked by washouts and poorer cement bond, relatively good cement bond exists below the interbeds and over the basalts that separate the interbeds.

Basalt lithologies are dominated by plagioclase and augite. Vein and vesicle filling materials include calcite and quartz (a variety of crypto-, micro-, and mega-crystalline forms); the most common alteration products—as determined from XRD and megascopic identification—are illite, zeolites, clinoptilolite, and celadonite. Pyrite is also locally present. Flow top breccias in the Grande Ronde qualitatively appear to contain more abundant alteration products than are present in flow tops of the more shallow basalts. The demonstration of regional correlation of flows by minor element geochemistry and determination of a robust basalt stratigraphy was one of the most fundamental activities involved in characterizing the Wallula pilot borehole.

Establishing the stratigraphic controls on reservoir and seal potential included the subsurface verification of formation differences observed in outcrop. In particular, thin pahoehoe flows in outcrops of the Wanapum are typically oxidized, with porous flow tops. In contrast, outcrops of the older Grande Ronde flows generally contain thicker, denser flows and fewer flow top breccias. This same pattern was observed in the subsurface. In addition, the Grande Ronde flows in the Wallula well contained fewer and thinner flow top breccias than the Grande Ronde in the Shell 1-10 Darcell Gas Exploration Well about 20 mi to the northeast (Figure 2.16). The decreased number and thickness of flow top breccias in the Grande Ronde at the Wallula site may be related to the formation of inflated lava flows (forming a lava lake) that thicken from immediately east of the Wallula well and westward into the Pasco Basin. Resistivity-based image logs in the lower part of the well contain features consistent with the flow of partially solidified lava within a thick, massive unit. Feeder dikes for the Grande Ronde outcrop to the east of Wallula, and gravity modeling conducted in association with characterization of the Wallula site suggests less depth to basement to the east, compatible with deposition as thin, hot flows that are less likely to form deep lava pools and are more likely to develop multiple brecciated tops.

### 2.3.4 Hydrologic Testing

As discussed in the *Wallula Pilot Field Activity Plan* (Spane et al. 2008), the primary objectives of the borehole test characterization program were to identify and characterize a suitable basalt interflow zone for a subsequent CO<sub>2</sub> injection (subject to Washington State Department of Ecology approval) field pilot study. General hydraulic property criteria for injection zone selection include Grande Ronde basalt interflow zones below ~2400 ft, having sufficient thickness ( $\geq 30$  ft), permeability ( $k \geq$  approximately 500 millidarcies at standard temperature and pressure), effective porosity ( $n_e \geq$  approximately 0.1), and composite, overlying caprock thicknesses ( $\geq$  approximately 100 ft). The depth selection criterion (i.e., shallowest acceptable reservoir horizon) is based on facilitating the possible geophysical monitoring and imaging of the CO<sub>2</sub> injected as a supercritical fluid. In addition, groundwater within the targeted interval was required to have elevated fluoride concentrations that would exceed the secondary and primary drinking water standards of 2.0 and 4.0 mg/L, respectively, as a potable water supply.

As previously discussed, hydrogeologic information was obtained primarily during borehole drilling/advancement using the progressive *drill-and-test* characterization strategy. This requires use of a downhole packer test system conveyed by a test tubing string to isolate the underlying test zone from the overlying open borehole section. The borehole test system used for the Wallula pilot hydrologic testing program was primarily manufactured by Baski, Inc. and included the following test components:

- Inflatable packer and associated packer inflation chamber for test zone isolation
- Downhole, temperature-compensated pressure transducers for test zone monitoring (both real-time and memory gauges)

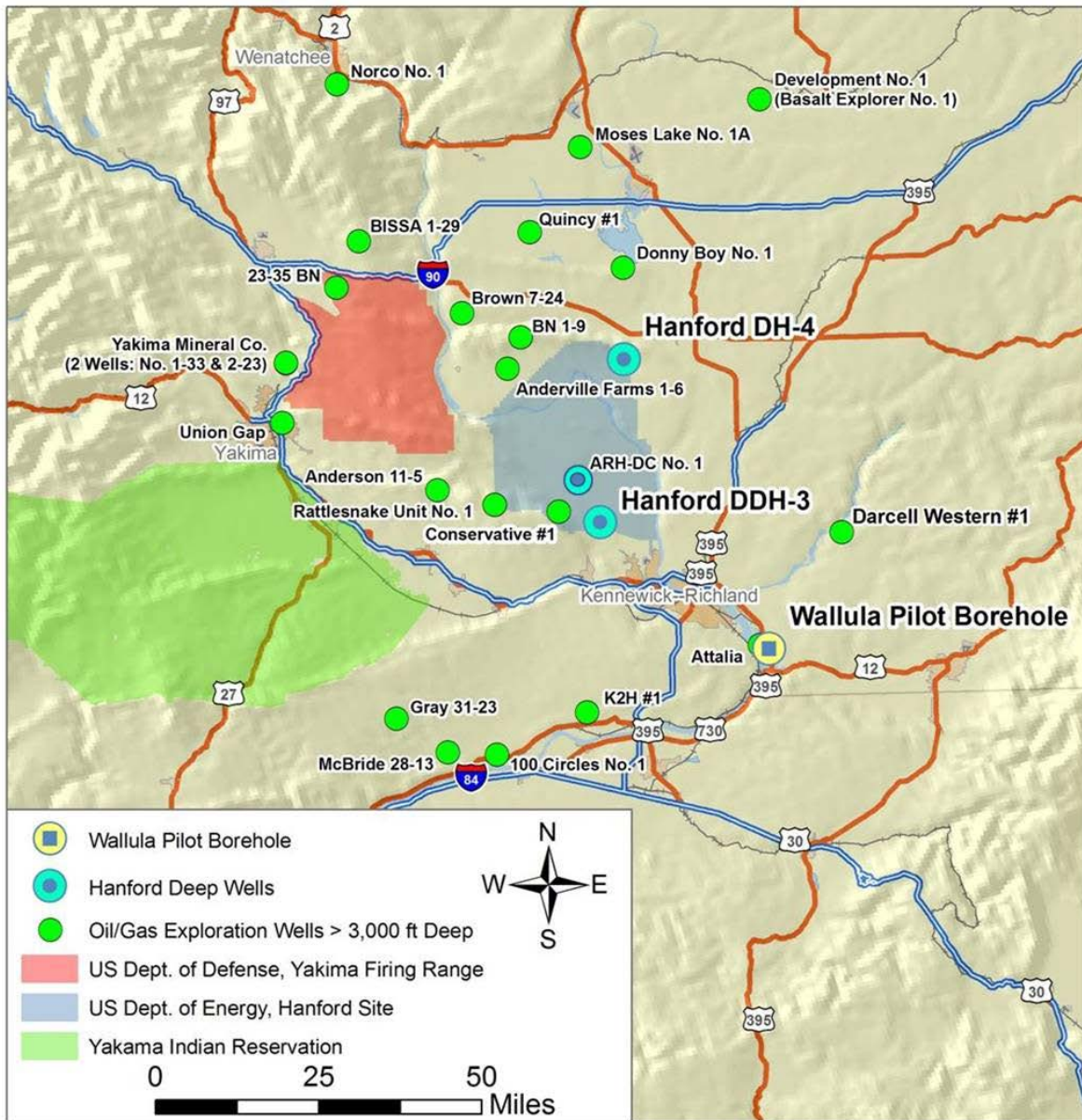


**Figure 2.16.** Location of the Shell 1-10 Darcell Gas Exploration Well and Other Deep Wells in the Region

- Downhole, pneumatic shut-in tool for test zone isolation
- Multiline, flat-pack cable (for packer inflation, shut-in tool operation, and real-time pressure transducer monitoring)
- Flat-pack cable power winch and reel (for cable deployment)
- Test tubing-string to convey the downhole test system to the test zone depth
- Regulated compressed nitrogen bottles for packer inflation and shut-in tool manipulation.

Figure 2.17 shows the as-built completion information for the Wallula pilot borehole and Figure 2.18 shows a schematic of the deployment of the downhole test system during borehole advancement. Data were collected during testing using manufacturer provided software, and were examined and stored on a field laptop computer. Hydrologic stresses imposed as part of the characterization process were produced using a downhole submersible pump within a cross-over, expanded section of the test tubing string, as illustrated in Figure 2.19. Isolation integrity of the test zone was evaluated by loading the annular zone above the inflated packer and between the test tubing string and 14-in. diameter casing with water at the beginning and end of each test zone characterization period, and observing test interval response with the real-time downhole pressure probe system. Hydraulic communication was detected only once following packer inflation for test zone isolation. This was corrected by repositioning the packer seat location a short distance along the borehole.

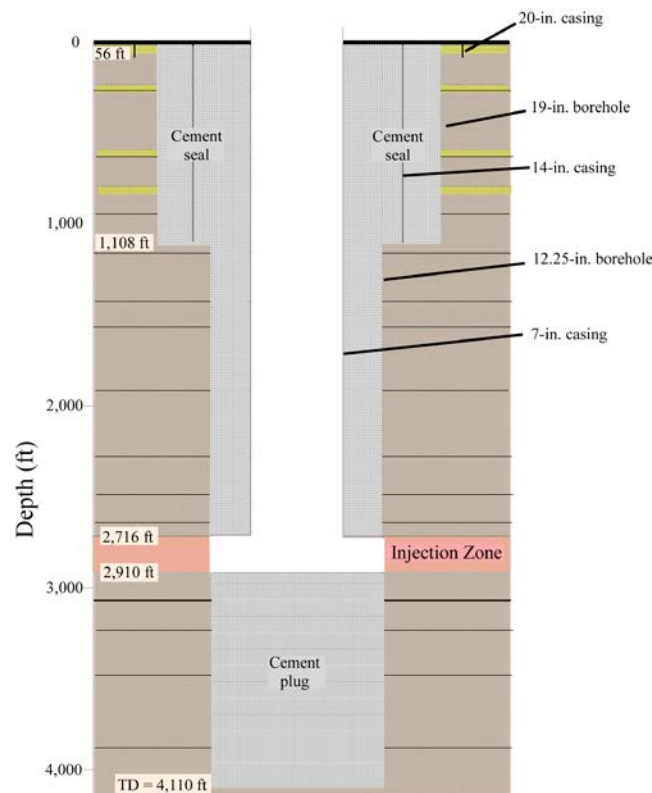


**Figure 2.17.** As-Built Completion for the Wallula Pilot Borehole

In all, six interflow test zone characterizations were conducted during active borehole advancement (Zones 1 through 5B). Immediately following completion of drilling activities, four additional interflow zones were characterized (Zones 6A, 6B, 6C, and 7) using the same downhole test system deployment used during borehole advancement. This was accomplished by simply repositioning the packer test system and sequentially characterizing different composite test sections within the lower section of the borehole. Based on the comparative results of these 10 test interval characterizations, a candidate injection test zone was identified between ~2716 and 2870 ft. To support quantitative characterization of this specific test interval, and to isolate this zone from the underlying open borehole section, a Weatherford bridge plug packer was set separately at a depth of 2913 ft.



A downhole memory pressure gauge was attached below the bridge-plug packer for assessing test zone isolation during this hydrologic test characterization phase. Two test sections were characterized sequentially within this identified candidate injection zone depth interval by repositioning the overlying downhole test system (Zone 8A: 2790 to 2913 ft; Zone 8B: 2688 to 2913 ft). As will be discussed in Section 2.3.4.1, Zone 8A contains only a minor amount of the composite test zone (Zone 8B) transmissivity. The majority of the test zone transmissivity occurs between the depth interval of 2688 and 2790 ft.

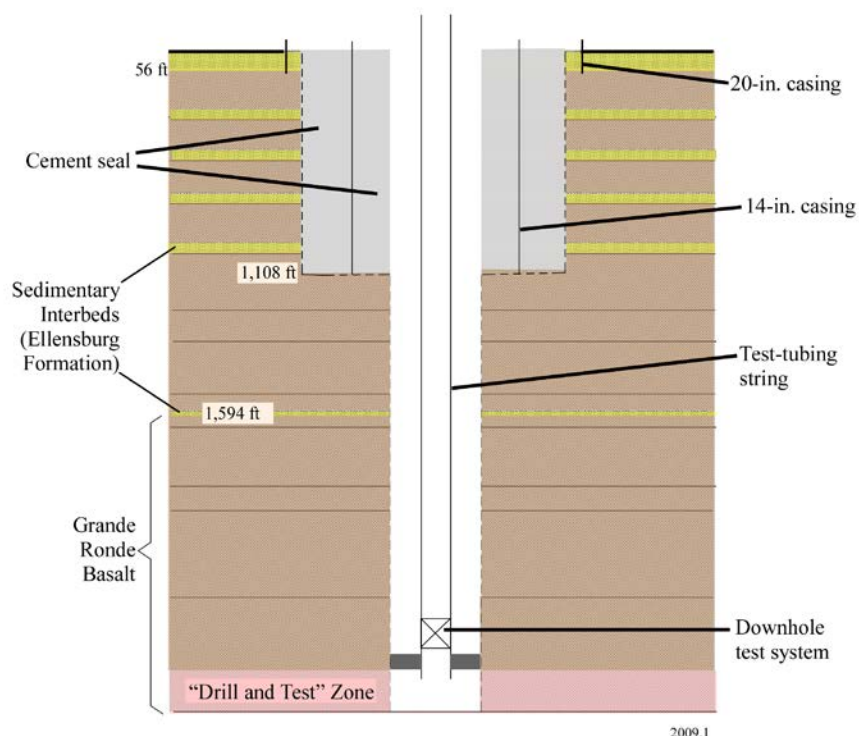


**Figure 2.18.** General Deployment of the Downhole Packer Test System during Borehole Advancement

Figure 2.20 shows a depiction of depth location for all 12 basalt interflow zone characterizations conducted within the Wallula pilot borehole during drilling and/or immediately prior to final well completion. In addition to the 12 basalt interflow zone tests, three low-permeability caprock test intervals (Zones 9, 10A, and 10B) were also characterized above the candidate injection Zone 8B. Table 2.4 summarizes the characterization activities conducted for the 12 basalt interflow and 3 low-permeability caprock intervals. Table 2.5 lists applicable hydrologic parameters and the relative investigative scale for the various hydraulic test methods used during the Wallula pilot borehole interflow and caprock zone characterizations. As indicated in Table 2.4, several hydrologic test methods generally were used for characterizing an individual test interval. This provides the opportunity for corroborating test parameter estimates over a range of investigative areas surrounding the borehole, as indicated in Table 2.5. A detailed description of the performance and analysis of the listed hydrologic test methods is presented in Reidel et al. (2002) and Spane (2008). A brief summary of these test discussions as they relate to the hydrologic characterization program conducted at the Wallula pilot borehole is presented in Appendix C. Miscellaneous pictures of hydrologic test equipment used during testing of Wallula pilot borehole test zones are provided in Appendix D.





**Table 2.5.** Summary of Hydrologic Test Methods Used for Wallula Pilot Test Site Characterization Investigation

Test Method	Hydrologic Parameter <sup>(a)</sup>						Test Scale		
	T	K <sub>h</sub>	S	S <sub>k</sub>	W <sub>L</sub>	L	Local	Intermed.	Large
Slug	√	√	x	x			√		
DST <sup>(b)</sup>	√	√	√	√		√	√	√	
Step-Drawdown/Recovery	√	√	√	√	√	√		√	
Constant-Rate Pumping – Drawdown & Recovery	√	√	√	√		√		√	√
Pulse <sup>(c)</sup>	√	√	x	x			√		
Multi-Step, Constant-Head Injection <sup>(c)</sup>	√	√		√		x	√		
Test History Matching <sup>(d)</sup>	√	√	√	√		x		√	√

(a) Hydrologic parameter nomenclature.

(b) DST = Drill stem test.

(c) Low-permeability, caprock test method.

(d) Superposition analysis method for analyzing a sequence of hydrologic tests.

T = Test interval transmissivity.

K<sub>h</sub> = Equivalent hydraulic conductivity; equal to T divided by test interval length or aquifer thickness.

S = Storativity; dimensionless.

S<sub>k</sub> = Well skin, dimensionless.

W<sub>L</sub> = Well loss.

L = Leakage response.

√ = Provides quantitative information.

x = Only provides inferential/qualitative information.

Figure 2.21 shows a preliminary transmissivity versus depth profile for the Wallula pilot borehole, as determined by field analyses of the 12 interflow zone tests. The transmissivity profile is reflective of the depth interval lengths within the borehole that were tested. Additional depth profile delineation is provided for test zones that were tested sequentially, using a common, fixed, lower borehole depth setting (e.g., Zones 6A, 6B, 6C; and 8A and 8B). In this situation, comparison of smaller test zone length values with the larger, composite test zone value provides the means for discriminating the bulk transmissivity distribution within the larger test zone interval. The preliminary field transmissivity values were primarily determined by analyzing the test zone hydrologic test results using a homogeneous formation, no well skin conceptual model approach. As indicated, a general decrease in test zone transmissivity with depth was exhibited for the site. More detailed analysis of hydrologic test interval characterization is currently ongoing, and will include test analyses based on heterogeneous formation, well skin, and multilayer analysis approaches. The results of the detailed hydrologic analysis will be reported in a subsequent document; however, the general decreasing transmissivity trend versus depth that is exhibited in Figure 2.21 is not expected to change substantially. This general decreasing transmissivity trend with depth pattern is consistent with results exhibited for Columbia River basalt interflow zones at a number of other (but not all) deep, intensively characterized Hanford Site basalt boreholes, as reported in Gephart et al. (1979), Spane (1982), DOE (1988), and Reidel et al. (2002). This apparent permeability-depth dependence is attributed to compaction (i.e., increasing effective stress), increased secondary mineral formation with depth, and, in some basinal geologic settings, increasing horizontal to vertical stress-field conditions (Reidel et al. 2005).

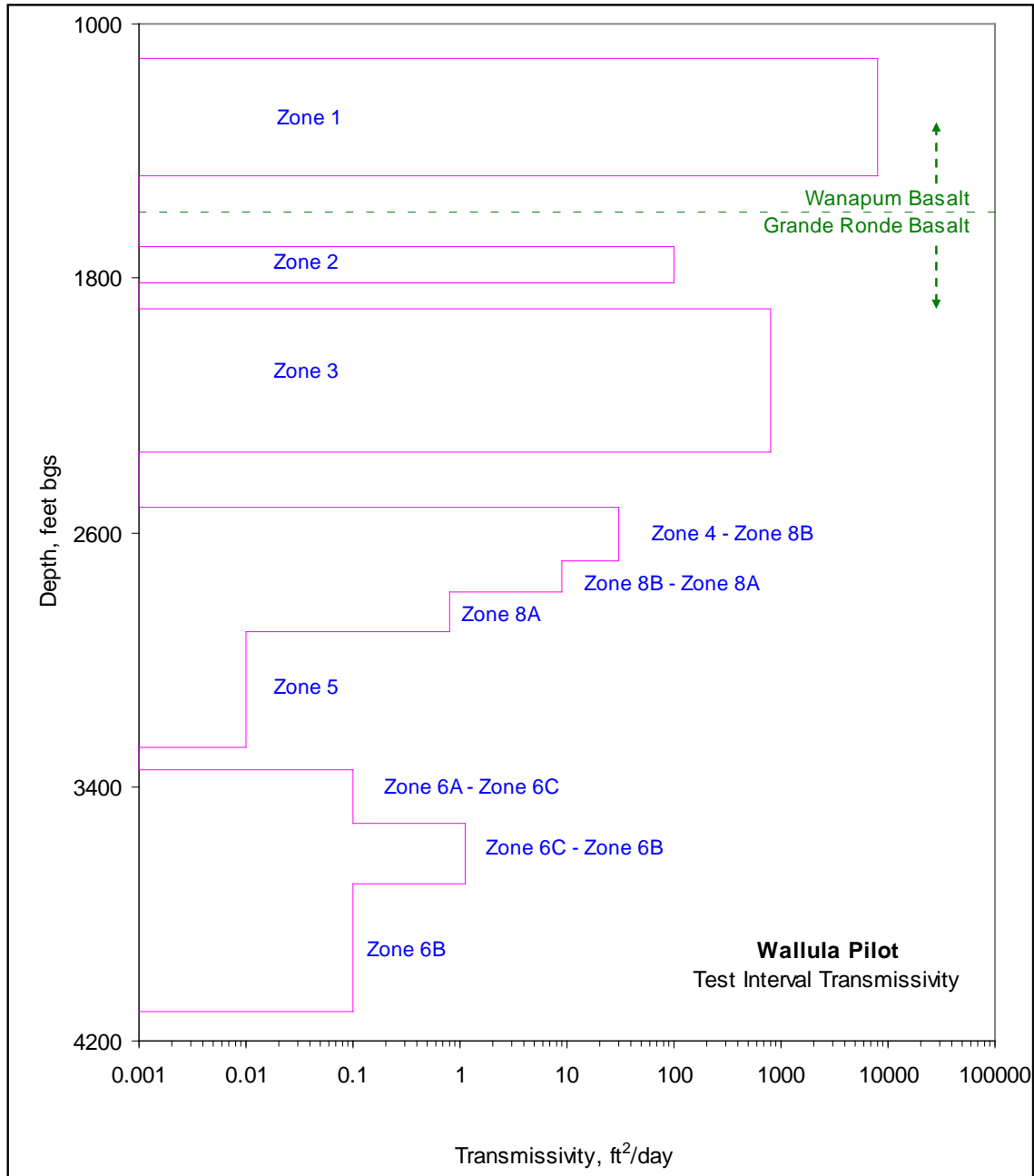


**Figure 2.21.** Wallula Pilot Basalt Interflow Transmissivity versus Borehole Depth

Observed hydraulic head measurements for the Wallula test zones are listed in Table 2.6. These measurements represent stabilized depth-to-water measurements that are recorded near the end or beginning of the hydraulic test zone characterization process. The hydraulic head measurements are based on a final ground-surface elevation survey of 363.99 ft mean sea level (MSL) (NAVD 88) that was surveyed for the site following well completion. The reported hydraulic head measurements are considered to be preliminary until final test zone analysis and site surveying are completed. It should also be recognized that observed hydraulic head measurements within deep boreholes can be highly influenced by the drilling process (over-/under-pressurization, formation thermal disequilibrium), fluid-column

effects (temperature profile distortions), and other extraneous natural/man-made-related effects (e.g., barometric pressure changes, river-stage fluctuations, distant extraction well pumping, etc.). This influence of antecedent drilling (commonly referred to as *borehole history effects*) are particularly manifest within low to intermediate permeability test formations, where these imposed conditions may require significant periods of time for their effect to stabilize or equilibrate, as noted in Pickens et al. (1987). Methods for accounting for some of these effects in hydraulic head calculations and conversions are presented in Spane and Mercer (1985), Spane and Thorne (1986), and Spane (1999).

**Table 2.6.** Preliminary Observed Hydraulic Head Measurements

Test Zone	Test Interval Depth, ft bgs <sup>(a)</sup>	Measurement Date	Observed Hydraulic Head <sup>(b)</sup> ft MSL	Comments
Zone 1	1108–1474	2/11/09	329	
Zone 2	1700–1814	2/19/09	329	
Zone 3	1895–2345	2/28/09	330	
Zone 4	2516–2798	3/10/09	326	
Zone 5A	3159–3279	3/18–20/09	ND	Test zone transmissivities are too low for reliable, stabilized hydraulic head measurement
Zone 5B	2910–3279			
Zone 6A	3340–4110	4/7–16/09	ND	Test zone transmissivities are too low for reliable, stabilized hydraulic head measurement
Zone 6B	3700–4110			
Zone 6C	3510–4110			
Zone 7	2698–4110	4/17/09	329	
Zone 8A	2790–2913	4/20–22/09	331	A depth-to-water measurement was not taken for Zone 8B
Zone 8B	2688–2913	4/22–24/09	ND	

(a) ft bgs = feet below ground surface; ground-surface elevation = 363.99 ft above mean sea level; NAVD 88 (Note: final vertical well survey conducted following well completion).

(b) Observed hydraulic head = ground-surface elevation minus depth-to-water measurement taken shortly after test zone isolation.

ND = Not determined.

Two general observations are evident concerning the preliminary hydraulic head conditions for the Wallula pilot borehole interflows listed in Table 2.6:

- An approximately 5-ft range in observed hydraulic head (i.e., 326 to 331 ft MSL) over the investigative depth
- Test zone hydraulic head values that are consistently lower than the operating reservoir elevation range of 335 to 340 ft MSL (datum: NGVD 29/47; 338 to 343 ft MSL NAVD 88) maintained for nearby Lake Wallula.

The small range in observed hydraulic head conditions is consistent with other detailed characterizations for deep Hanford Site boreholes also situated in the Pasco Basin. It is interesting to note that the lowest observed hydraulic head (326 ft MSL) was exhibited for Zone 4, which includes two adjacent interflow zones immediately below the Umtanum basalt. The Umtanum basalt is a regionally extensive hydrogeologic unit that can act as secondary caprock horizon, caused by the low-permeability characteristics and significant thickness of its flow interior section.

The observed test zone hydraulic head values are 7 to 12 ft lower than the operating reservoir range for nearby Lake Wallula, which was created in 1954 during the construction of McNary Dam. Because of its proximity to the Columbia River/Lake Wallula, hydraulic heads within the Wallula pilot interflow test zones were expected to be higher than the operating reservoir elevation. Because of the preliminary nature of the observed hydraulic head values, it is uncertain what hydrologic conditions are responsible for the lower-than-expected head values. Possible explanations include lack of complete hydrologic equilibration during the past 55 years following Lake Wallula creation, and distant, regional groundwater development within this formation section of the Columbia River Basalt. Groundwater-level monitoring is currently ongoing for the Wallula well completion interval (i.e., 2716 to 2910 ft). These baseline monitoring data will provide information concerning the temporal, seasonal, and long-term groundwater response characteristics for deep basalt formations at the Wallula test site location. Frequency- and time-domain analysis of these baseline data will help identify the hydrologic head relationship between deep basalt groundwater and nearby Lake Wallula. A summary of applicable baseline analytical methods is presented in Spane (1999, 2002).

#### **2.3.4.1 Injection Zone Characterization**

The 194-ft open-well completion zone of 2716 to 2910 ft contains three Grande Ronde flowtop/interflow zones: Slack Canyon flow #2 (2720.5 to 2768.5 ft), Slack Canyon flow #1 (2797.5 to 2811.5 ft), and the Ortley flowtop (2837.5 to 2866.5 ft). Because of the relatively thin intervening basalt flow interior sections between the Slack Canyon flow tops #1 and #2, and between the lower Slack Canyon and underlying Ortley basalts, this composite open zone completion is considered to be a single, hydraulically communicative, hydrogeologic unit. Within this 194-ft open-well completion interval, the principal zones containing effective permeability for transmission of groundwater and subsequent CO<sub>2</sub> injection are anticipated to be the three flow tops for the previously identified basalt flows. Collectively, 91 ft of brecciated flow top material is present, and is distributed as follows: 48 ft for the Slack Canyon flow top #2 (2720.5 to 2768.5 ft); 14 ft for the Slack Canyon flow top #1 (2797.5 to 2811.5 ft); and 29 ft for the Ortley flow top (2837.5 to 2866.5 ft).

As indicated in Table 2.3 and Table 2.4, two depth intervals within and encompassing the open-well completion zone of 2716 to 2910 ft were tested during the course of the open borehole testing. Zone 8A examined the lower section between 2790 and 2913 ft while Zone 8B hydraulically characterized the encompassing depth interval 2688 and 2913 ft (see Figure 2.22). A comparative examination of hydrologic test results for the two zones indicates that the lower two flow top zones (i.e., the Ortley and Slack Canyon flow #1) contain only ~10% or less of the total completion zone composite transmissivity. This is displayed qualitatively by the differences exhibited for normalized slug test recovery response results for the two zones, shown in Figure 2.23. In this test response comparison, slower test recovery is associated with lower test zone transmissivity. As indicated in Figure 2.23, Zone 8B recovers ~10 times faster than indicated for the normalized test response for Zone 8A. Because Zone 8B encompasses Zone 8A, this indicates—by application of the superposition principle (Reilly et al. 1987)—that the majority of the Zone 8B composite transmissivity (i.e., ~90%) occurs within the 48-ft flow top of the Slack Canyon flow #2 (2720.5 to 2768.5 ft).

As listed in Table 2.2, a series of hydrologic tests were performed for test Zone 8B. The hydrologic tests were conducted between April 22 and 24, 2009, and included the following: cyclic constant-rate pumping tests, slug and drill-stem (DST) tests. Figure 2-24 shows the downhole pressure response recorded for Zone 8 during the sequence of slug and DST testing.

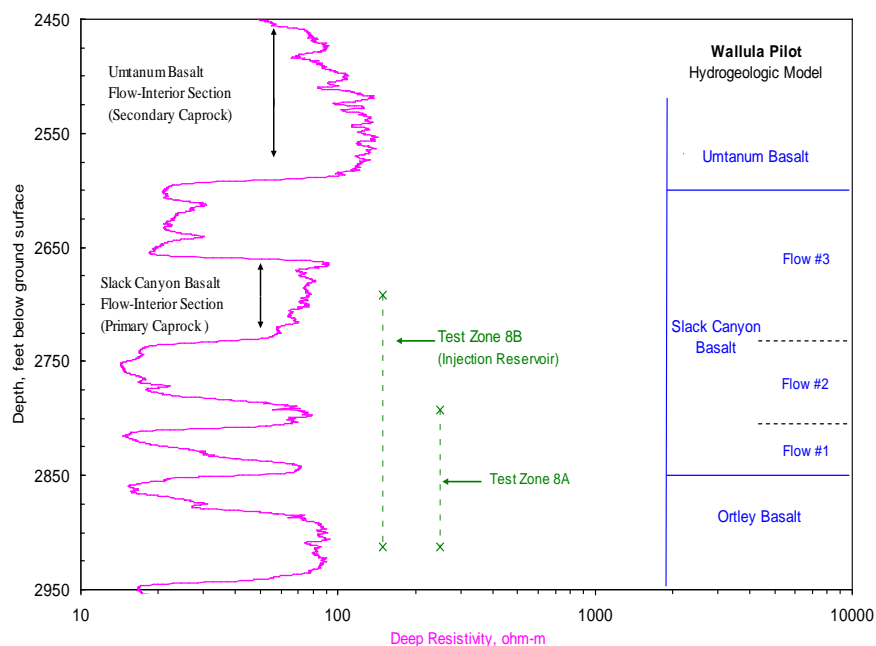


**Figure 2.22.** Borehole Hydrologic Test Zones within the Completed Well Injection Zone Horizon (2716 to 2910 ft)

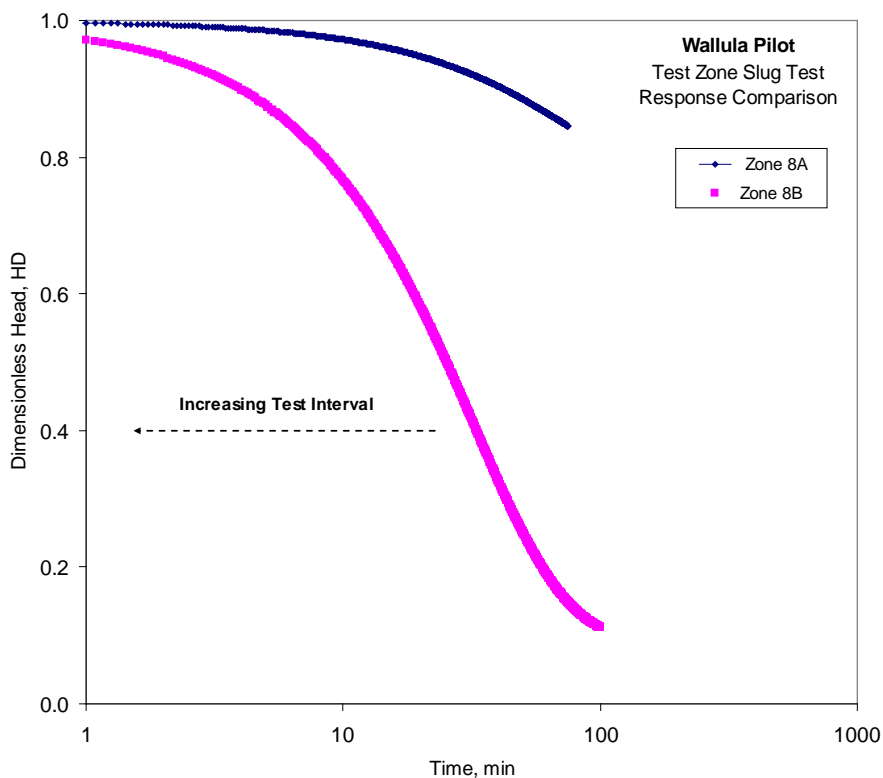


**Figure 2.23.** Slug Test Zone Response Comparison

Preliminary analysis of results for individual hydraulic characterization tests provided the following hydrologic property estimate ranges for Zone B and the final well completion zone: transmissivity,  $T = 9.8$  to  $19.8 \text{ ft}^2/\text{day}$ ; hydraulic conductivity,  $K = 0.108$  to  $0.218 \text{ ft/day}$ ; intrinsic permeability,  $k = 44$  to  $90$  millidarcies at standard temperature and pressure; storativity,  $S = 1.0\text{E-}5$  (assumed); and well skin,  $S_k = 0$  to  $+6.0$ . Figure 2.25 shows an example of an initial field test analysis and associated analysis parameters for a slug withdrawal test (SW #1). This is the first test within the hydrologic test characterization sequence performed for Zone 8B that is shown in Figure 2.24. More quantitative analysis of the hydrologic characterization tests conducted for Zone 8B will reduce the hydrologic property estimate range currently assigned for the well completion injection zone.

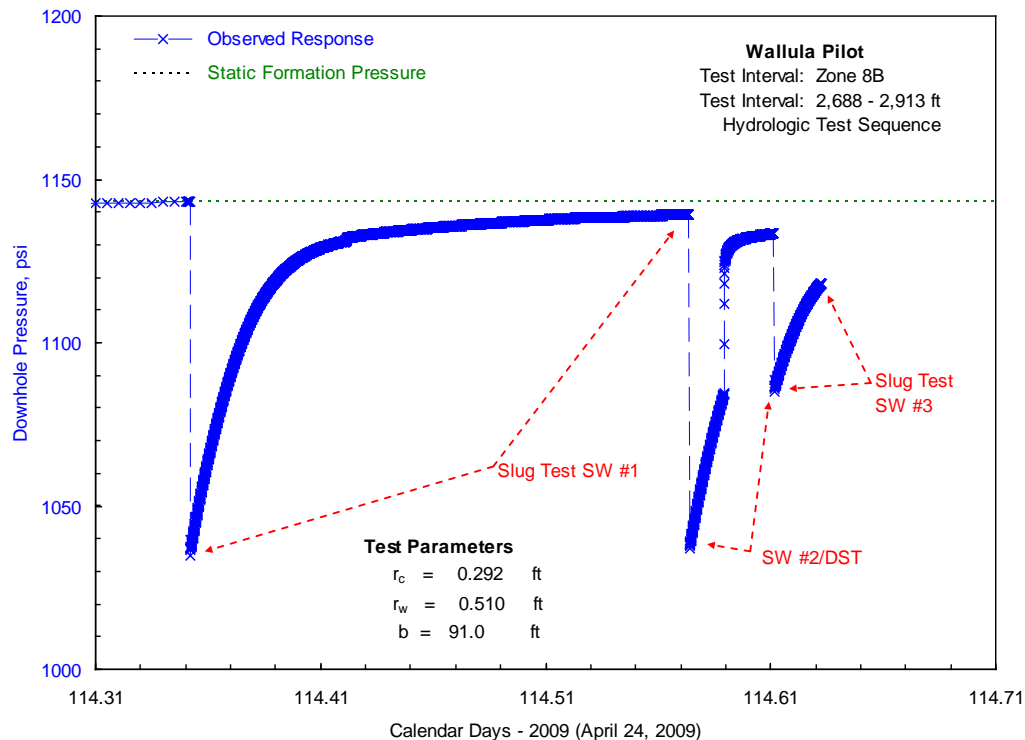


**Figure 2.24.** Hydrologic Test Characterization Sequence: Zone 8B

The previous discussion assumes that the hydrologic property values are uniform for the three flow top horizons intersected within the well completion interval. However, as noted previously, the transmissivity distribution within the well completion zone does not appear to be uniform, with ~90% of the composite  $T$  being associated with the upper 48-ft Slack Canyon flow top #2. Given this assumed  $T$  distribution condition within the Wallula well completion zone, an average hydraulic conductivity,  $K$ , range of  $0.184$  to  $0.371 \text{ ft/day}$  is indicated for this upper flow top zone. This is equivalent to a calculated average intrinsic permeability,  $k$ , range of  $75$  to  $150$  millidarcies at standard temperature and pressure for the upper 48-ft flow top interval. In comparison, the lower two flow top intervals within the well completion zone (i.e., Slack Canyon flow #1 and Ortley flow tops) have a composite effective thickness of  $43 \text{ ft}$ , and an average calculated  $K$  and  $k$  estimate range of  $0.023$  to  $0.046 \text{ ft/day}$ , and  $9$  to  $19$  millidarcies at standard temperature and pressure, respectively.

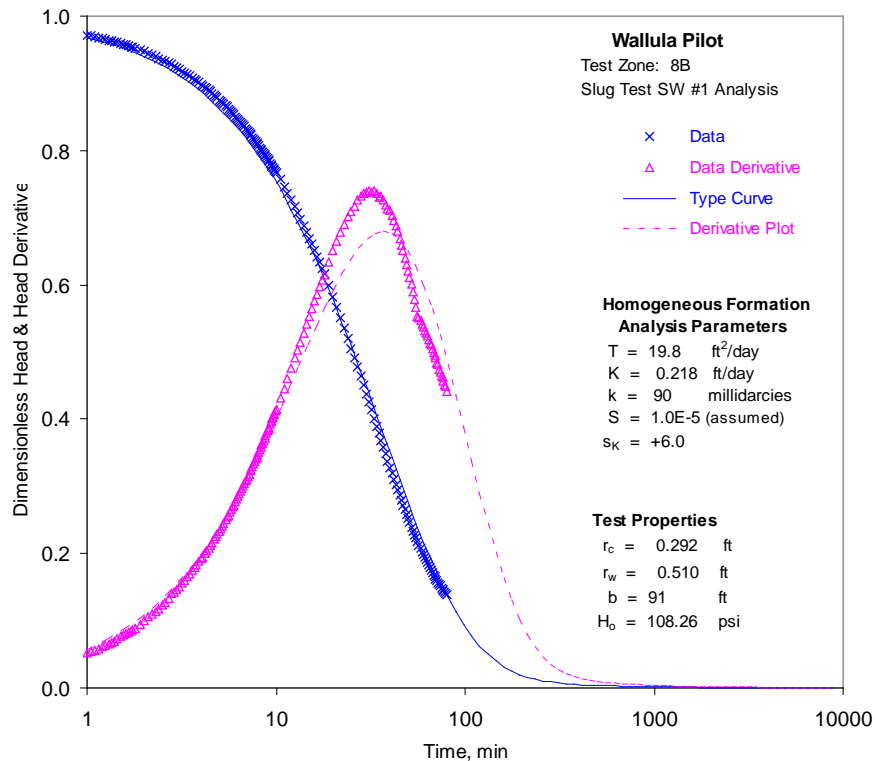


**Figure 2.25.** Preliminary Zone 8B Slug Test Analysis

No hydrologic characterization tests were performed on the injection zone immediately following well completion activities. A series of hydrologic tests are planned for the injection zone, prior to implementing the active CO<sub>2</sub> field pilot injection test study. The preinjection hydrologic tests to be performed depend on available funding to support this characterization element, but may include the following:

- Tracer injection and pump back (for estimating injection zone effective porosity)
- Dynamic flowmeter/pumping test (for quantifying the permeability distribution within the injection zone)
- Long-term constant-rate pumping test and recovery (for lateral hydrologic boundary and leakage response detection).

#### 2.3.4.2 Caprock Zone Characterization

Three low-permeability flow interior/caprock test intervals (Zones 9, 10A, and 10B) were also characterized above the candidate injection Zone 8B. The caprock tests had open borehole test interval lengths ranging between 35 and 99 ft (top inflatable packer is 4.5 ft in length; Tables 2.5 and 2.6 test/depth interval listings are referenced to the top of the top packer depth setting). Figure 2.26 shows the location of the caprock tests in relationship with the well injection zone horizon (i.e., 2716 to 2910 ft). Multistep, constant-head injection pressure tests were conducted for all three caprock horizons, with surface injection pressures ranging between 0 and a maximum 150 psi. The multistep injection tests were completed over test periods ranging between 4.5 and 5.5 hours, with individual injection steps generally e 1 hour in duration. Injection pressure was provided by high-pressure gas cylinders and adjusted



appropriately using a precision pressure regulator. Injection rates were calculated by monitoring the decline of water within a 1/2-in. inside diameter (ID) sight-tube mounted on the side of a 2.45-ft-long, 8-in.-ID wellhead injection chamber. This provided injection flow-rate measurement capabilities to 0.1 mL/min. A surface sunscreen enclosure was used during the daylight hours to minimize adverse thermal effects imposed by direct sun exposure on the surface injection wellhead test equipment. A picture of the wellhead injection system is shown in Appendix D.

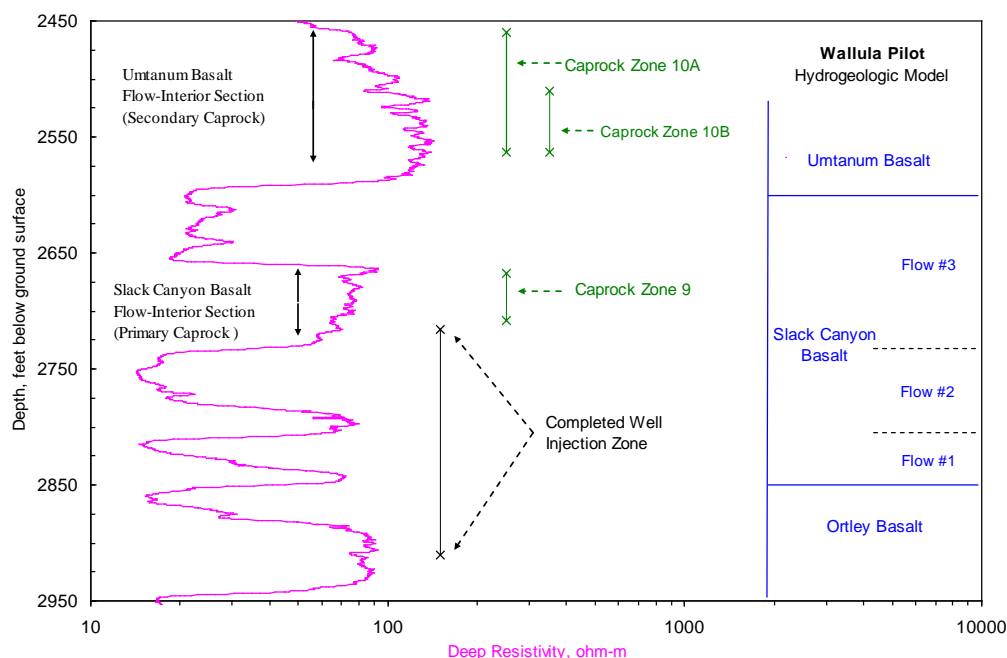


**Figure 2.26.** Caprock Hydrologic Test Zones above the Completed Well Injection Zone Horizon (2716 to 2910 ft)

Methods used in the analysis of the Wallula multistep, constant-head injection tests are discussed in Appendix C. Preliminary analysis results provided average K estimates for the three caprock intervals ranging between  $\sim 1.0\text{E}^{-12}$  to  $1.0\text{E}^{-13}$  m/sec (i.e.,  $\sim 0.01$  to  $\sim 0.1$  microdarcies at standard temperature and pressure). This is consistent with low-permeability, Hanford Site basalt flow interior tests reported in Eslinger (1986). In this previous study, a statistical analysis was performed on 13 individual Grande Ronde basalt flow-interior, borehole field tests (for test-section lengths ranging between  $\sim 35$  and 200 ft). The results of the statistical study provided a geometric mean value for Grande Ronde Basalt flow interiors of  $4.9 \times 10^{-13}$  m/sec ( $\sim 0.05$  microdarcies at standard temperature and pressure) as reported in Eslinger (1986). These extremely low-permeability values suggest that overlying thick basalt flow interior sections (e 50 ft) represent an effective caprock for isolating  $\text{CO}_2$  injected into underlying Wallula completion zone flow tops. This injection zone isolation is based on the existence of pervasive low-permeability caprock conditions (as indicated by test results from Zones 9, 10A, and 10B), and assumes the absence of nearby localized, cross-cutting, geologic features; e.g., faults, tectonic fractures/joints.

**Table 2.7.** Pertinent Information Pertaining to Hydrochemical/Microbiological Sampling

Sampling Date	Test Zone	Test Interval Depth, ft bgs <sup>(a)(b)</sup>	Groundwater Volume Developed, gallons	Comments
2/13/09	Zone 1	1108–1474	1,798,000 <sup>(c)</sup>	Sampling occurred near the end of a ~24-hr constant-rate pumping test conducted with a line-shaft turbine pump (@~1,250 gpm
2/20/09	Zone 2	1700–1814	79,000	Sampling occurred near the end of a ~21-hr constant-rate pumping test conducted with a submersible pump
3/1/09	Zone 3	1895–2345	113,000	Sampling occurred near the end of a ~19-hr constant-rate pumping test conducted with a submersible pump
3/9/09	Zone 4	2516–2798	35,500	Sampling occurred near the end of a ~27-hr constant-rate pumping test conducted with a submersible pump
4/13/09	Zone 6A	3340–4110	8800	Sampling occurred near the end of a ~94-hr cyclical pumping test conducted with a submersible pump
4/23/09	Zone 8B	2688–2913	3275	Sampling occurred near the end of a ~15-hr cyclical pumping test conducted with a submersible pump

(a) ft bgs = feet below ground surface; ground-surface elevation = 363.99 ft above mean sea level; NAVD 88 (Note: final vertical well survey conducted following well completion).

(b) Upper test interval depth indicative of top of packer depth setting or well casing depth; lower test interval depth indicates either bottom of borehole at the time of testing (for Zones 1 through 6A) or top of lower bridge plug packer (for Zone 8B). Note: top packer = 4.5 ft in length.

(c) Does not include additional volume pumped for prior step-drawdown test.  
gpm = gallons per minute.

### 2.3.5 Hydrochemistry and Isotopic Sampling

Groundwater samples were collected from six Wallula borehole test zones prior to final well completion. The samples were collected at the end of long-duration, constant-rate pumping or cyclical pumping characterization periods primarily using a downhole submersible pump (note: Zone 1 collected samples using a line-shaft turbine pump). Collection of the samples at the end of the pumping periods provided for maximum test zone development and removal/minimization of potential antecedent drilling or open borehole conditions. Samples were collected during the course of pumping and field analyses performed for specific electrical conductance, pH, and alkalinity. These field hydrochemical parameters were used in monitoring and assessing test zone development. Final formal hydrochemical samples were collected at the surface through a diverted discharge line using a stainless-steel manifold equipped with a “Tee” fitting and a manual valve. Switching the valve diverted flow through the Tee branch into 1/4-in. outside diameter (OD) polyethylene tubing. In most cases, sample water was passed directly through an in-line 0.45-µm filter and then into sample bottles containing preservatives where appropriate. For Zones 6A and 8B, the sample water was especially turbid, and several liters of unfiltered water were collected in a large carboy and then filtered using a peristaltic pump and in-line filters. Duplicate and field blank samples were collected during the sampling of Zone 6A. Duplicate bottles were filled sequentially using the peristaltic pump and in-line filter assembly. The field blank samples consisted of

distilled and de-ionized water that had been passed through an in-line filter. All samples were stored in coolers containing ice and were delivered to the analyzing laboratory's local receiving facility as soon as practical (i.e., the same day or the morning of the next day when sampling was completed after normal business hours). Chain-of-custody paperwork was filled out at the time of sample collection, and the forms signed by appropriate personnel when the samples were transferred to the receiving facility.

Samples were shipped overnight from the receiving facility to General Engineering Laboratories (GEL) in Charleston, South Carolina, and analyzed using standard analysis protocols (see Appendix E for a listing of the methods used and the results). GEL is accredited by Washington State and is audited annually by the U.S. Department of Energy's Consolidated Audit Program (DOECAP). Sample results were transmitted to Battelle in hardcopy and electronic formats, and the values entered into a database for evaluation. In addition to the sample analyses already performed, samples were also collected for the possible characterization of a suite of isotopic and gas analyses, including the following: dissolved gases, helium-4, stable isotopes [ $C^{13}$ ,  $C^{13}(CH_4)$ ,  $H^2$ ,  $H^2(CH_4)$ ,  $O^{18}/O^{16}$ ,  $S^{34}$ ], and unstable isotopes ( $H^3$ ,  $C^{14}$ , uranium disequilibrium,  $Cl^{36}$ ). Selected samples will be submitted for this second cycle of hydrochemical test zone characterization and reported at a later date.

Results from major and trace metal inorganic analyses listed in Appendix E indicate that all Wallula pilot sampled test zones are of similar hydrochemical character and can be classified as a relatively dilute, sodium-bicarbonate chemical water type. The Wallula basalt groundwaters exhibit hydrochemical characteristics similar to other *geochemically evolved* basalt groundwaters within the region. Basalt groundwater typically evolves from a relatively dilute calcium-magnesium bicarbonate hydrochemical type near recharge areas and slowly changes to a more mineralized, sodium bicarbonate to sodium bicarbonate-chloride groundwater laterally at more distant groundwater-flow system locations and vertically with depth. Discussions pertaining to hydrochemical evolutionary characteristics and geochemical controls influencing Columbia River basalt hydrochemistry are presented in a number of reports including Gephart et al. (1979), Spane et al. (1982), DOE (1988), Whiteman et al. (1994), Spane and Webber (1995), and Reidel et al. (2002, 2005). Generally speaking, the basic geochemical processes controlling mineral equilibria and basalt hydrochemical development that are recognized in these previous reports include hydrolysis of volcanic glass phase reactions within the basalt, calcite, and silicate mineral precipitation, sulfate reduction, and cation exchange.

Consistent with these geochemical processes, basalt groundwaters sampled at the Wallula pilot borehole generally exhibit the following:

- Elevated pH, fluoride, silica, bicarbonate, and sodium
- Decreased concentrations of calcium, magnesium, and sulfate.

Of relevance to the pilot study is the elevated pH (9.0 to 9.7) and relatively high fluoride concentrations (3.2 to 11.9 mg/L). Generally, pH and fluoride concentrations increase with increasing test zone depth. While the total dissolved solids concentration level could make this water protected under the U.S. Environmental Protection Agency's *Safe Drinking Water Act*, the State of Washington uses a different standard for permitting sequestration projects. Washington State is one of the most progressive states on CO<sub>2</sub> policy and carbon sequestration standards. Accordingly, exceedance of MCLs listed in 40 CFR 141.62 is the standard adopted in Washington State for permitting geologic sequestration projects under WAC 173-218-115. The targeted injection zone, consisting of breccia zones associated with three basalt flows between 2716 to 2910 ft, was hydrochemically characterized during sampling of test

Zone 8B. Groundwater sampled from this zone has a fluoride concentration level of 4.98 mg/L, which exceeds both the secondary and primary drinking water standards of 2.0 and 4.0 mg/L, respectively.

### 2.3.6 Microbiological Studies

Knowledge of the deep subsurface biosphere has grown in 20 years to include an understanding of the conditions that determine microbial distribution, quantity of biomass, diversity, and activity (Fredrickson and Balkwill 2006). Subsurface microbes are metabolically active and alter the water and rock chemistry where they live. In turn, these microbes are responsive to the abiotic conditions of these systems and are structured along the chemical and physical gradients imposed upon them.

Computational studies that address how the Columbia River basalts (CRB) groundwater and CO<sub>2</sub> alter basalt minerals predict a decrease in pH from 7.6 to 4 with a corresponding release of cations from basalt minerals (McGrail et al. 2006) after injection of supercritical CO<sub>2</sub>. With time and distance from the injection well, CO<sub>2</sub> changes from a supercritical free phase to carbonic acid dissolved in water to aqueous bicarbonate ion and ultimately to solid carbonate minerals.

Injection of supercritical CO<sub>2</sub> into the CRB and the associated pH changes, rock-water reactions, and temporary increase in solution products (e.g., cations of Fe, Al, Mg, Ca) in surrounding strata will impose pH and cationic gradients on microbial communities. New microbial communities will live in the low pH and high-dissolved cation concentrations derived from CO<sub>2</sub>-induced alteration of basalts. These cells will be situated along a continuum of precipitated carbonate minerals as the system buffers the CO<sub>2</sub>. The overall objective of the microbial studies work conducted on the Wallula pilot borehole is to further understanding of how subsurface microbial communities respond to supercritical CO<sub>2</sub> injection, and to understand this response in the context of geochemical and mineralogical profiles that result from chemical reactions of basalt with CO<sub>2</sub> and re-precipitation of carbonate minerals. Several questions relevant to the biogeochemistry of supercritical CO<sub>2</sub> storage in deep basalts that are expected to be answered post-injection include the following:

- How will natural subsurface microbial communities be restructured in response to the chemical and physical gradients associated with supercritical CO<sub>2</sub> storage?
- Are there specific microbes that are adapted to survive conditions consistent with supercritical CO<sub>2</sub> alteration of basalt minerals?
- Do microbes that become established in subsurface strata exposed to supercritical CO<sub>2</sub> and the associated alteration products play a role in plugging fractures or pore space?
- Can microbes facilitate mineral dissolution and precipitation reactions that neutralize CO<sub>2</sub> induced acidity?

The changes in chemistry corresponding to supercritical CO<sub>2</sub> emplacement may stress microbes native to the formation. Exposure to supercritical CO<sub>2</sub> may be lethal to some microbes; however, some can survive such exposure (Mitchell et al. 2008, 2009) and certainly at some distance from the injected supercritical fluid more general survival and adaptation would be expected. To evaluate survival and adaption patterns post-injection, part of the drilling and characterization program for the Wallula Pilot included collection of microbial cells from water samples from five test intervals in the CRB, as illustrated in Figure 2.27. Cells were collected by filtering water that had been produced from the

selected intervals in the basalts, and were matched with washed samples of basalt cuttings obtained from comparable depths in the borehole. Samples were also matched with samples used to determine the water chemistry, hydrological features of the basalt interflow zones, and the mineralogical characteristics of the basalts.

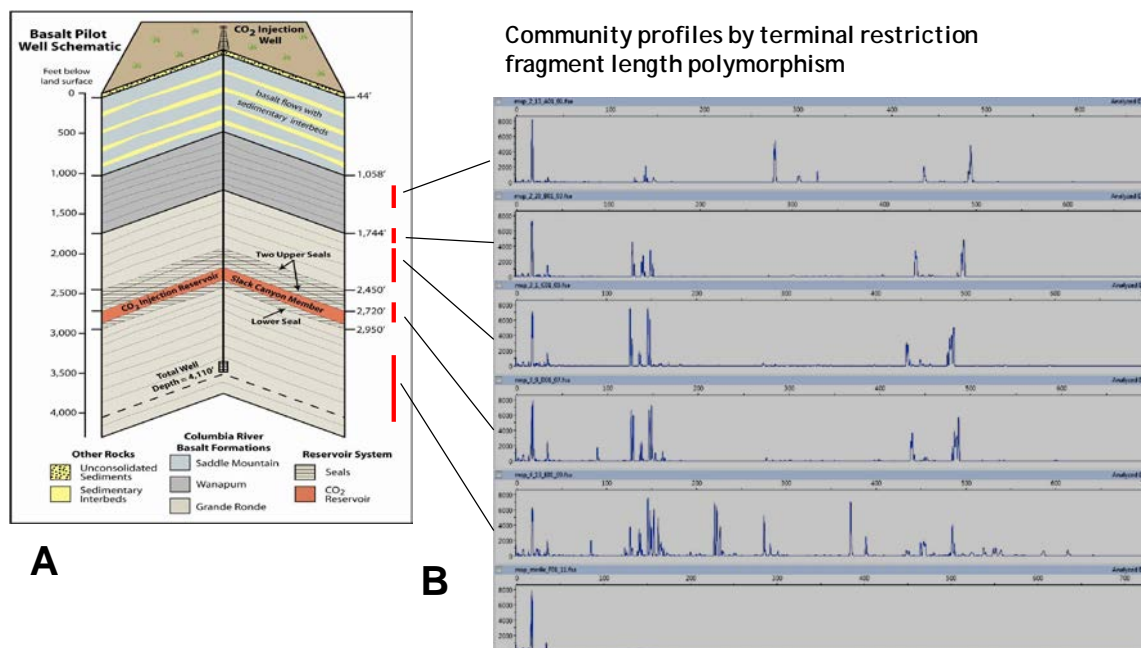


**Figure 2.27.** Five Intervals were Packed Off in the Wallula Pilot Well and Sampled for Free-Living Microbial Cells in Groundwater (red bars in A) and Terminal Restriction Fragment Length Polymorphism (t-RFLP) Profiles from the Five Respective Intervals (B). Peaks appearing along the x-axis of the five t-RFLP plots represent amplified DNA fragments that correspond to distinct microbial taxa (species) filtered from the groundwater at different depths in the well.

The presence of microbes was confirmed at all five depths sampled in the well. Attempts were made to detect both bacteria and archaea (two distinct types of microbes); however, only bacterial DNA could be extracted and amplified. It is possible the method used to extract DNA was not suitable for archaea. Microbial community diversity analyses (terminal restriction fragment-length polymorphism) indicated the presence of diverse microbial communities at and above the depths where CO<sub>2</sub> injection will occur. Microbial communities found in the Wanapum and the upper Grande Ronde strata are somewhat similar to each other and distinct from microbes found in the lower Grande Ronde and Wanapum layers. Quantitative polymerase chain reaction (PCR), a molecular method used to enumerate selected genes in a sample, was used to detect and quantify the 16S rRNA gene. This gene is present in all living cells and is a signature of cell viability. Battelle researchers' determinations of the quantity of 16S rRNA gene copies in the cells filtered from the water samples indicated that free-living biomass at the different depths ranged from  $3 \times 10^3$  to  $9 \times 10^5$  cells per mL. This free biomass (i.e., that which is planktonic in an aquifer and not attached to the solid substrate) is often considered to be less than 1% of the total biomass in the

subsurface (Lehman et al. 2001). Thus, based on prior subsurface microbiology studies, it is not unreasonable to expect that considerably more cells may exist that are attached to the basalt than are free-living or planktonic in the water.

Additional work is in progress to determine the types of bacteria present in the DNA extracted from the cells at different depths by comparing the DNA signature sequence data obtained from the 16S rRNA gene to that of known cells. This information will provide limited insight into the metabolic capabilities that might be expected of the bacteria in the basalt aquifers.

## **3.0 Injection Discussion and Planning**

### **3.1 Target Formation Description**

Based on characterization results obtained during drilling, three basalt breccia zones were identified between the depth interval of 2716 and 2910 ft (Table 2.1) as being suitable injection reservoirs for a subsequent CO<sub>2</sub> injection pilot study. The targeted injection reservoir lies stratigraphically below the massive Umtanum Member of the Grande Ronde Basalt, whose flow-interior section possesses regionally recognized low-permeability characteristics. The identified composite injection zone reservoir provides a unique and attractive opportunity to scientifically study the reservoir behavior of three interconnected reservoir intervals below primary and secondary caprock confining zones.

### **3.2 Injection Simulation Analysis**

Simulations of a pilot-scale CO<sub>2</sub> injection into the flow tops of individual basalt flows in the Grande Ronde Basalt at Wallula, Washington, were performed using the STOMP-H<sub>2</sub>O-CO<sub>2</sub>-NaCl model simulator (White and Oostrom 2006). The model for the CO<sub>2</sub> injection simulations included three injection horizons: the Ortley flow top (OFT), the Slack Canyon #1 flow top (SCFT1) and the Slack Canyon #2 flow top (SCFT2). The injection zone flow top intervals possess moderately high permeabilities and are overlain by two thick-flow interior/caprock intervals (i.e., the Umtanum and Slack Canyon #3) exhibiting low-permeability, confining-layer conditions. Separating the individual injection zone flow tops are relatively thin, intervening flow interiors that have expected low-permeability conditions.

#### **3.2.1 Hydraulic Properties**

Hydraulic properties for each model layer were determined from hydraulic test results described in Section 2.3.4. Horizontal hydraulic conductivities for each layer are shown in Table 3.1. The hydraulic conductivity for the SCFT2 is the highest, at  $6.35 \times 10^{-5}$  cm/sec, while hydraulic conductivities for the SCFT1 and OFT are 8 times lower, at  $8.2 \times 10^{-6}$  cm/sec. Vertical hydraulic conductivities were assumed to be one order of magnitude lower than the horizontal hydraulic conductivities. Flow tops were assumed to have 10% porosity and flow interiors to have 1% porosity.

Unsaturated flow properties of the basalt flows intersected by the Wallula pilot borehole have not been measured and were assumed for each of the materials (White et al. 2006), as listed in Table 3.2. The unsaturated hydraulic properties for the flow tops are similar to those of gravel, whereas the flow interiors were assigned higher air-entry pressure to reflect the smaller pore size inherent for their lower permeability.

A hydrostatic gradient of 0.435 psi/ft was assumed based on observed formation pressure versus depth measurements exhibited for a deep Hanford Site characterization borehole, RRL-2, as reported in Strait and Spane (1982). Formation temperature was assumed to be 94.59°F at a depth of 2930.5 ft, with a geothermal gradient of -0.0147°F/ft, based on observed measurements within the Wallula pilot borehole.

**Table 3.1.** Hydraulic Properties and Depth of Basalt Flows at Wallula

Abbr.	Model Layer	Top, ft	Bottom, ft	Thickness, ft	K, cm/sec	Porosity, %
UFI	Umtanum flow interior (secondary seal)	2442.5	2577.5	135	$1.00 \times 10^{-12}$	1
SCFT3	Slack Canyon #3 porosity zone (no injection)	2577.5	2645.5	68	$1.47 \times 10^{-4}$	10
SCFI3	Slack Canyon #3 flow interior (primary seal)	2645.5	2720.5	75	$3.00 \times 10^{-12}$	1
SCFT2	Slack Canyon #2 flow top porosity zone (injection)	2720.5	2768.5	48	$6.53 \times 10^{-5}$	10
SCFI2	Slack Canyon #2 flow interior (seal)	2768.5	2797.5	29	$3.00 \times 10^{-11}$	1
SCFT1	Slack Canyon #1 flow top porosity zone (injection)	2797.5	2811.5	14	$8.20 \times 10^{-6}$	10
SCFI1	Slack Canyon #1 flow interior (seal)	2811.5	2837.5	26	$3.00 \times 10^{-11}$	1
OFT	Ortley flow top porosity zone (injection)	2837.5	2866.5	29	$8.20 \times 10^{-6}$	10
OFI	Ortley flow interior (lower confining zone)	2866.5	2930.5	64	$1.00 \times 10^{-12}$	1

**Table 3.2.** Brooks-Corey Function Parameters

	Air-Entry Pressure, cm	$\lambda$	Residual Saturation
UFI	154	4.033	0.01
SCFT3	54	4.033	0.01
SCFI3	154	4.033	0.01
SCFT2	54	4.033	0.01
SCFI2	154	4.033	0.01
SCFT1	54	4.033	0.01
SCFI1	154	4.033	0.01
OFT	54	4.033	0.01
OFI	154	4.033	0.01

Two-dimensional simulations with a cylindrical coordinate grid were developed for the model simulations. The model domain extended from 2930.5 ft in depth to 2442.5 ft in depth (488 ft total), with a radial width of 1000 ft surrounding the injection well. A vertical grid spacing of 2 ft was used, with a radial grid spacing set at 5 ft. Homogeneous layers were assumed throughout (Figure 3.1). Simulations were limited in scope to include only multiphase flow behavior and did not include chemical reactions with the basalts. Reactive transport simulations are in progress and will be discussed in subsequent publications.



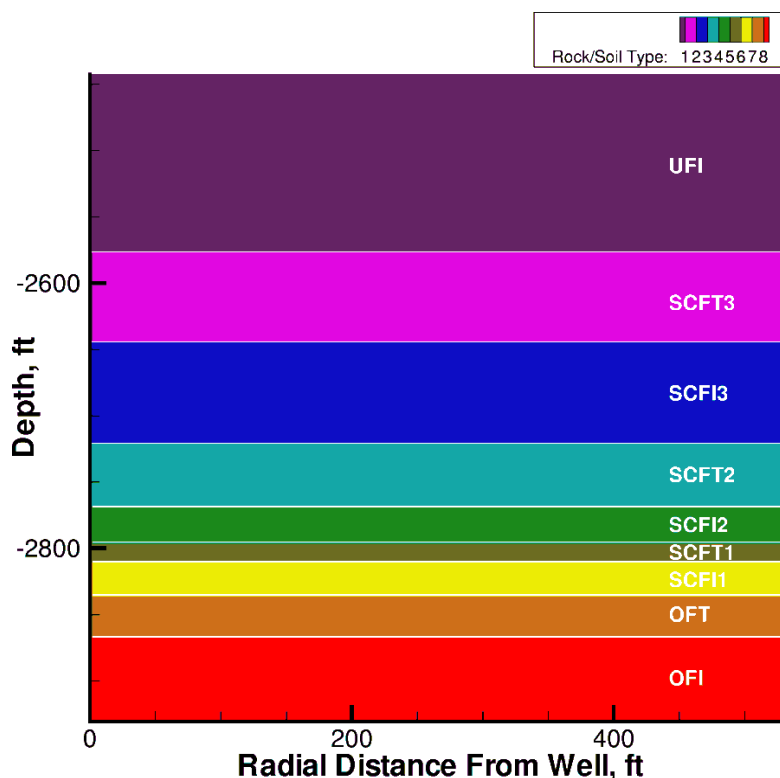


**Figure 3.1.** Lithologic Units for Simulation of Pilot-Scale CO<sub>2</sub> Injection at Wallula

### 3.2.2 Simulation Results

The total mass of CO<sub>2</sub> modeled for the injection simulations was 1000 metric tons (MT), which was injected over a time period of either 14 or 30 days. For possible pilot study design considerations, three different injection scenarios were considered:

1. Scenario 1: simultaneous injection into the OFT, SCFT1, and SCFT2 over a period of 14 days
2. Scenario 2: injection only into the SCFT2 over a period of 14 days
3. Scenario 3: injection only into the OFT over a period of 30 days.

Results from the various injection simulation scenarios will be used in the final design of the CO<sub>2</sub> injection field pilot study. A brief description of the three scenario injection simulations is provided in Section 3.2.2.1.

#### 3.2.2.1 Scenario 1: Injection into OFT, SCFT1, and SCFT2

Simulation results for the composite, open-borehole injection into the OFT, SCFT1, and SCFT2 (Scenario 1) indicate that most of the injected CO<sub>2</sub> flows into the SCFT2 (Figure 3.2). This zonal preferential injection of CO<sub>2</sub> is a result of the higher permeability exhibited by SCFT2. The density of the injected supercritical CO<sub>2</sub> is 66% of that exhibited by groundwater at the prevailing formation temperature and pressure conditions. Because supercritical CO<sub>2</sub> does not displace all of the groundwater within the formation pore space, the average fluid-density contrast is 75% to 100% of that exhibited by

the initial formation water (Figure 3.3). The radius of the injected supercritical CO<sub>2</sub> from the Wallula pilot borehole well increases from 100 ft after the active 2 weeks of injection to 180 ft at 1 year after the start of injection (Figure 3.4 and Figure 3.5). The simulated increase in downhole pressure within the injection zone/well bore is less than 110 psi (Figure 3.6). One year after the start of injection, 18% of the injected CO<sub>2</sub> has dissolved into the aqueous-groundwater phase (Figure 3.7).

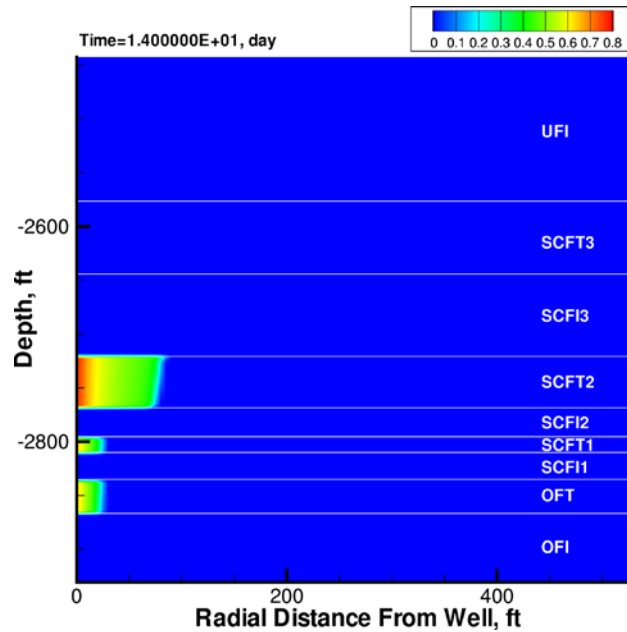


**Figure 3.2.** CO<sub>2</sub> Saturation in the Ortley, Slack Canyon #1 and Slack Canyon #2 Flow Tops Immediately after 1000 MT Supercritical CO<sub>2</sub> Injection

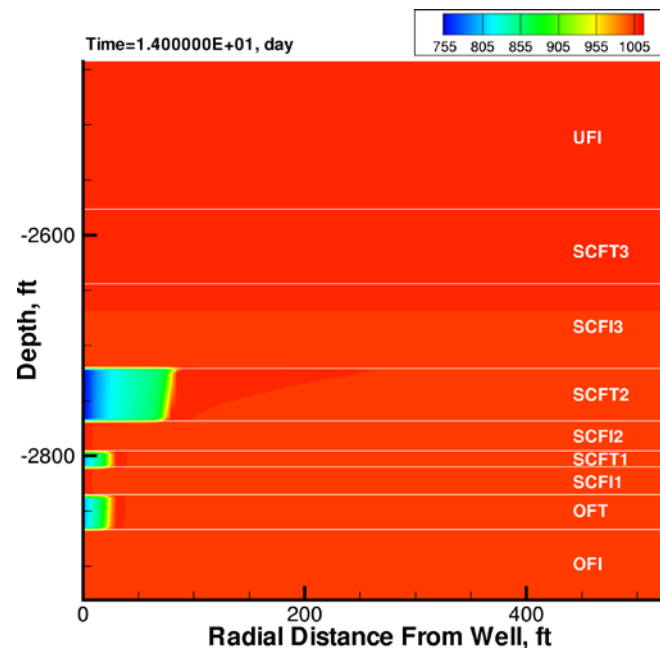


**Figure 3.3.** Fluid Density (kg/m<sup>3</sup>) in the Ortley, Slack Canyon #1, and Slack Canyon #2 Flow Tops Immediately after 1000 MT Supercritical CO<sub>2</sub> Injection

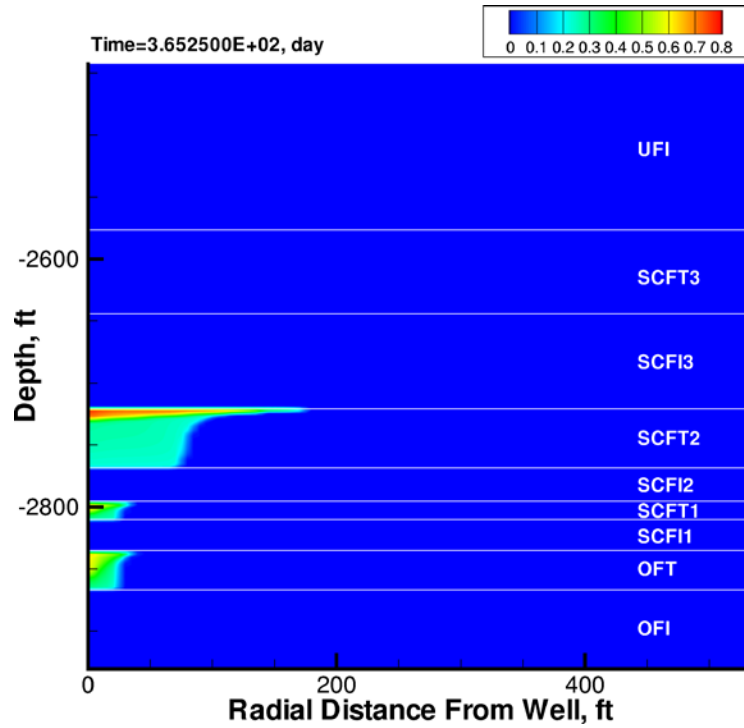


**Figure 3.4.** CO<sub>2</sub> Saturation in the Ortley, Slack Canyon #1 and Slack Canyon #2 Flow Tops 1 Year after Start of 1000 MT Supercritical CO<sub>2</sub> Injection

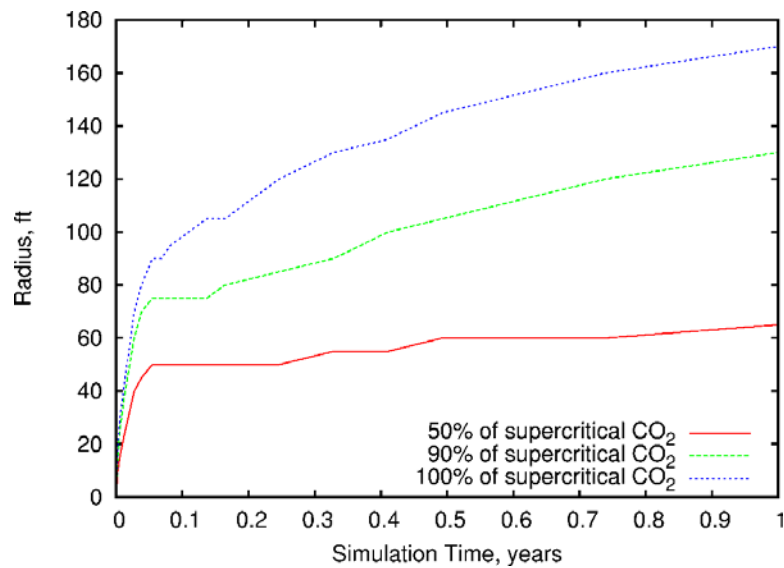


**Figure 3.5.** Radii Containing 50%, 90%, and 100% of 1000 MT of Supercritical CO<sub>2</sub> Injected into the Ortley, Slack Canyon #1 and Slack Canyon #2 Flow Tops

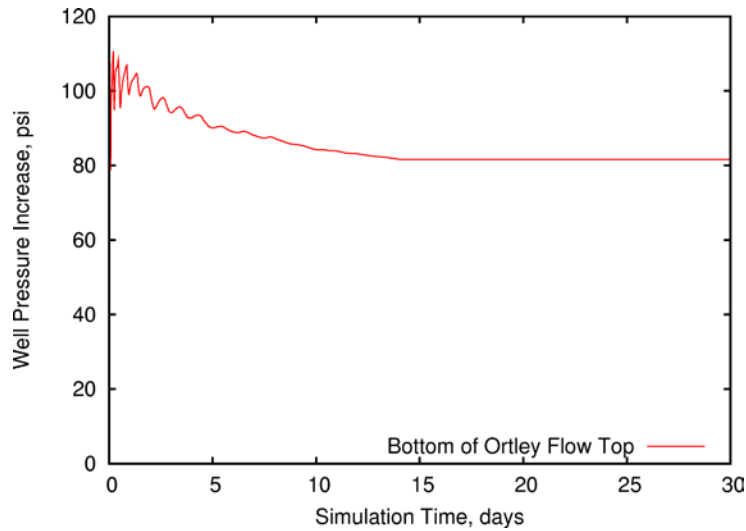


**Figure 3.6.** Increase in Well Pressure during Injection of Supercritical CO<sub>2</sub> into the Ortley, Slack Canyon #1, and Slack Canyon #2 Flow Tops

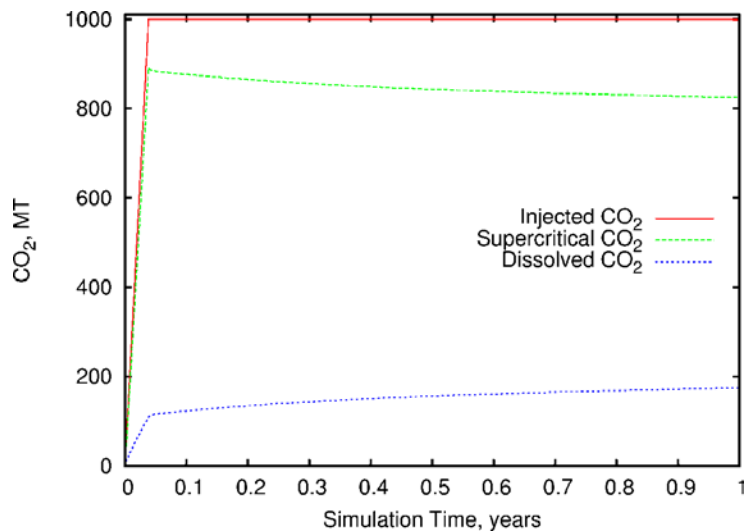


**Figure 3.7.** Phase Distribution of 1000 MT of Supercritical CO<sub>2</sub> Injected into the Ortley, Slack Canyon #1 and Slack Canyon #2 Flow Tops

### 3.2.2.2 Scenario 2: Injection into Slack Canyon #2 Flow Top (SCFT2)

Because most of the CO<sub>2</sub> injected in the previous Scenario 1 ended up in the SCFT2, a simulation assuming all CO<sub>2</sub> is injected directly into the SCFT2 does not produce significantly different results (Figure 3.8). The density of the injected supercritical CO<sub>2</sub> is 66% of that exhibited by groundwater at prevailing formation temperature and pressure conditions. Because supercritical CO<sub>2</sub> does not displace all of the groundwater within the formation pore space, the average fluid density contrast is 75% to 100% of initial formation water (Figure 3.9). The radius of the injected supercritical CO<sub>2</sub> from the Wallula pilot borehole well increases from 100 ft after the active 2 weeks of injection to 180 ft at 1 year after the start of injection (Figure 3.10 and Figure 3.11). The simulated increase in downhole pressure within the

injection zone/well bore is less than 120 psi (Figure 3.12). One year after the start of injection, 18% of the injected CO<sub>2</sub> has dissolved into the aqueous-groundwater phase (Figure 3.13).

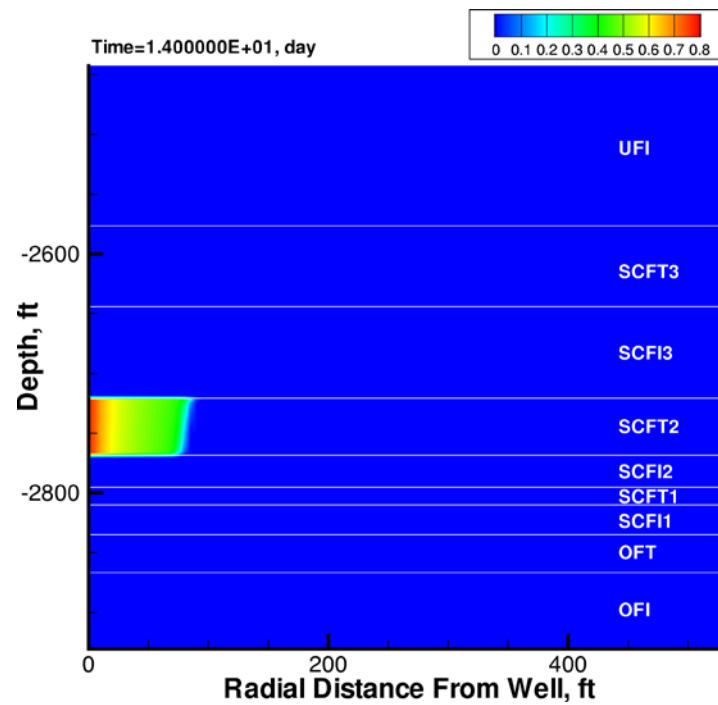


**Figure 3.8.** CO<sub>2</sub> Saturation in the Slack Canyon #2 Flow Top, Immediately after 1000 MT Supercritical CO<sub>2</sub> Injection

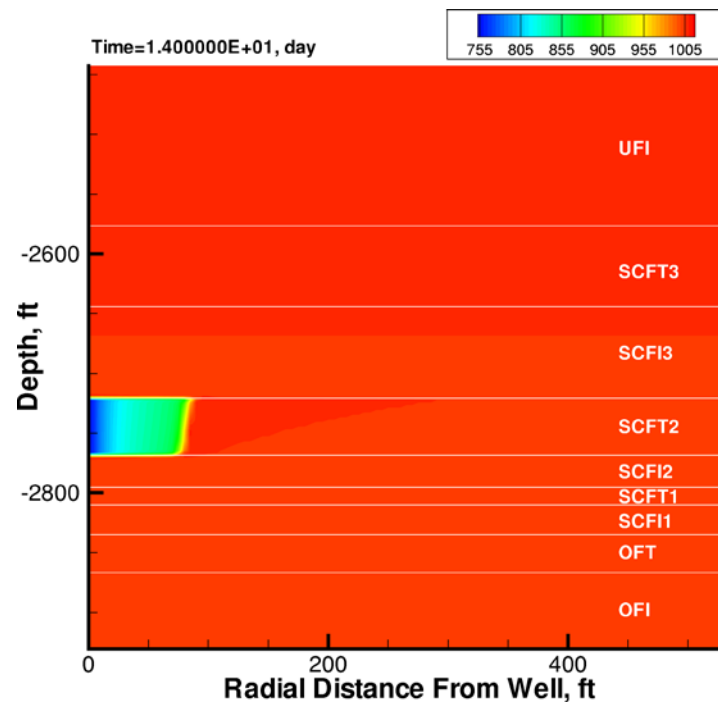


**Figure 3.9.** Fluid Density (kg/m<sup>3</sup>) in the Slack Canyon #2 Flow Top, Immediately after 1000 MT Supercritical CO<sub>2</sub> Injection

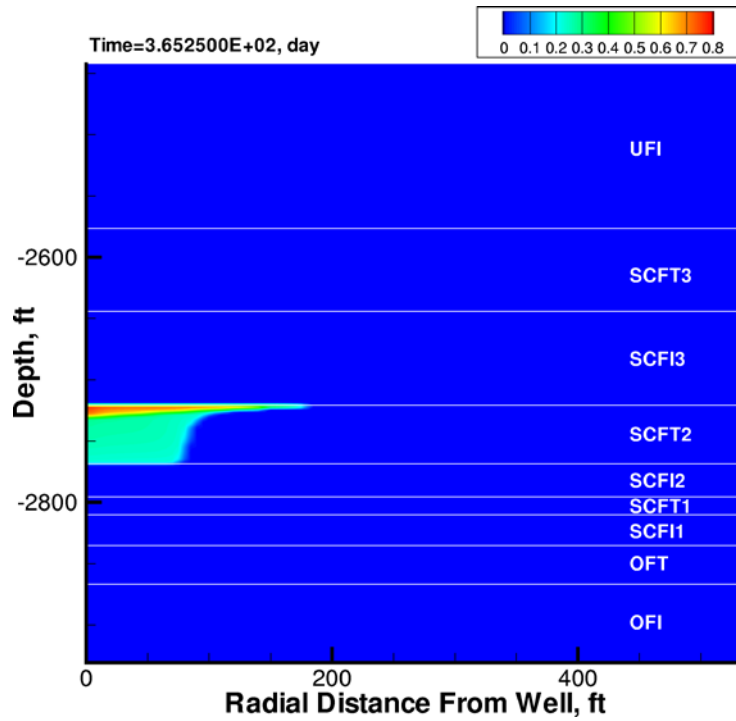


**Figure 3.10.** CO<sub>2</sub> Saturation in the Slack Canyon #2 Flow Top, 1 Year after Start of 1000 MT Supercritical CO<sub>2</sub> Injection

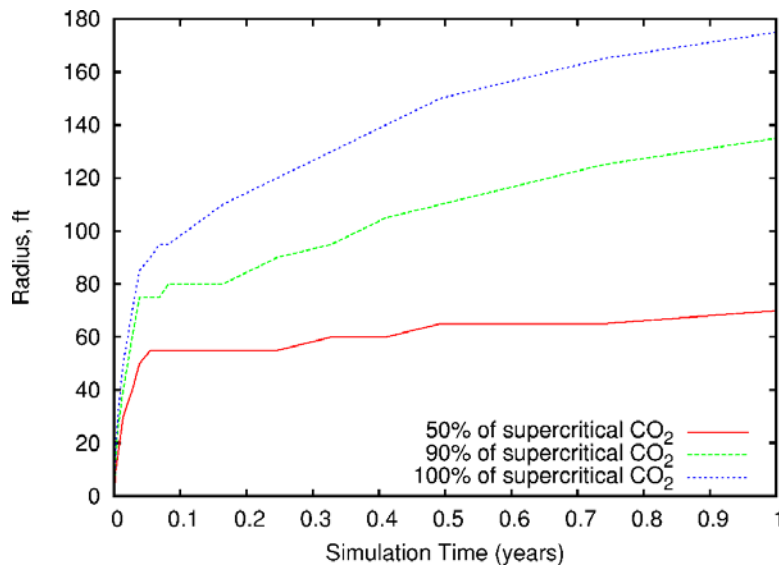


**Figure 3.11.** Radii Containing 50%, 90%, and 100% of 1000 MT of Supercritical CO<sub>2</sub> Injected into the Slack Canyon #2 Flow Top

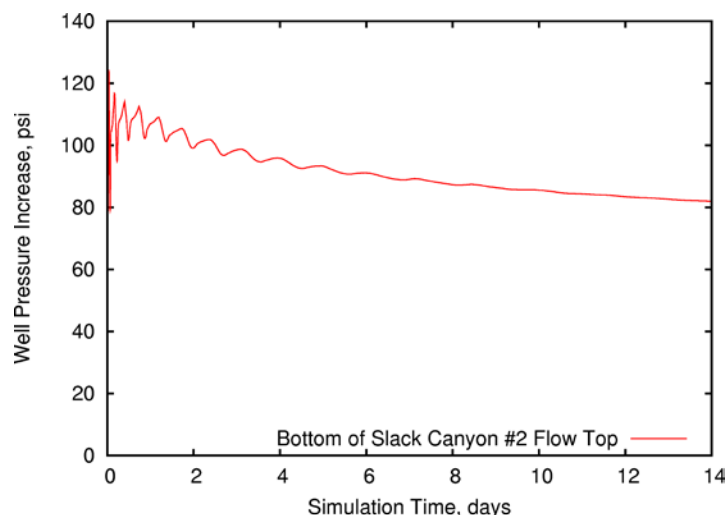


**Figure 3.12.** Increase in Well Pressure During Injection of Supercritical CO<sub>2</sub> into the Slack Canyon #2 Flow Top

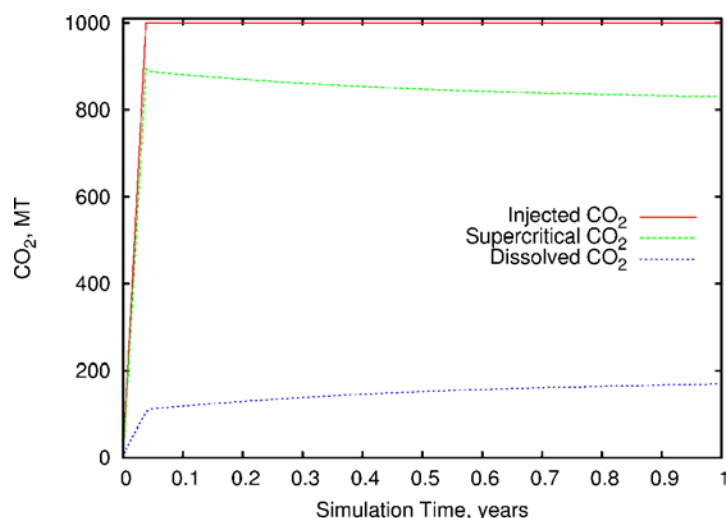


**Figure 3.13.** Phase Distribution of 1000 MT of Supercritical CO<sub>2</sub> Injected into the Slack Canyon #2 Flow Top

### 3.2.2.3 Scenario 3: Injection into Ortley Flow Top

A simulation assuming all CO<sub>2</sub> is injected into the OFT produces a similar predicted plume radius to injection into the SCFT2 (Scenario 2; Figure 3.14). Although the OFT is thinner than the SCFT2 with identical porosity, the lower permeability of the OFT results in a more compact CO<sub>2</sub> plume. As for Scenarios 1 and 2, the density of the injected supercritical CO<sub>2</sub> is 66% of that exhibited by groundwater at prevailing formation temperature and pressure conditions. Because supercritical CO<sub>2</sub> does not displace all of the groundwater in the formation pore space, the average fluid density contrast is 80% to 100% of initial formation water (Figure 3.15). The radius of the injected supercritical CO<sub>2</sub> from the Wallula pilot well increases from 100 ft at 2 weeks after the start of injection to 120 ft at 1 year after the start of injection (Figure 3.16 and Figure 3.17). Most of the supercritical CO<sub>2</sub> mass appears to be stable after

1 year, but a part of the plume continues to spread after this time. Because of the lower permeability, the simulated increase in downhole pressure within the injection zone/well bore is ~600 psi above the original reservoir pressure (Figure 3.18), five times greater than for injection into the SCFT2. One year after the start of injection, 10% of the injected CO<sub>2</sub> has dissolved into the aqueous-groundwater phase (Figure 3.19).

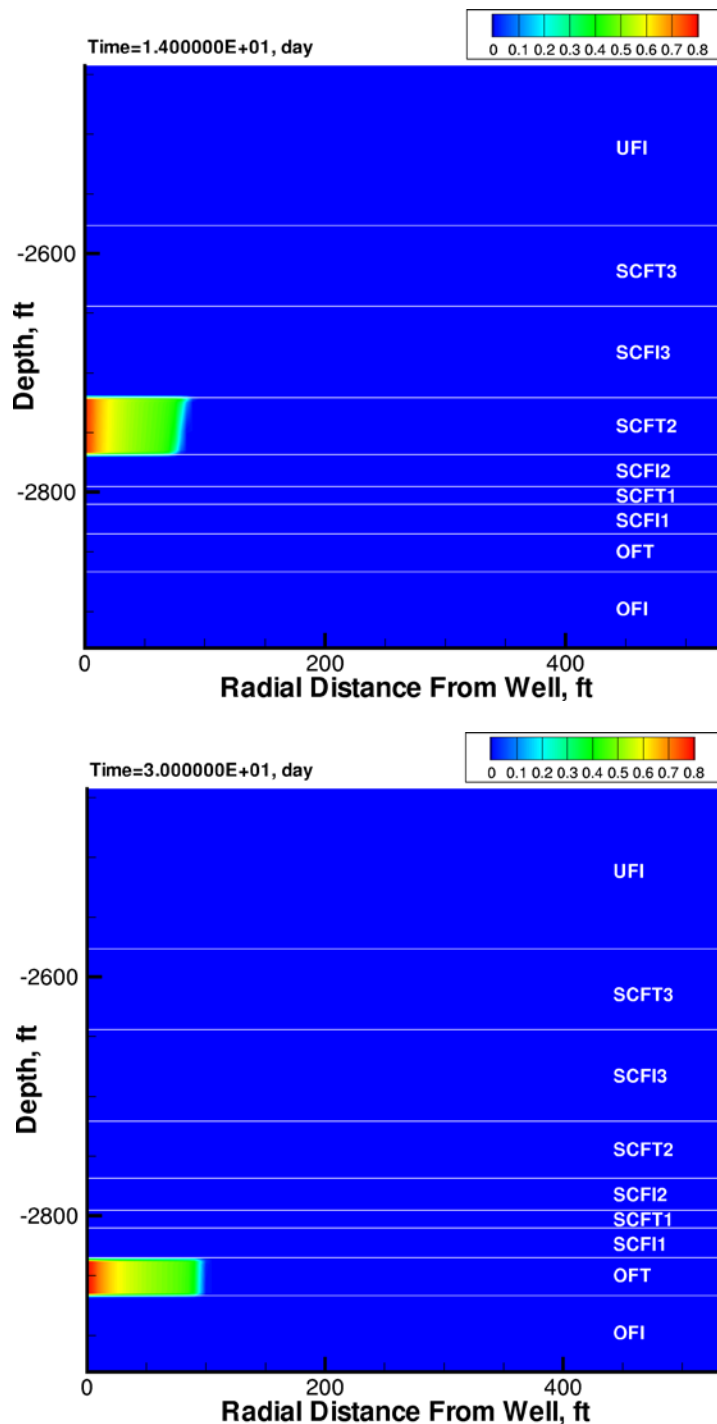


**Figure 3.14.** CO<sub>2</sub> Saturation in the Ortley Flow Top Immediately after 1000 MT Supercritical CO<sub>2</sub> Injection



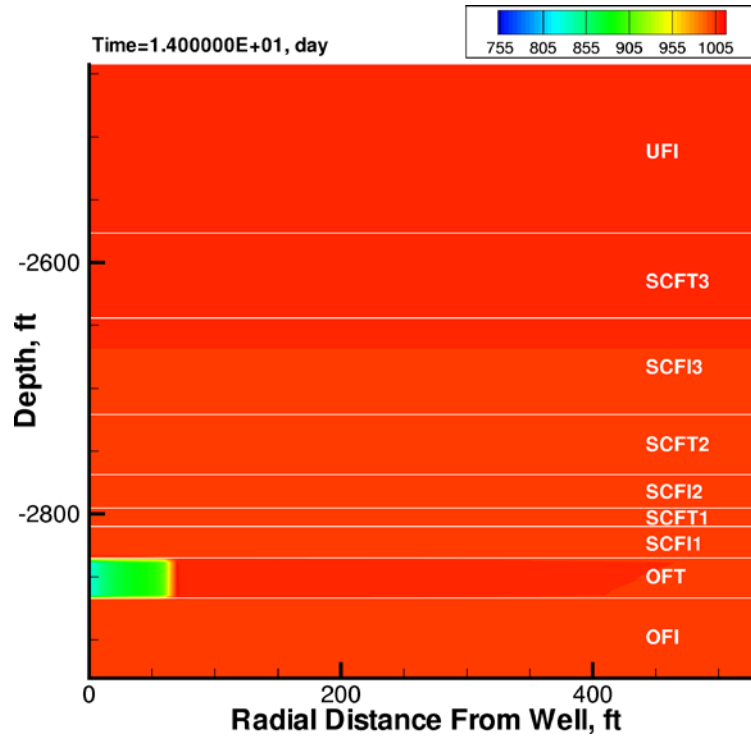


**Figure 3.15.** Fluid Density ( $\text{kg/m}^3$ ) in the Ortley Flow Top, Immediately after 1000 MT Supercritical  $\text{CO}_2$  Injection

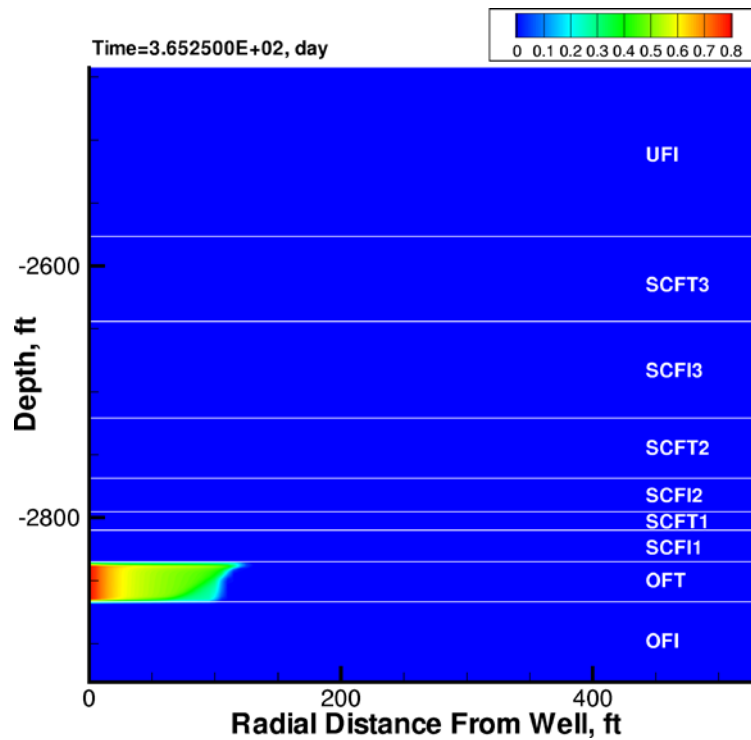


**Figure 3.16.**  $\text{CO}_2$  Saturation in the Ortley Flow Top, 1 Year after Start of 1000 MT Supercritical  $\text{CO}_2$  Injection

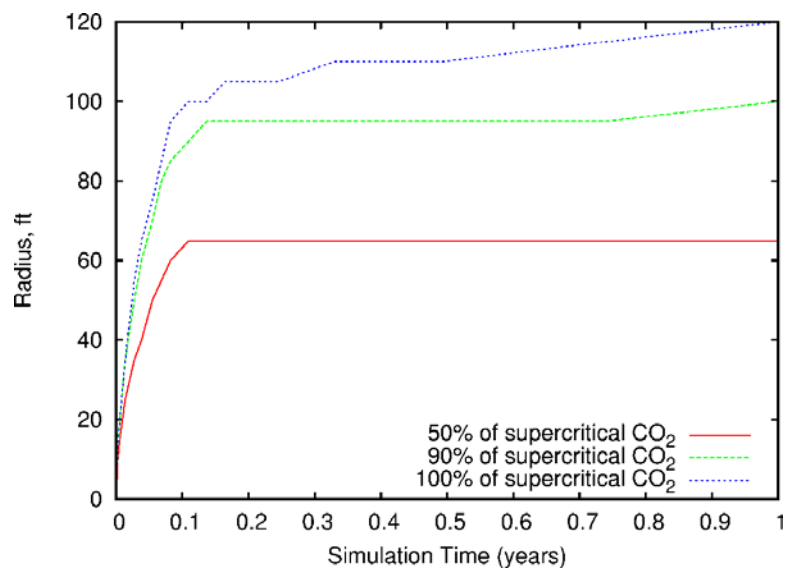


**Figure 3.17.** Radii Containing 50%, 90%, and 100% of 1000 MT of Supercritical CO<sub>2</sub> Injected into the Ortley Flow Top

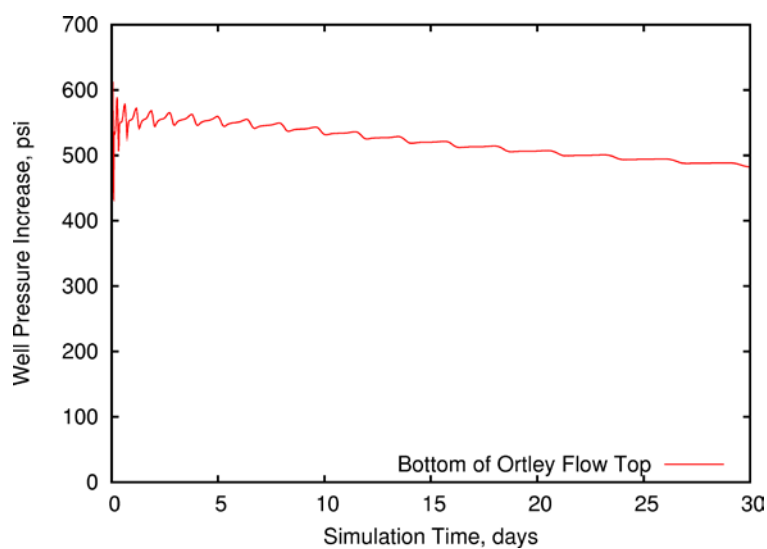


**Figure 3.18.** Increase in Well Pressure during Injection of Supercritical CO<sub>2</sub> into the Ortley Flow Top

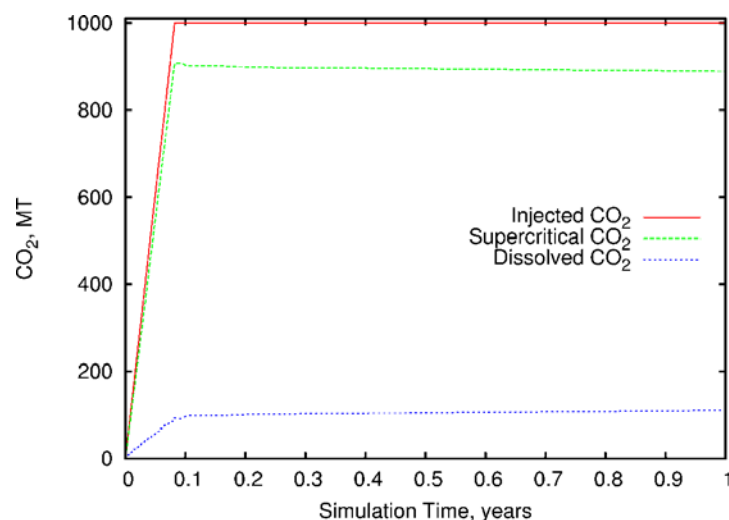


**Figure 3.19.** Phase Distribution of 1000 MT of Supercritical CO<sub>2</sub> Injected into the Ortley Flow Top

### 3.3 Injection Procedures

The principal focus of the injection phase is to provide the following:

1. Safely inject liquid CO<sub>2</sub> and several tracers incorporated in the CO<sub>2</sub> into basalt interflows within the well completion zone (2716 to 2910 ft)
2. Delineate the extent of the injected CO<sub>2</sub> plume within the host injection reservoir zone
3. Assess both test formation and well annular pressure responses for potential hydrologic leakage response effects (i.e., hydraulic communication) from the extended CO<sub>2</sub> injection, as monitored using geophysical sensors and standard hydrologic pressure monitoring systems.

Baseline conditions established during the preinjection characterization phase will serve as the basis for delineating plume migration during and following the active CO<sub>2</sub> injection phase.

Prior to initiation of CO<sub>2</sub> injection, the candidate injection interflow zone will be isolated within the completed well with a downhole packer-downhole shut-in valve test system. This packer test system is similar to the packer test system successfully deployed during the detailed borehole characterization phase of the Wallula pilot borehole. During the borehole characterization phase, 15 test zones within the open borehole were successfully isolated and characterized. The main difference in packer deployment from the previous borehole characterization phase is that during CO<sub>2</sub> injection, the packer will be set within the 7-in. cemented casing string immediately above the open borehole injection horizon. Salient downhole test system components include the following: inflatable packer, real-time downhole pressure probes (to monitor injection reservoir and overlying annular pressures), and a downhole shut-in tool valve assembly for test zone isolation at reservoir depth. The associated pressure responses at the injection well during the active CO<sub>2</sub> injection phase will be monitored and analyzed for indications of possible changes in injection zone hydraulic and storage properties, and diagnostic formational leakage response characteristics. As previously noted, the pressure responses will be monitored in real time using sensitive, programmable, downhole pressure transducers for maximum monitoring surveillance flexibility. Pressure measurements will be observed and stored both at the injection well site and telemetered to a data acquisition system located at Battelle.

The final logistics and delivery of CO<sub>2</sub> to the field site are currently in the design phase. Current plans, however, include the transportation of CO<sub>2</sub> by rail from the source/supplier directly to a side rail spur immediately adjacent to the field pilot study area. A scaffold system may be used to convey the CO<sub>2</sub> the short distance over a small access road and/or perimeter fencing to a surface storage container/vessel. The CO<sub>2</sub> will be maintained at a relatively uniform temperature (i.e., close to or slightly above the ~95 degrees formation temperature), within the storage vessel during the entirety of the injection phase. Efforts will be implemented to maintain a continuous, constant CO<sub>2</sub> injection rate, although a systematic, pulsed injection option is possible due to CO<sub>2</sub> supply disruptions. The CO<sub>2</sub> injection rate selected for the field pilot study will be based on the finalized estimated injection zone hydraulic and storage properties obtained during the borehole and preinjection characterization phase. Based on preliminary numerical modeling simulations and preliminary injection reservoir hydraulic property estimates, the active CO<sub>2</sub> injection phase will likely be completed within a 2-week period, assuming no delays in delivery of CO<sub>2</sub> to the site. A suite of partitioning and conservative hydrochemical tracers will also be incorporated and administered at the beginning and near the end of the injection phase and monitored for detection through geochemical sampling.

### **3.4 Monitoring Program**

This section provides a brief overview of the planned monitoring program for the Wallula pilot borehole. At least 30 days prior to injection, a field activity plan will be issued providing detailed procedures to be followed both during and after the CO<sub>2</sub> injection has been completed at the site.

#### **3.4.1 Atmospheric Monitoring**

An eddy covariance system will be installed at the field site to detect the very unlikely event of CO<sub>2</sub> leakage from the subsurface. The technique provides coverage over a broader monitoring area than is possible with soil gas probes (see Section 3.4.2) but has inherently lower sensitivity. The eddy covariance (correlation) method is an established micrometeorological technique that has been used for years to measure the flux of heat and other scalars between the atmosphere and the earth's surface. In the open-path eddy covariance method, CO<sub>2</sub> flux is determined by simultaneously measuring wind speed and direction, temperature, humidity, and the atmospheric concentrations of CO<sub>2</sub>, which are then used to compute CO<sub>2</sub> flux (the amount of CO<sub>2</sub> released per unit area per unit time). In this method, CO<sub>2</sub> concentrations are measured using an open-path infrared gas analyzer. A data logger records synchronized data from the sensors and the results of an online CO<sub>2</sub> flux calculation.

#### **3.4.2 Soil Monitoring**

Although reservoir simulations indicate it is physically impossible for any CO<sub>2</sub> to reach the surface during or after CO<sub>2</sub> injection, a dedicated soil gas probe will be installed within the projected CO<sub>2</sub> bubble radius around the test well. Vadose zone soil gas samples would begin being collected monthly as early as possible ahead of CO<sub>2</sub> injection (to establish background variability) and would continue on a regular basis until site closure. Soil-gas samples would be analyzed for CO<sub>2</sub>, tracers introduced with the CO<sub>2</sub>, and other target analytes (such as CH<sub>4</sub>).

### 3.4.3 Water Chemistry

The packer test system (discussed in Section 3.3) will be used to periodically collect fluid and/or gas samples from the test zone. Water chemistry analysis will be performed to determine critical parameters needed to track progression towards geochemical conditions suitable for carbonate mineral precipitation and for comparison with preinjection reactive transport simulations. Parameters to be measured include the following: pH, Eh, dissolved O<sub>2</sub>, temperature, conductivity, major and minor trace elements, stable isotopes, tracers, colloids, and microbes.

### 3.4.4 Preclosure Characterization

A residence time of 12 to 24 months is anticipated for the injected CO<sub>2</sub> to contact and react with the basalt reservoir before initiating preclosure characterization activities. The primary objective of this phase is to characterize the in-situ geochemical reactions of the injected CO<sub>2</sub> within the reservoir host rock horizon, and to assess any potential changes to hydraulic and storage characteristics within the injection interflow zone. The preclosure characterization phase will be implemented following completion of the designed injection residence period. Preclosure characterization activities include drilling at least one deviated geochemical corehole, conducting a suite of wireline borehole geophysical surveys, and performing a series of comparative hydrologic tests.

The slant or deviated geochemical corehole(s) will be drilled after removal of the downhole packer monitoring system. The corehole(s) will be deviated at an angle (using an installed borehole wedge) that will ensure intersecting the injection zone horizon at a to-be-determined radial distances from the injection well. The primary objective of this preclosure characterization activity is to retrieve injection zone basalt cores for detailed geochemical characterization of potential secondary mineralization that may be associated with the CO<sub>2</sub> injection process. This is a key preclosure characterization activity for verifying and assessing in-situ CO<sub>2</sub> reaction/mineralization rates.

Selected wireline borehole geophysical surveys will be conducted within the borehole prior to corehole drilling. The post-injection geophysical surveys selected will be based on an evaluation of wireline survey results conducted during the preinjection phase characterization. The preclosure wireline geophysical information will be compared with the results obtained during the preinjection characterization phase to evaluate potential formational property changes in the area immediately surrounding the borehole due to the CO<sub>2</sub> injection.

Additionally, the series of detailed hydrologic tests conducted during the preinjection phase will be repeated during the preclosure characterization. The associated pressure responses will be monitored in a similar fashion. The preclosure tests will be compared to preinjection results to assess potential formational property changes (i.e., transmissivity, storativity, leakage) over the local and intermediate-scale distance.

## **4.0 Public Outreach**

Stakeholder and public engagement is a critical component of any geologic sequestration project. Success or failure of public engagement on geologic sequestration projects has direct ramifications for application of the technology not only in the immediate region of the project, but has national and international impacts as well. Effective engagement of a broad spectrum of people and organizations is needed.

The objective of the stakeholder engagement efforts undertaken by the Wallula Pilot Project team is to build understanding of project objectives, conduct of activities, and potential benefits with local and regional stakeholder groups and the public. First, a brief historical background is provided of stakeholder activities and events that have impacted the project.

### **4.1 Historical Background**

In April 2007, PNWD and BSCSP were invited by the Port of Walla Walla to conduct a field pilot study on Port-owned land regarding CO<sub>2</sub> sequestration in basalt formations. The demonstration site was at that time under consideration by industry for construction of a 750-MW IGCC power plant that would require CCS. The site is located in a rural area, zoned heavy industrial, with agricultural and livestock management the principal businesses in the surrounding region. As a result of this invitation from the Port, Battelle staff stopped further search efforts at locating a field site in the NW to conduct the pilot.

Battelle staff participated in extensive stakeholder engagement activities, beginning in late July 2007. Meetings were held in Seattle with the Northwest Energy Coalition and Climate Solutions, important non-governmental organizations groups, and various newspaper editors. Numerous laboratory and field site tours were held that included visits from the Northwest Energy Coalition, Department of Ecology, Council on Trade & Economic Development, and several newspaper and magazine reporters. A public meeting was held on October 11, 2007, in Walla Walla to give an overview of the pilot project. Approximately 40 people attended and no opposition to the pilot project was voiced at that time.

In December 2007, support for the IGCC plant was terminated by the major financial backer and a land purchase option contract between the Port and the developer expired. Shortly thereafter, local public opposition to the proposed IGCC plant began to rapidly increase. As a result of these external events, Battelle was requested to seek an alternative site. In April 2008, Battelle staff began efforts to find an alternative location to conduct the pilot study that would preserve investments made in the surface seismic survey conducted in December 2007.

In May 2008, Battelle staff contacted management at the Boise White Paper mill located approximately 1/2 mile from the Port property site. Negotiations to conduct the pilot on their property were successfully concluded in August 2008 with the signing of a Land Use Agreement. Part of that agreement was to develop and execute a formal stakeholder engagement plan. This included hiring an Outreach

Coordinator to lead the effort. The engagement plan was formulated and revised through August and September 2008. The objectives of the stakeholder engagement plan included the following:

- Developing basic project information materials with key messages about the project, including information for citizens, interest groups, elected officials, and media.
- Identifying people and organizations in the local area that will have an interest in the pilot project, and proactively approaching them to explain the purpose, process, and expected outcomes, and to learn about their questions and concerns.
- Working to resolve issues raised by stakeholders, and keeping them informed as the pilot project proceeds to try to address their concerns and help them appreciate the potential contribution of this technology to clean energy and climate change goals.
- Identifying and engaging with a broader set of stakeholders with a statewide and regional view about the potential of emerging technology to address energy and climate change goals, as a foundation for permitting, sharing results, and potential future application of the technologies in areas beyond the Wallula community.

Execution of the engagement plan began in October 2008. A fact sheet and question and answer sheet were drafted. Meetings with community leaders were conducted to describe the new partnership and emphasize the distinctions between the pilot project and prior commercial interests in the area. The outreach team also met with key media leads before the partnership between Battelle and the paper mill was announced to answer any questions and clarify any misconceptions. After the announcement, the team met with dozens of stakeholders and several community groups representing a broad range of interests to describe the project and answer questions. The outreach coordinator from both Battelle and the paper mill attended as well as senior management from the paper mill and a technical CCS lead from Battelle. These discussions were frank and a commitment was made to share correspondence between Battelle/paper mill staff and the State regulator to demonstrate the team's interest in being transparent. In addition to interviews and small meetings/focus groups with stakeholders, an open house and tours were provided. Geology classes from a local college toured CCS laboratories and the drilling site. This engagement resulted in summer interns being hired and increasing the community's awareness and understanding of CCS.

The outreach team emphasized the win-win attributes of the project and how the paper mill was being proactive to investigate the feasibility of capturing and storing its CO<sub>2</sub> onsite. Through the various community engagement approaches and accurate media coverage, there was a much better understanding of the pilot project's objective and improved public trust. Battelle staff plan to continue a vigorous stakeholder engagement effort moving forward into the next phase of the pilot project.

## 5.0 References

- 40 CFR 141.62. 2009. “National Primary Drinking Water Regulations, Maximum Contaminant Levels for Inorganic Contaminants.” *Code of Federal Regulations*, U.S. Environmental Protection Agency.
- Alfredsson HA, BS Hardarson, H Franzson, and SR Gislason. 2008. “CO<sub>2</sub> Sequestration in Basaltic Rock at the Hellisheidi Site in SW Iceland: Stratigraphy and Chemical Composition of the Rocks at the Injection Site.” *Mineral. Mag.* 72(1):1–5.
- Bjornstad BN. 2009. *Geologic Sampling and Analysis Plan for the Wallula Deep-Basalt, Pilot Borehole*. PNWD-4123, Battelle Pacific Northwest Division, Richland, Washington.
- DOE. 1988. *Site Characterization Plan, Reference Repository Location, Hanford Site, Washington*. DOE/RW-0164, Vol. 2, U.S. Department of Energy, Washington, D.C.
- Eslinger PW. 1986. *Probability Distribution of Horizontal Hydraulic Conductivity in Grande Ronde Basalt Flow Interiors*. Computational Brief, CB No. 550, Rockwell Hanford Operations, Richland, Washington.
- Flaathen TK, EH Oelkers, and SR Gislason. 2008. “The Effect of Aqueous Sulphate on Basaltic Glass Dissolution Rates.” *Mineral. Mag.* 72(1):39–41.
- Fredrickson JK and DL Balkwill. 2006. “Geomicrobial Processes and Biodiversity in the Deep Terrestrial Subsurface.” *Geomicrobiol. J.* 23(6):345–356.
- Gephart RE, RC Arnet, RG Baca, LS Leonhart, and FA Spane. 1979. *Hydrologic Studies within the Columbia Plateau, Washington: An Integration of Current Knowledge*. RHO-BWI-ST-5, Rockwell Hanford Operations, Richland, Washington.
- Goldberg DS, T Takahashi, and AL Slagle. 2008. “Carbon Dioxide Sequestration in Deep-Sea Basalt.” *Proceedings of the National Academy of Sciences of the United States of America* 105(29):9920–9925.
- Gysi AP and A Stefansson. 2008. “Numerical Modelling of CO<sub>2</sub>-Water-Basalt Interaction.” *Mineral. Mag.* 72(1):55–59.
- Johnson DM, PR Hooper, and RM Conrey. 1999. “XRF Analyses of Rocks and Minerals for Major and Trace Elements on a Single Low-Dilution Li-Tetraborate Fused Bead.” In *Advances in X-Ray Analyses*, Vol. 41, International Centre for Diffraction Data, Newtown Square, Pennsylvania, pp. 843–867.
- Khalilabad MR, G Axelsson, and SR Gislason. 2008. “Aquifer Characterization with Tracer Test Technique; Permanent CO<sub>2</sub> Sequestration into Basalt, SW Iceland.” *Mineral. Mag.* 72(1):121–125.
- Lehman RM, FS Colwell, and GA Bala. 2001. “Attached and Unattached Microbial Communities in a Simulated Basalt Aquifer under Fracture- and Porous-Flow Conditions.” *Appl. Environ. Microb.* 67(6):2799–2809.
- Matter JM, T Takahashi, and D Goldberg. 2007. “Experimental Evaluation of In Situ CO<sub>2</sub>-Water-Rock Reactions During CO<sub>2</sub> Injection in Basaltic Rocks: Implications for Geological CO<sub>2</sub> Sequestration.” *Geochem. Geophys. Geosy.* 8.



- McGrail BP, AM Ho, SP Reidel, and HT Schaef. 2003. "Use and Features of Basalt Formations for Geologic Sequestration." In *Proceedings of the Sixth International Conference on Greenhouse Gas Control Technologies*, Vol. II (ed. J Gale and Y Kaya), Elsevier Science Limited, Kidlington, Oxford, United Kingdom, pp. 1637–1640.
- McGrail BP, HT Schaef, AM Ho, YJ Chien, JJ Dooley, and CL Davidson. 2006. "Potential for Carbon Dioxide Sequestration in Flood Basalts." *J. Geophys. Res.-Sol. Ea.* 111(B12).
- Mitchell AC, AJ Phillips, MA Hamilton, R Gerlach, WK Hollis, JP Kaszuba, and AB Cunningham. 2008. "Resilience of Planktonic and Biofilm Cultures to Supercritical CO<sub>2</sub>." *J. Supercrit. Fluids* 47(2):318–325.
- Mitchell AC, AJ Phillips, R Hiebert, R Gerlach, LH Spangler, and AB Cunningham. 2009. "Biofilm Enhanced Geologic Sequestration of Supercritical CO<sub>2</sub>." *Int. J. Greenh. Gas Con.* 3(1):90–99.
- NAVD88. 1988. North American Vertical Datum of 1988.
- NGVD 29/47. 1973. National Geodetic Vertical Datum of 1929.
- Pickens JF, GE Grisak, JD Avis, DW Belanger, and M Thury. 1987. "Analysis and Interpretation of Borehole Hydraulic Tests in Deep Boreholes - Principles, Model Development, and Applications." *Water Resour. Res.* 23(7):1341–1375.
- Prasad PSR, DS Sarma, L Sudhakar, U Basavaraju, RS Singh, Z Begum, KB Archana, CD Chavan, and SN Charan. 2009. "Geological Sequestration of Carbon Dioxide in Deccan Basalts: Preliminary Laboratory Study." *Curr. Sci. India* 96(2):288–291.
- Reidel SP. 2005. "A Lava Flow without a Source: The Cohasset Flow and Its Compositional Components, Sentinel Bluffs Member, Columbia River Basalt Group." *J. Geol.* 113:1–21.
- Reidel SP, VG Johnson, and FA Spane. 2002. *Natural Gas Storage in Basalt Aquifers of the Columbia Basin, Pacific Northwest USA: A Guide to Site Characterization*. PNNL-13962, Pacific Northwest National Laboratory, Richland, Washington.
- Reidel SP, FA Spane, and VG Johnson. 2005. *Potential for Natural Gas Storage in Deep Basalt Formations at Canoe Ridge, Washington State: A Hydrogeologic Assessment*. PNNL-15386, Pacific Northwest National Laboratory, Richland, Washington.
- Reilly TE, OL Franke, and GD Bennett. 1987. "The Principle of Superposition and Its Application in Ground-Water Hydraulics." In *Techniques of Water-Resources Investigations*, Chapter B6, Applications of Hydraulics, United States Geological Survey, Denver, Colorado, pp. 28.
- Schaef HT and BP McGrail. 2009. "Dissolution of Columbia River Basalt under Mildly Acidic Conditions as a Function of Temperature: Experimental Results Relevant to the Geological Sequestration of Carbon Dioxide." *Appl. Geochem.* 24(5):980–987.
- Spane FA. 1982. "Hydrologic Studies within the Pasco Basin." In *Proceedings of 1982 National Waste Terminal Storage Program Information Meeting*, U.S. Department of Energy, DOENWTS-30, pp. 23–28.
- Spane FA. 1999. *Effects of Barometric Fluctuations on Well Water-Level Measurements and Aquifer Test Data*. PNL-13078, Pacific Northwest Laboratory, Richland, Washington.

Spane FA. 2002. "Considering Barometric Pressure in Groundwater Flow Investigations." *Water Resour. Res.* 38(6):14/1–18.

Spane FA. 2008. *Results of Detailed Hydrologic Characterization Tests Conducted within Ohio Geological Survey CO<sub>2</sub> No. 1 Well*. PNWD-4000, Battelle Pacific Northwest Division, Richland, Washington.

Spane FA and RB Mercer. 1985. *HEADCO: A Program for Converting Observed Water Levels and Pressure Measurements to Formation Pressure and Standard Hydraulic Head*. RHO-BW-ST-71P, Rockwell Hanford Operations, Richland, Washington.

Spane FA and PD Thorne. 1986. *Comparison of Calculated and Observed Hydrostatic Pressure Measurements at Borehole DC-8*. RHO-BW-ST-74P, Rockwell Hanford Operations, Richland, Washington.

Spane FA and WD Webber. 1995. *Hydrochemistry and Hydrogeologic Conditions within the Hanford Site Upper Basalt Confined Aquifer System*. PNNL-10817, Pacific Northwest National Laboratory, Richland, Washington.

Spane FA, DL Graham, and RW Bryce. 1982. *Hydrochemical and Isotopic Content of Basalt Groundwaters beneath the Hanford Site, Washington*. RHO-BW-SA-190P, Rockwell Hanford Operations, Richland, Washington.

Spane FA, BP McGrail, EC Sullivan, DS Goldberg, TL McLing, RS Weeks, and RW Smith. 2008. *Field Activity Plan: Characterization Test for CO<sub>2</sub> Sequestration in the Columbia River Basalt Group*. PNWD-3844, Revision 1, Battelle Pacific Northwest Division, Richland, Washington.

Strait SR and FA Spane, Jr. 1982. *Preliminary Results of Hydrologic Testing the Composite Umtanum Basalt Flow Top at Borehole RRL-2*. SD-BWI-TI-105, Rev. 0, Rockwell Hanford Operations, Richland, Washington.

Tingay M, J Reinecker, and B Müller. 2008. *Borehole Breakout and Drilling-Induced Fracture Analysis from Image Logs*. German Research Centre for Geosciences, Potsdam, Germany. Available at [http://dc-app3-14.gfz-potsdam.de/pub/introduction/introduction\\_frame.html](http://dc-app3-14.gfz-potsdam.de/pub/introduction/introduction_frame.html).

WAC-173-160-420. "General Construction Requirements for Resource Protection Wells." *Washington Administrative Code*, Olympia, Washington.

WAC-173-160-430. "Minimum Casing Standards." *Washington Administrative Code*, Olympia, Washington.

WAC-173-160-442. "Limitations for Use of Drilling Materials." *Washington Administrative Code*, Olympia, Washington.

WAC-173-160-444. "Standards for Use of Polymers and Additives." *Washington Administrative Code*, Olympia, Washington.

WAC-173-160-450. "Well Sealing Requirements." *Washington Administrative Code*, Olympia, Washington.

WAC 173-218-115. “Specific Requirements for Class V Wells Used to Inject Carbon Dioxide for Permanent Geologic Sequestration. ” Available at <http://apps.leg.wa.gov/WAC/default.aspx?cite=173-218-115>. Last accessed December 30, 2009.

White MD, BP McGrail, HT Schaef, and DH Bacon. 2006. “Numerically Simulating Carbonate Mineralization of Basalt with Injection of Carbon Dioxide into Deep Saline Formations.” In *Proceedings of XVI International Conference on Computational Methods in Water Resources*, Technical University of Denmark, Proceedings available at <http://proceedings.cmrw-xvi.org/contributionDisplay.py?contribId=246&sessionId=3&confId=a051>.

White MD and M Oostrom. 2006. *STOMP Subsurface Transport over Multiple Phases, Version 4.0, User's Guide*. PNNL-15782, Pacific Northwest National Laboratory, Richland, Washington.

Whiteman KJ, JJ Vaccaro, JB Gonthier, and HH Bauer. 1994. *The Hydrogeologic Framework and Geochemistry of the Columbia Plateau Aquifer System, Washington, Oregon, and Idaho*. Professional Paper 1413-B, U.S. Geological Survey, Washington, D.C.

Zoback MD. 1999. *Fracture Permeability and in Situ Stress in the Dixie Valley, Nevada, Geothermal Reservoir*. DOE/ID/13452, Stanford University, Stanford, California. Available at <http://www.osti.gov/bridge/servlets/purl/12560-O4jzXN/webviewable/12560.pdf>.